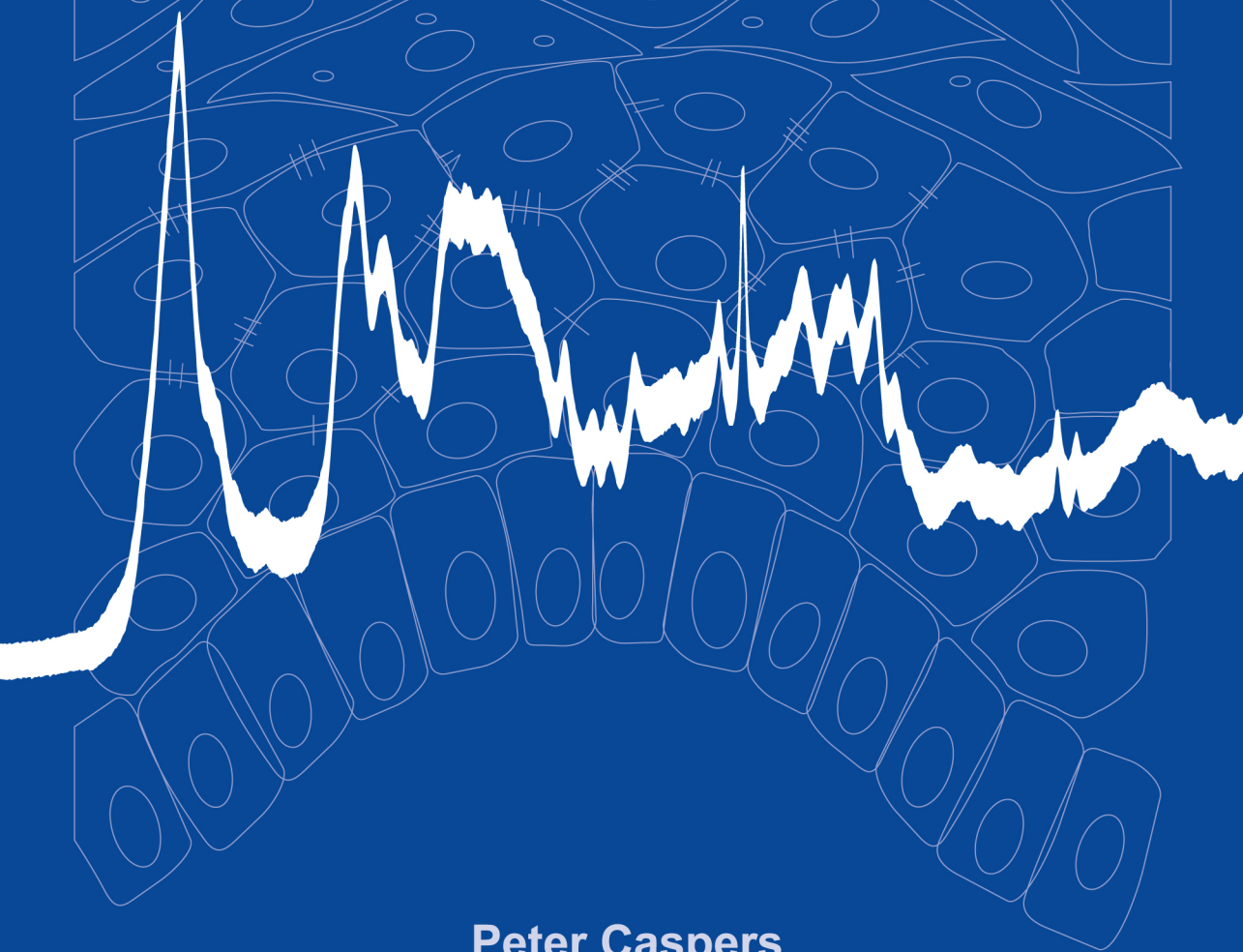


In vivo skin characterization
by
confocal Raman microspectroscopy



Peter Caspers

**In vivo skin characterization
by confocal Raman microspectroscopy**

Peter Caspers

Printed by Optima Grafische Communicatie, Rotterdam

ISBN 90-6734-366-8

© 2003 by P.J. Caspers.

© 1998 Chapter 2, © 2000 Chapter 4, by John Wiley & Sons, Ltd.

© 2001 Chapter 3, by The Society for Investigative Dermatology, Inc.

© 2002 Chapter 5, by Plenum Publishing Corporation.

© 2003 Chapter 6, by the Biophysical Society.

**In vivo skin characterization
by confocal Raman microspectroscopy**

In vivo karakterisering van de huid
met confocale Raman microspectroscopie

Proefschrift

ter verkrijging van de graad van doctor aan de
Erasmus Universiteit Rotterdam
op gezag van de
Rector Magnificus

Prof.dr.ir. J.H. van Bommel

en volgens besluit van het College voor Promoties.

De openbare verdediging zal plaatsvinden op
woensdag 17 september 2003 om 13:45 uur
door

Peter Jacobus Caspers
geboren te Amsterdam

Promotiecommissie

Promotor:

Prof.dr. H. A. Bruining

Overige leden:

Prof.dr. J. W. Oosterhuis

Prof.dr. H. A. M. Neumann

Dr.ir. H. J. C. M. Sterenberg

Copromotor:

Dr.ir. G. J. Puppels

voor Belinda

*“Fanatisme is: je krachtsinspanning verdubbelen
nadat je je doel vergeten bent.”*

George Santayana, 1863-1952

Contents

Chapter 1	Introduction	9
	1.1 Human skin	
	1.2 Methods for skin characterization	
	1.3 Raman spectroscopy	
	1.4 History of Raman spectroscopy	
	1.5 This thesis	
Chapter 2	In vitro and in vivo Raman spectroscopy of human skin	25
Chapter 3	In vivo confocal Raman microspectroscopy of the skin: noninvasive determination of molecular concentration profiles	43
Chapter 4	Automated depth-scanning confocal Raman microspectrometer for rapid in vivo determination of water concentration profiles for human skin	67
Chapter 5	Monitoring the penetration enhancer dimethyl sulfoxide in human stratum corneum in vivo by confocal Raman spectroscopy	81
Chapter 6	Combined in vivo confocal Raman spectroscopy and confocal microscopy of human skin	91
Chapter 7	Conclusions and prospects	109
Chapter 8	Summary	117
	Samenvatting	123
	Dankwoord	
	Curriculum vitae	
	Publications	

Introduction

Chapter

1

Abstract

Various areas of skin research depend on detailed knowledge of the molecular composition of skin and molecular structure of skin constituents. On a microscopic scale the skin is a highly heterogeneous tissue. Molecular composition and structure vary tremendously, depending on depth and location on the body, and may be affected by skin disorders and environmental factors such as sun exposure, seasonal variation, and cosmetic or medical treatments can influence the molecular properties of the skin. For many aspects of skin research or skin characterization, noninvasive methods are particularly welcome. This is partly because they cause less discomfort for the patient or volunteer, as the skin is not damaged, but more importantly because noninvasive methods enable investigation of the skin in its natural state, without affecting its integrity, morphology or molecular composition. Only noninvasive measurements can be performed repeatedly on the same skin area, and can thus be used to monitor skin changes. The aim of the work presented in this thesis was to develop confocal Raman microspectroscopy as a noninvasive technique for qualitative and quantitative analysis of the molecular composition of the human skin *in vivo*.

1.1 Human skin

The skin is the largest human organ, covering an area of about 2 m^2 for an adult. Anatomically the skin consists of two layers: the *epidermis* is a stratified epithelium lying on top of a fibroelastic tissue called the *dermis*. The skin is connected to the body by a layer of fatty connective tissue, the subcutis, which dissipates mechanical stress and allows the skin to follow the motions of the body.

Dermis

The dermis is a fibroelastic connective tissue, which gives the skin tensile strength. It contains nerves, blood vessels, lymph vessels, muscles, hair follicles, sweat glands and sebaceous glands. The total thickness of the dermis varies from 1 mm to a maximum of 4 mm on the back. The dermal blood vessels are organized in two layers oriented parallel to the skin surface. These networks of microcirculatory elements, or plexes, are connected by vertical blood vessels and terminate in fine capillary networks just beneath the epidermis. The proteins collagen and elastin are primarily responsible for the tensile strength of the dermis. Collagen is the major structural protein and represents 75% of the dry weight and 90% of the total protein content of the dermis. In hydrated tissue, the proportion of collagen is still 20% (wt.). Collagen fibers are composed of microfibrils that in turn are formed by collagen molecules called tropocollagen. The molecule consists of three polypeptide chains, wrapped around one another in a triple helix. In adult skin 80% of the total collagen is of type I, 15% of type III and the remaining 5% exists of type IV, V, VI and VII.¹

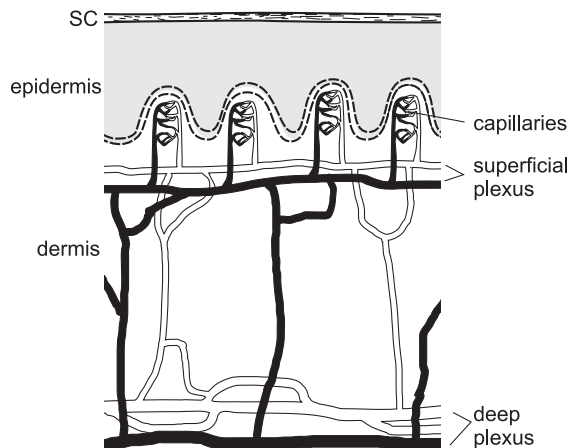


Figure 1. The dermal vasculature, showing the deep plexus, the superficial plexus and the capillary loops.

Epidermis

The epidermis is a stratified epithelium of cornifying cells. The principal cell type of the epidermis is the keratinocyte, containing filaments of the protein keratin, which give the cell its structural stability.

In much smaller quantities three other types of cells are found in the epidermis: melanocytes, which produces the skin pigment melanin, Langerhans cells, important for immunological function and Merkel cells, which are thought to have a sensory function. The total thickness of the epidermis lies between 50 and 150 μm . Perhaps the most important function of the epidermis is to produce the stratum corneum (SC). This outermost layer of the skin is a thin sheet of dead cornified cells, which forms the primary barrier to water loss and invasion of microbes and chemicals.

In a process of continuous differentiation, the keratinocytes migrate upward, accumulating keratin. In the final stage the keratinocyte is fully cornified and desquamates at the skin surface. The complete differentiation process from basal cell until desquamation takes about 15-30 days. In the epidermis four sub layers can be distinguished, which represent the successive stages of differentiation of the keratinocytes. (1) The differentiation process starts at the *stratum basale* or the germinative layer, consisting of large cubic cells. This is the innermost layer of the epidermis, separated from the dermis by a continuous basal membrane. (2) Once the cells start to migrate they enter the *stratum spinosum*, comprised of polyhedral cells with a spine-like appearance caused by bundles of tonofilaments that, with conventional microscopy, are seen to cross intercellular spaces and form contacts between adjacent keratinocytes.²

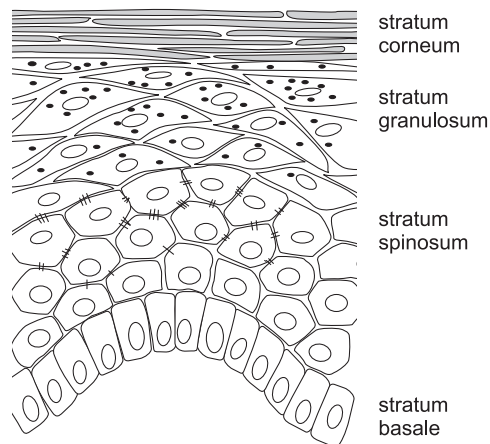


Figure 2. Schematic drawing of the epidermis. Four major layers of cells are distinguished: the basal layer (stratum basale); the spinous layer (stratum spinosum); the granular layer (stratum granulosum), containing keratohyalin granules which are shown here as black spots; and the stratum corneum.

The following layer is the *stratum granulosum*, comprised of several layers of flattened cells filled with keratohyalin granules, which are visible with light microscopy. Keratohyalin granules contain histidine-rich and cysteine-rich proteins, which are the precursor of filaggrin (*filament aggregating protein*). This protein plays a role in the aggregation of keratin filaments within the cornified cells. Filaggrin also provides the pool of free amino acids in the SC, which make up the natural moisturizing factor. In the upper part of the stratum spinosum submicroscopic granules start to appear, the origin of which is thought to be the Golgi apparatus. These granules are abundantly present in the stratum granulosum. At high magnification using electron microscopy, the granules exhibit a lamellar structure comprised of lipids (sterols, phospholipids and cerebrosides) and several hydrolytic enzymes. (4) Finally the keratinocytes abruptly transform into flat, fully keratinized, enucleate cells to form the *stratum corneum*. The lamellar granules have discharged their contents into the intercellular spaces, forming a matrix of lamellar lipids surrounding the flattened cornified cells. The thickness of the SC is approximately 15 μm on most parts of the body. The architecture of flat cornified cells embedded in a matrix of lamellar lipids renders an almost impermeable barrier that keeps water in and harmful substances and microorganisms out of the body.

Molecular composition of the Stratum Corneum (SC)

Keratin The major structural protein in epidermis is keratin. The name keratin refers to a family of fibrous proteins which historically have a variety of different classifications, according to molecule mass, acidity, structure and cysteine content. Keratins are sometimes divided in ‘soft keratins’ (those of the skin) and ‘hard keratins’ (those in hardened tissues such as hair, feather and nail). Another classification originates from Australian research on wool, as it was found that extracts of wool contained different amounts of cysteine, a sulfur rich amino acid that contributes to the rigidity of the fibers by forming disulfide links. The terms ‘high sulfur keratins’ (>20% cysteine) and ‘low sulfur keratins’ (<3% cysteine) refer to these differences in sulfur content of the protein.³ More important for characterization of human epidermis is a classification based on protein secondary structure, which is thought to play a role in the barrier function of the SC. Keratin can be divided into α - and β -keratin, according to the α -helical or β -sheet secondary conformation. Keratin in human SC is for about 90% composed of α -keratin and for 10% of β -keratin.⁴ Based on Raman spectroscopic investigation of isolated sheets of SC, Anigbogu *et al.* reported a somewhat larger fraction of β -keratin: 16% β -keratin and 84% α -keratin. For the total dry weight fraction of SC this is 54% and 10% respectively.⁵

Lipids The majority of skin lipids is found in the epidermis. The complex epidermal lipid contents changes substantially as the keratinocytes differentiate. The main lipids in the basal layer are membrane lipids (phospholipids and cholesterol) and a small amount of triglycerides, which may serve as a potential source of energy for the metabolically very active cells. In the spinous layer lamellar bodies are formed within the cells. They contain phospholipids (34%), sphingolipids (23%, ceramides and cerebrosides) and cholesterol (15%).⁶ In the transition to the fully cornified SC large changes in the epidermal lipid con-

tents take place. The most prominent changes are the disappearance of phospholipids and glycosylceramides in the SC.

The lipid content in SC consists mainly of cholesterol, ceramides and fatty acids. Although many studies have been reported about SC lipids and their structures, little consensus exists about the quantity of the different classes of lipids in SC. One of the problems in the analysis of epidermal lipids may be contamination from non-epidermal lipids. In several studies of non-human epidermal lipids triglycerides are included as a major constituent of lipids extracted from isolated epidermis. Most likely the origin of these triglycerides is a contamination with subcutaneous fat during sample preparation. Also the distinction between skin surface lipids from sebum, mainly triglycerides, fatty acids, wax esters and squalene, and the non-polar epidermal lipids may cause problems. A review of the composition of epidermal lipids and of different determination methods is presented by Wertz and Downing.⁶

Water The SC is a barrier that separates the viable cells of the epidermis from the environment. The inner cell layer of the SC covers the viable cells of the epidermis, which contain approximately 70% (wt.) water. The outer surface of the SC faces the environment and the cells are hydrated to a much lower degree, largely depending on the environmental humidity. It is clear therefore, that a steep water gradient must exist in the SC. This gradient has been determined for isolated SC using X-ray microanalysis, but *in vivo* evidence has been lacking.^{7;8}

It has been known for a long time that the SC itself requires a certain hydration level in order to maintain its integrity and its barrier function. Water provides flexibility and deprived of water, the SC becomes brittle and may crack or fissure.⁹ In recent years, it has become apparent that water acts in more subtle ways than simply increasing flexibility of the SC. Corneocyte desquamation, the shedding of cells from the SC surface, is a delicate process in which the integrity of the SC barrier is to be maintained. In healthy skin the loss of corneocytes is precisely balanced by the rate of keratinocyte proliferation. The process of desquamation is regulated by enzymes, which are critically influenced by the water content in the tissue (reviewed in Harding *et al.*¹⁰). Perturbation of this process results in dry flaky, scaly skin, which is a very common problem for both healthy people and for a variety of diseases. In a number of studies the amount of water in the SC has been related to the condition of dry skin. However, a reduced water content in all dry skin conditions has not been conclusively shown.¹¹⁻¹³

Natural moisturizing factor (NMF) In order for the SC to maintain an optimal level of moisturization it produces a very efficient humectant known as the natural moisturizing factor (NMF). The NMF is a mixture of amino acids, derivatives of amino acids and specific salts and is found exclusively in the SC cells. The constituent chemicals are highly water soluble and hygroscopic and will absorb atmospheric water even at relative humidities as low as 50%. This allows the SC to maintain water even when the outer surface is exposed to a relatively dry environment. Studies have revealed that filaggrin is the sole source of all the amino acid derived components of NMF. The protein was first discov-

ered as being necessary in organizing the keratin filaments as the granular cell made its transition into a corneocyte, hence the name filaggrin (*filament aggregating protein*). The NMF precursor protein is called profilaggrin and is located in the keratohyalin granules, which are found in the stratum spinosum and granulosum layers of the viable epidermis. As the granule cell makes the transition into a corneocyte the profilaggrin is released after species-specific dephosphorylation and undergoes proteolytic processing. Filaggrin then facilitates the bundling of the keratin intermediates filaments to form macro fibrils, which subsequently form the bulk of the corneocyte proteins. After the epidermal water permeability barrier is established, filaggrin is hydrolyzed and converted into NMF in an abrupt process that takes place in the lower few cell layers of the SC. The conversion of filaggrin into NMF is an enzymatic process that, like many other enzymatic processes in the SC, is critically influenced by the level of hydration in the tissue (review by Harding, 2000).¹⁰

1.2 Methods for skin characterization

Much of our fundamental knowledge of the epidermis has been obtained by the use of a wide variety of experimental methods, most of which are more or less invasive, i.e. they required isolation of skin tissue or skin constituents, for instance by cutting, clipping, stripping with adhesive tape or extraction with various solvents. The actual analysis is then performed *in vitro* on isolated skin material. By definition, invasive methods disturb the skin tissue. Extraction or isolation of material influences the remaining skin and alters its molecular composition, which limits the possibilities for monitoring changes in the skin, whether induced or natural, over a certain period of time. Moreover, the molecular composition of the samples of skin material may change during the processes of isolation or extraction. For instance, a method often used to isolate SC from excised skin is to separate the epidermis from the underlying tissue by immersion in hot water, followed by enzymatic digestion of the viable cells. Although the remaining sheet of SC appears intact, it can be assumed that a portion of the soluble compounds has been washed out and that the molecular structure of lipids and proteins has changed. The problem of perturbation of the molecular composition is of particular importance when physiological parameters such as hydration and pH are investigated, as these can easily be affected.

A common method for *in vivo* investigation of the stratum corneum is tape stripping, based on the removal of SC layers by successive applications of adhesive tape. Various methods can then be employed to analyze the removed skin material on the tape strips such as spectroscopic inspection of the strips,^{14, 15} electron diffraction¹⁶ and solvent extraction followed by chromatography.¹⁷⁻²⁰ Alternatively, the stripped skin area can be investigated upon removal of successive cell layers from the skin. This method has been used to obtain information about changes across the thickness of the SC of pH,²¹ NMF,²² lipids and hydration.²³⁻²⁵ Weighing of the tape strips before and after application determines the amount of skin material on the strips, which provides an estimate of the number of cell layers removed by each stripping and concomitantly the depth that is reached after a number of strippings. However, the variability in the amount of removed skin material prohibits an accurate estimated, particularly because a single strip contains material from differ-

ent cell layers due to folds and furrows in the skin.²⁶ As a monitoring technique tape stripping is less appropriate, because it completely or partly removes the stratum corneum from the studied skin area.

Noninvasive methods

Noninvasive methods can be used to avoid the problems of disturbing the molecular composition of the skin or uncertainties that are a result of sample preparation. To this end, a limited number of techniques have been employed such as Magnetic Resonance Imaging (MRI), techniques based on the electrical properties of the skin and optical methods.

MRI can be used to distinguish different tissues and to determine the water content in these tissues. A main requirement for imaging different skin layers is a high spatial resolution in the depth direction. In a conventional MRI system the axial resolution is in the order of several hundreds of microns. The limiting factor for spatial resolution is the strength of the magnetic field that can be created within the tissue. In high resolution MRI, the probing volume is kept small, which makes it possible to create a stronger field within the tissue. In this way a resolution of about 70 μm in the direction perpendicular to the skin surface has been achieved, which enabled delineation of the epidermis *in vivo*.²⁷ However, this is still far away from the resolution required to detect molecular gradients in the SC.

Methods based on the *electrical properties* of skin have found a widespread use in assessing skin hydration (reviewed by Loden, 1995).¹³ Generally these instruments detect changes in impedance, conductance or capacitance of the skin. These electrical properties are highly susceptible to moisture levels in the skin, and therefore are thought to reflect the hydration status of the skin. Measurement of the electrical properties of the skin is simple and the required equipment is relatively cheap, which may have contributed to the widespread use of these methods. Nevertheless, electrical measurements have several limitations, which make their value as a method to obtain a better understanding of the hydration properties of the skin questionable. Electrical measurements provide only qualitative information about changes in skin hydration, but no quantitative measure of the actual water content is provided. Besides, apart from water, many other factors can influence the electrical properties of the skin and affect the measurement. Another limitation is that the measurement volume (i.e. the skin volume that contributes to the measured signal) is only poorly defined. Since the water content across the SC exhibits a steep gradient (this thesis, chapter 3), it remains unclear whether and how a change in the reading of the instrument reflects a change in the hydration profile. The method is also quite sensitive to irregularities of the skin such as furrows and sweat glands. The upper SC cells are sensitive to changes in hydration when the measurement probe occludes the skin. This will flatten the loose cells on the skin surface and change the contact area between the skin and the probe. Hence, small changes at the skin surface can have strong effects on the apparent hydration status of the skin.

A number of highly developed *optical* methods has been employed in skin research. *In vivo* microscopic techniques such as Confocal Scanning Laser Microscopy (CSLM) and two-photon fluorescence microscopy enable *in vivo* imaging of the skin with high spatial

resolution and high contrast. Contrast in CSLM is obtained from variations of the refractive index in the tissue. A more detailed description of CSLM, including examples of its application to skin studies, is given in chapter 6. The contrast mechanism of two-photon microscopy originates from excitation of endogenous fluorescent compounds.^{28; 29} Although two-photon microscopy discriminates between fluorescent and non-fluorescent compounds, the possibilities to distinguish between different molecules are limited. CSLM and two-photon microscopy are essentially imaging techniques, providing information about skin architecture rather than information about molecular composition. The second type of information can be obtained by various spectroscopic techniques. Fluorescence spectroscopy is such a technique, and has recently been used in studies aiming at detection and classification of pathologic tissue³⁰ and effects of aging and UV exposure.^{31;}³² However, the molecular specificity of fluorescence spectroscopy is limited and investigations have been directed at the use of exogenous fluorescent markers to overcome this limitation.^{33; 34}

Molecular specificity without the use of exogenous markers is provided by vibrational spectroscopy: Infrared (IR) spectroscopy and Raman spectroscopy. Vibrational spectroscopy is based on the interaction of light with molecular vibrations. Analysis of the spectrum of the scattered (Raman) or absorbed (IR) light provides very detailed information about the molecular vibrations in the studied material. Such a ‘vibrational spectrum’ is a unique fingerprint for a given molecule and can be used to detect and identify the molecular constituents of a complex sample such as a biological tissue.

1.3 Raman spectroscopy

The Raman effect

When the electric component of light interacts with matter, part of the light will be deflected from the direction of the incident electromagnetic wave. This is referred to as scattering. There are three basic types of light scattering. The dominant type is elastic scattering or Rayleigh scattering, which involves no energy transfer in the scattering event and consequently the scattered light has the same frequency as the incident light. The two other basic types of light scattering are inelastic, which means that energy is transferred in the scattering event and that the scattered light has a frequency different from the incident light. If the frequency of the scattered light is higher than that of the incident light, the process is called Stokes Raman scattering. A decrease of the frequency of the scattered photons is called anti-Stokes Raman scattering.

Scattering of light by a molecule can be described in terms of classical mechanics, in which a molecule is treated as a harmonic oscillator. A molecule can store energy, thereby increasing its internal vibrational motion. This is in analogy with two particles connected by a spring. When the spring is stretched and released, the particles start to oscillate. Vibrational energy can be added to the system, which increases the amplitude of the oscillation.

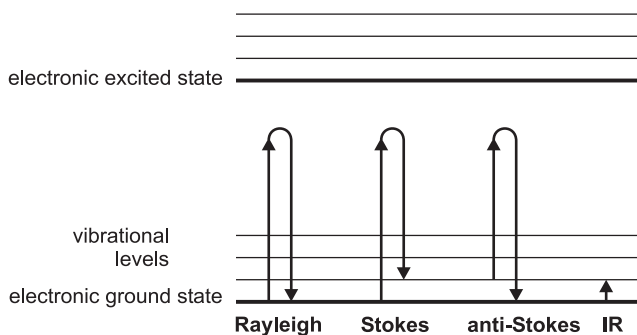


Figure 3. Energy level diagrams showing inelastic scattering (Rayleigh), elastic scattering (Stokes and anti-Stokes) and Infrared absorption (IR).

In the classical-mechanical view, a molecule can increase its vibrational motion upon absorption of electromagnetic energy and decrease its vibrational motion upon dissipation of electromagnetic energy. However, the internal vibrations of a molecule are quantized and can occur only at discrete energies or vibrational states. As a result a molecule can absorb or emit energy in discrete units only, as it changes from one vibrational state to another.

In a Raman scattering event, a change in the vibrational energy of a molecule results in an equal shift of energy of the scattered photon. A decrease of vibrational motion of a molecule adds to the energy of the scattered photon, producing an anti-Stokes shift. Vice versa, an increase of vibrational motion of a molecule is subtracted from the energy of the scattered photon, producing a Stokes shift. In a typical Raman experiment, a sample is irradiated by monochromatic light. The spectrum of light scattered from the sample generally contains a component of elastic scattered light (Rayleigh), together with spectral contributions of inelastic scattered light (Stokes and anti-Stokes), which has several different frequencies. The shifts in energy of the elastic scattered components correspond to vibrational energy levels of the molecules in the irradiated sample. The exact energy needed to excite a molecular vibration depends on the mass of the atoms involved in the vibration and the type of chemical bonds between these atoms. The energy may be influenced by molecular structure, interactions between molecules and the chemical microenvironment of groups of atoms involved in the vibration. Molecules may have a great number of independent vibrational modes ($3N-6$ for a molecule consisting of N atoms), many of which can be excited by a Raman scattering event. This means that a molecule has a unique combination of vibrational levels and that its Raman spectrum is highly molecule specific. Moreover, Raman scattering is a linear process, i.e. the number of Raman scattered photons is directly proportional to the number of irradiated molecules. Hence, the intensity of a Raman band is proportional to the concentration of the respective compound. Therefore the positions, relative intensities and shapes of the bands in a Raman spectrum carry detailed, quantitative information about the molecular composition of a sample and about molecular structures and interactions present.³⁵

Raman Instrumentation

A Raman spectrometer essentially consists of a monochromatic light source, a sample stage and a spectrometer. Upon irradiation of a sample, light is scattered in all directions. Scattered light is collected in the sample stage and directed towards a spectrometer. In the spectrometer the different frequency components contained in the scattered light are separated and recorded to produce a Raman spectrum. Scattered light includes both elastic and Raman scattered components. Since the elastic scattered light is many orders of magnitude more intense than the Raman scattered light, additional filtering is required in order to suppress the elastic component and enable detection of the Raman scattered fraction.

The Raman spectrometer used for the skin studies described in this thesis (figure 1 in chapter 3), was a dispersive CCD-based (Charge Coupled Device) system. Raman signals are relatively weak due to the low efficiency of the Raman scattering process. Therefore, efficient detection of the Raman signal is important, particularly for *in vivo* applications, when long signal collection times are generally not opportune. In a CCD-based spectrometer the different wavelengths of the scattered light are dispersed by an optical grating and projected on a CCD detector. This is essentially a large array of detectors that enables simultaneous recording of a complete Raman spectrum in a single exposure. The resulting detection efficiency is greatly enhanced as compared to the multiplexing Fast-Fourier Transform (FFT) Raman systems that were initially used in Raman investigations of the skin.³⁶

Sufficient spatial resolution in the depth direction is a prerequisite for discriminating between the different skin layers and to study molecular variations within the SC. To this end, the principle of confocal Raman microspectroscopy was applied in the design of a sample stage for *in vivo* investigation of the skin. Raman microspectroscopy exploits the principles of confocal microscopy to obtain spectra from specific regions in a sample. This method has been optimized by Puppels *et al.*, which enabled them to study macromolecules within single living cells and chromosomes.^{37; 38} In the sample stage for skin measurements the laser light is focused via a microscope objective in a small region in the skin. Scattered light that emerges from this irradiated volume is collected by the microscope objective and projected onto the core of an optical fiber. The core of the optical fiber acts as a pinhole and permits only light emerging from the region where the laser light is focused to enter the fiber, whereas light from out-of-focus regions is blocked. The focus from which scattered light is detected and the focus irradiated by the laser coincide, hence the name ‘confocal’.

The light source in our experiments was a titanium-sapphire laser, pumped by an argon-ion laser. This system offered the flexibility of wavelength selection over a wide range. It is however expensive and takes much space. In the near future, small solid-state lasers will be the lasers of choice for Raman systems and it is to be expected that their price will drop rapidly to a fraction of that of the current laser systems.

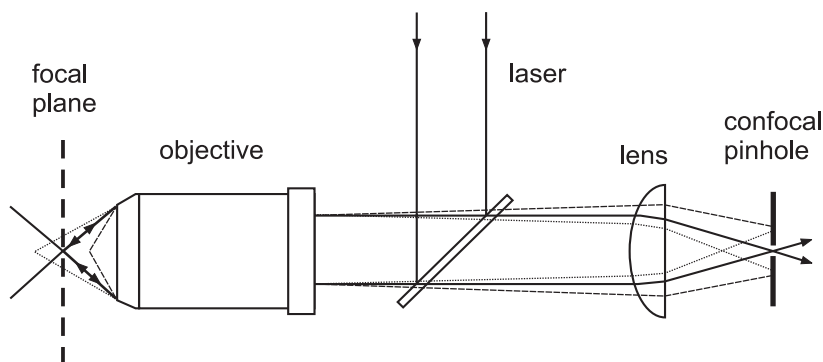


Figure 4. Confocal principle of a Raman microspectrometer. Laser light is focused in the focal plane by a microscope objective. Scattered light is collected by the same microscope objective and projected on a confocal pinhole. Only light emerging from the focal region passes through the pinhole.

1.4 History of Raman spectroscopy

“We are obviously at the fringe of a fascinating new region of experimental research, which promises to throw light on diverse problems relating to radiation and wave theory, X-ray optics, atomic and molecular spectra, fluorescence and scattering, thermodynamics and chemistry. It all remains to be worked out”. The Indian physicist C. V. Raman spoke these words in 1928 in a lecture about a new type of light scattering. Raman and his co-worker K. S. Krishnan had observed that when a liquid sample was irradiated by an intense light source, a fraction of the scattered light had a wavelength different from the wavelengths of the incident light. The shift in wavelength was associated with a change in the rotational and vibrational energy and therefore gave information about the energy levels of the irradiated molecules contributed to the understanding of molecular structure. This phenomenon had been predicted on theoretical grounds five years earlier by Adolf G. Smekal.³⁹ With their publication in *Nature*⁴⁰ Raman and Krishnan were the first to publish experimental evidence for the phenomenon. At the same time in Moscow, G.S Landsberg and L.I. Mandel’shtam had discovered the light scattering phenomenon independently from Raman and Krishnan in Calcutta, but their study was published just a few months after Raman and Krishnan’s.⁴¹ However, the phenomenon was called the ‘Raman effect’ and two years after the discovery Raman was awarded the Nobel Prize for physics.

Interest in the new phenomenon was great and numerous publications devoted to the Raman effect appeared in the first decade after its discovery. Then, after a rapid initial growth, the popularity of Raman spectroscopy as an analytical method declined. The Raman effect is a relatively inefficient process and Raman signals are extremely weak. This required an intense monochromatic light source and sensitive detection equipment, for which spectroscopists at that time used a mercury lamp and photographic paper and exposure times of hours or even days. Because of the technical hurdles and because of the development of Infrared Spectroscopy, which was closely related to Raman spectroscopy

but technically more simple to apply, researchers lost interest in Raman spectroscopy and Infrared Spectroscopy became the dominant technique after the second world war.

Interest in Raman spectroscopy was rekindled after the invention of the laser in the 1960's. The laser was a powerful, highly monochromatic light source that could easily be focused, enabling irradiation of a sample with high intensity. Another step forward was the development of electronic measuring devices such as photomultiplier tubes and photodiode arrays, which provided sensitive detectors for the relatively weak Raman signals. Tedious work with photographic film and extremely long exposure times could now be abandoned. Today, Raman spectroscopy is a well-established technique with widespread application in many fields. Particularly, with ever continuing developments in small lasers, sensitive detection equipment and fast computers, the technique is entering the clinical realm.

1.5 This thesis

The number of noninvasive research methods to study the molecular composition of the skin is limited. Existing methods lack either the spatial resolution or the molecular specificity to enable investigation of the presence and distribution molecular compounds in the stratum corneum, without interfering with the studied skin area. The objective of the work described in this thesis was to develop a method based on confocal Raman spectroscopy as a noninvasive technique for qualitative and quantitative analysis of the molecular composition of the human skin and the stratum corneum in particular.

Chapter 2 describes the exploratory work that served as the basis for the development of *in vivo* confocal Raman spectroscopy of human skin. In this study *in vitro* Raman spectra of microtomed cross sections of human skin were measured. Distinct Raman signals of the SC, viable epidermis and dermis provided insight into the differences in molecular composition between the different skin layers. A Raman instrument for rapid collection of *in vivo* Raman spectra of the skin was developed. Spectra were recorded from several locations on the arms and hands. It was shown that Raman spectra could be recorded *in vivo* from different layers of the skin. Variations in the Raman spectra obtained from different skin sites could be qualitatively explained, based on variations of the concentrations of six of the major constituents of NMF.

In chapter 3 the framework that had established in the previous chapter is filled in. *In vivo* confocal Raman spectroscopy is presented as a method to measure molecular concentration profiles in the skin. It is demonstrated that the method can be used to determine the water concentration in the SC as a function of distance to the skin surface and *in vivo* water concentration profiles have been determined for the arm and the thenar. The distribution of NMF in the SC was investigated by determining concentration profiles of NMF constituents. This experiment provided *in vivo* evidence that NMF is formed in the lower part of the SC.

Chapter 4 describes an improved design of the Raman instrument for rapid, automated recording of water concentration profiles in the skin. The application was demonstrated by recording water concentration profiles before and after thorough hydration of the skin, which considerably increased the water content in the SC.

In chapter 5 the possibility is probed to use Raman spectroscopy for monitoring of topically applied substances. A small dose of the penetration enhancer dimethyl sulfoxide (DMSO) was applied to the skin and concentration profiles were measured in order to monitor the distribution of DMSO as a function of depth and time. DMSO could still be detected for up to 72 hours after application.

Chapter 6 describes the realization of the plans that had been proposed earlier in chapter 4: the combination of *in vivo* confocal Raman spectroscopy with an imaging technique. This chapter describes a combined confocal Raman microspectrometer with a confocal scanning laser microscope, enabling simultaneous spectroscopic examination and imaging of skin morphology *in vivo*, which allows direct comparison of molecular composition with skin architecture. For instance, *in vivo* concentration profiles of water and NMF were determined and cross sectional images were recorded simultaneously, showing the precise location of the measured profiles. Also the possibility to target specific skin structures (sweat ducts, sebaceous units and capillary loops, for instance) and to study their molecular compositions was demonstrated.

In chapter 7 a general conclusion is drawn from the work described in this thesis and the prospects of *in vivo* confocal Raman microspectroscopy for fundamental skin research and its application in clinical dermatology are discussed.

References

1. Odland, G. F. 1991. Structure of the skin. *In* Physiology, Biochemistry and molecular Biology of the Skin. L. A. Goldsmith, editor. Oxford University Press, New York. 3-62.
2. Jakubovic, H. R., and A. B. Ackerman. 1992. Structure and function of skin: development, morphology, and physiology. *In* Dermatology. S. L. Moschella and H. J. Hurley, editors. W. B. Saunders company, Philadelphia. 3-87.
3. Bowden, P. E. 1993. Keratins and other epidermal proteins. *In* Molecular aspects of dermatology. G. C. Priestley, editor. John Wiley & Sons, Chichester. 3-62.
4. Baden, H. P., L. A. Goldsmith, and L. Bonar. 1973. Conformational changes in the -fibrous protein of epidermis. *J Invest Dermatol.* 60:215-8.
5. Anigbogu, A. N. C., A. C. Williams, B. W. Barry, and H. G. M. Edwards. 1995. Fourier transform Raman spectroscopy of interactions between the penetration enhancer dimethyl sulfoxide and human stratum corneum. *Int J Pharm.* 125:265-282.
6. Wertz, P. W., and D. T. Downing. 1991. Epidermal lipids. *In* Physiology, Biochemistry and molecular Biology of the Skin. L. A. Goldsmith, editor. Oxford University Press, New York. 205-236.
7. Warner, R. R., M. C. Myers, and D. A. Taylor. 1988. Electron probe analysis of human skin: determination of the water concentration profile. *J Invest Dermatol.* 90:218-24.

8. von Zglinicki, T., M. Lindberg, G. M. Roomans, and B. Forslind. 1993. Water and ion distribution profiles in human skin. *Acta Derm Venereol.* 73:340-3.
9. Blank, I. H. 1952. Factors which influence the water content of the stratum corneum. *J Invest Dermatol.* 18:433-440.
10. Harding, C. R., A. Watkinson, and A. V. Rawlings. 2000. Dry skin, moisturization and corneodesmolysis. *Int J Cosmet Science.* 22:21-52.
11. Jemec, G. B., and J. Serup. 1992. Scaling, dry skin and gender. A bioengineering study of dry skin. *Acta Derm Venereol Suppl.* 177:26-8.
12. Linde, Y. W. 1992. Dry skin in atopic dermatitis. *Acta Derm Venereol Suppl.* 177:9-13.
13. Loden, M. 1995. Biophysical properties of dry atopic and normal skin with special reference to effects of skin care products. *Acta Derm Venereol Suppl (Stockh).* 192:1-48.
14. Lademann, J., H. Weigmann, C. Rickmeyer, H. Barthelmes, H. Schaefer, G. Mueller, and W. Sterry. 1999. Penetration of titanium dioxide microparticles in a sunscreen formulation into the horny layer and the follicular orifice. *Skin Pharmacol Appl Skin Physiol.* 12:247-56.
15. Weigmann, H., J. Lademann, H. Meffert, H. Schaefer, and W. Sterry. 1999. Determination of the horny layer profile by tape stripping in combination with optical spectroscopy in the visible range as a prerequisite to quantify percutaneous absorption. *Skin Pharmacol Appl Skin Physiol.* 12:34-45.
16. Pilgram, G. S., A. M. Van Pelt, F. Spies, J. A. Bouwstra, and H. K. Koerten. 1998. Cryo-electron diffraction as a tool to study local variations in the lipid organization of human stratum corneum. *J Microsc.* 189:71-8.
17. Pratzel, H., and P. Fries. 1977. Modification of relative amount of free amino acids in the stratum corneum of human epidermis by special factors of the environment. I. The influence of UV-irradiation (author's transl). *Arch Dermatol Res.* 259:157-60.
18. Weigmann, H., J. Lademann, R. v Pelchrzim, W. Sterry, T. Hagemester, R. Molzahn, M. Schaefer, M. Lindscheid, H. Schaefer, and V. P. Shah. 1999. Bioavailability of clobetasol propionate-quantification of drug concentrations in the stratum corneum by dermatopharmacokinetics using tape stripping. *Skin Pharmacol Appl Skin Physiol.* 12:46-53.
19. Pirola, R., S. R. Bareggi, and G. De Benedittis. 1998. Determination of acetylsalicylic acid and salicylic acid in skin and plasma by high-performance liquid chromatography. *J Chromatogr B Biomed Sci Appl.* 705:309-15.
20. Alberti, I., Y. N. Kalia, A. Naik, J. D. Bonny, and R. H. Guy. 2001. In vivo assessment of enhanced topical delivery of terbinafine to human stratum corneum. *J Control Release.* 71:319-27.
21. Öhman, H., and A. Vahlquist. 1994. In vivo studies concerning a pH gradient in human stratum corneum and upper epidermis. *Acta Derm Venereol.* 74:375-9.
22. Rawlings, A. V., I. R. Scott, C. R. Harding, and P. A. Bowser. 1994. Stratum corneum moisturization at the molecular level. *J Invest Dermatol.* 103:731-741.
23. Potts, R. O., D. B. Guzek, R. R. Harris, and J. E. McKie. 1985. A noninvasive, in vivo technique to quantitatively measure water concentration of the stratum corneum using attenuated total-reflectance infrared spectroscopy. *Arch Dermatol Res.* 277:489-495.
24. Bommannan, D., R. O. Potts, and R. H. Guy. 1990. Examination of stratum corneum barrier function in vivo by infrared spectroscopy. *J Invest Dermatol.* 95:403-8.
25. Brancaleon, L., M. P. Bamberg, T. Sakamaki, and N. Kollias. 2001. Attenuated total reflection-Fourier transform infrared spectroscopy as a possible method to investigate biophysical parameters of stratum corneum in vivo. *J Invest Dermatol.* 116:380-6.

26. van der Molen, R. G., F. Spies, J. M. van 't Noordende, E. Boelsma, A. M. Mommaas, and H. K. Koerten. 1997. Tape stripping of human stratum corneum yields cell layers that originate from various depths because of furrows in the skin. *Arch Dermatol Res.* 289:514-8.
27. Richard, S., B. Querleux, J. Bittoun, I. Idy-Peretti, O. Jolivet, E. Cermakova, and J. L. Leveque. 1991. In vivo proton relaxation times analysis of the skin layers by magnetic resonance imaging. *J Invest Dermatol.* 97:120-5.
28. Masters, B. R., P. T. So, and E. Gratton. 1998. Multiphoton excitation microscopy of in vivo human skin. Functional and morphological optical biopsy based on three-dimensional imaging, lifetime measurements and fluorescence spectroscopy. *Ann N Y Acad Sci.* 838:58-67.
29. Hendriks, R. F. M., and G. W. Lucassen. 2001. Two-photon fluorescence and confocal video microscopy of in-vivo human skin. In *Multiphoton microscopy in biomedical sciences*. A. Periasamy and P. T. So, editors. SPIE, San Jose, CA. 287-293.
30. Wagenieres, G. A., W. M. Star, and B. C. Wilson. 1998. In vivo fluorescence spectroscopy and imaging for oncological applications. *Photochem Photobiol.* 68:603-632.
31. Brancalion, L., G. Lin, and N. Kollias. 1999. The in vivo fluorescence of tryptophan moieties in human skin increases with UV exposure and is a marker for epidermal proliferation. *J Invest Dermatol.* 113:977-82.
32. Kollias, N., R. Gillies, M. Moran, I. E. Kochevar, and R. R. Anderson. 1998. Endogenous skin fluorescence includes bands that may serve as quantitative markers of aging and photoaging. *J Invest Dermatol.* 111:776-80.
33. Wennberg, A. M., F. Gudmundson, B. Stenquist, A. Ternesten, L. Molne, A. Rosen, and O. Larko. 1999. In vivo detection of basal cell carcinoma using imaging spectroscopy. *Acta Derm Venereol.* 79:54-61.
34. Svanberg, K., I. Wang, S. Colleen, I. Idvall, C. Ingvar, R. Rydell, D. Jocham, H. Diddens, S. Bown, G. Gregory, S. Montan, S. Andersson-Engels, and S. Svanberg. 1998. Clinical multi-colour fluorescence imaging of malignant tumours-- initial experience. *Acta Radiol.* 39:2-9.
35. Koningstein, J. A. 1971. Introduction to the theory of the Raman effect. D. Reidel Publishing Company, Dordrecht.
36. Barry, B. W., H. G. M. Edwards, and A. C. Williams. 1992. Fourier Transform Raman and infrared vibrational study of human skin: assignment of spectral bands. *J Raman Spectroscopy.* 23:641-645.
37. Puppels, G. J., M. van Rooijen, C. Otto, and J. Greve. 1993. Confocal Raman Microspectroscopy. In *Fluorescent and luminescent probes for biological activity*. W. T. Mason, editor. Academic Press, San Diego. 237-258.
38. Puppels, G. J., F. F. M. de Mul, C. Otto, J. Greve, M. Robert-Nicoud, D. J. Arndt-Jovin, and T. M. Jovin. 1990. Studying single living cells and chromosomes by confocal Raman microscopy. *Nature.* 347:301-303.
39. Smekal, A. 1923. Zur Quantentheorie der Dispersion. *Naturwissenschaften.* 11:873-875.
40. Raman, C. V., and K. S. Krishnan. 1928. A new type of secondary radiation. *Nature.* 121:501-502.
41. Landsberg, G. S., and L. I. Mandelshtam. 1928. *Naturwissenschaften.* 16:557.

In vitro and in vivo Raman spectroscopy of human skin

Biospectroscopy
1998, 4: S31-S39

Chapter

2

P.J. Caspers
G.W. Lucassen
R. Wolthuis
H.A. Bruining
G.J. Puppels

Abstract

Noninvasive techniques that provide detailed information about molecular composition, structure, and interactions are crucial to further our understanding of the relation between skin disease and biochemical changes in the skin, as well as for the development of penetration enhancers for transdermal drug administration. In this study we present *in vitro* and *in vivo* Raman spectra of human skin. Using a Raman microspectrometer, *in vitro* spectra were obtained of thin cross sections of human skin. They provided insight into the molecular composition of different skin layers. Evidence was found for the existence of a large variation in lipid content of the stratum corneum. A simple experimental setup for *in vivo* confocal Raman microspectroscopy of the skin was developed. *In vivo* Raman spectra of the stratum corneum were obtained at different positions of the arm and hand of three volunteers. They provided evidence for differences in the concentration of natural moisturizing factor at these positions.

Introduction

The skin is a highly heterogeneous tissue composed of layers that differ in morphology and molecular composition. Conventionally the skin is divided in two major layers, the dermis and epidermis. The dermis is the inner layer that varies in thickness from 1 to 4 mm. It is largely composed of collagens (primarily types I and III), which represent approximately 75% of the dry weight of the dermis. On top of the dermis lies the epidermis, which varies in thickness from 40 μm in the eyelids to more than 1 mm on the palms. This stratified epithelium primarily consists of cornifying cells called *keratinocytes*. Of particular interest is the stratum corneum or horny layer, which forms the outermost layer of the epidermis. It consists of flat terminally differentiated keratinocytes embedded in a matrix of lamellar lipids.^{1, 2} The water barrier function and the cellular water-binding capability of the stratum corneum are crucial for healthy skin. Therefore, the medical and pharmaceutical implications of a better understanding of these mechanisms in the stratum corneum are considerable.

Raman spectroscopy is a nondestructive technique with a wide range of possible applications in the field of biomedical research. Because the technique can be used noninvasively, it is of particular interest to skin research. For example, it has been demonstrated that changes in molecular structure and composition as a result of disease are reflected in the Raman spectra.³⁻⁵ Moreover, because clinical disease symptoms are preceded by molecular changes, this technique could prove valuable for an early, *in vivo* diagnosis of a large class of skin diseases. Another field of interest is skin permeability. Human skin is a highly effective barrier to water, chemicals, and microbes. This also limits transdermal drug administration. The structure and composition of stratum corneum lipids are recognized as playing a dominant role in this barrier function of the skin. Considerable effort has been undertaken to elucidate the mechanisms involved in this barrier function, using techniques such as X-ray diffraction and electron microscopy.⁶⁻⁸ Raman spectroscopy could play an important complementary role in this line of research.

Raman and Infrared (IR) spectroscopy are complementary techniques. However, Raman spectroscopy has certain advantages, such as its relative insensitivity to water, that justify its increasing popularity for skin characterization.⁹ In previous studies Fourier Transform (FT) Raman spectroscopy was used *in vitro* to study the isolated stratum corneum of human, mammalian and reptilian skin,⁹⁻¹⁶ the structure of stratum corneum lipids,¹⁷ and the effects of the penetration enhancer dimethyl sulfoxide on the structure of stratum corneum lipids and proteins.¹⁸ In other *in vitro* studies abnormalities were reported in the Raman spectra of malignant and benign skin lesions, and differences were observed between Raman spectra of basal cell carcinoma and normal skin.^{4, 5} Most Raman spectroscopic studies of the horny layer were performed on isolated stratum corneum by using harsh chemical and physical methods to separate this membrane from the skin.¹² These methods may cause artifacts due to changes in the molecular structure and composition during sample preparation. FTIR was also applied *in vivo* on human stratum corneum.^{19, 20} The use of attenuated total reflectance FTIR spectroscopy, however, is limited to the upper few microns of the stratum corneum because of the limited penetration depth of mid- and far-IR

light in skin. Near-IR light can penetrate deeper into the skin. An *in vivo* FT-Raman spectrum was published by Williams *et al.*¹² showing signal contributions of collagen. Shim and Wilson²¹ used fiber optic probes to obtain *in vivo* Raman spectra of the skin. The use of fiber optics will be essential in the development of clinical applications. However, signal to noise levels that are achieved are still rather low, and the particular probe used by Shim and Wilson would not enable a separation of signal contributions from different skin layers, as was also the case in the FT-Raman experiment mentioned above.

The aim of this study was to develop a methodology that would enable the recording of Raman spectra of various skin layers *in vivo* in order to obtain information about the molecular composition and molecular structure. In preparation for this work Raman spectra of different skin layers were recorded *in vitro*. Raman spectra are presented of the stratum corneum, the epidermis below the stratum corneum, and the dermis. These were obtained from unfixed thin sections of skin, prepared at -20°C with a microtome. The use of frozen sections has the advantage that the different skin layers can be studied without the need for chemical and physical treatments of the skin sample to separate the layers. A confocal Raman design was developed that enabled rapid *in vivo* collection of Raman spectra directly from the skin. *In vivo* spectra were obtained for different skin layers and for the stratum corneum at different anatomical regions.

Materials and Methods

Sample preparation

Skin samples for *in vitro* measurements were obtained from female breast biopsies, which were performed during breast reduction surgery. Immediately after excision the samples were put in a capsule and frozen in isopentane cooled with liquid nitrogen. Cross sections of 6- and 20- μm thickness were cut with a microtome at -20°C and the frozen sections were stored at -80°C until use. One sample of male abdominal skin was obtained *post mortem*. Before the measurements the samples were thawed at 0°C and subsequently acclimatized for several hours at room temperature and 100% humidity. Multiple thin sections were cut for the *in vitro* experiments. For each of the unstained sections used in Raman experiments, a consecutive section was stained with hematoxylin and eosin. The stained sections were used as a reference to locate the boundaries between the different skin layers in the unstained sections. Biochemical compounds were purchased from Sigma-Aldrich and used in the Raman experiments without further purification.

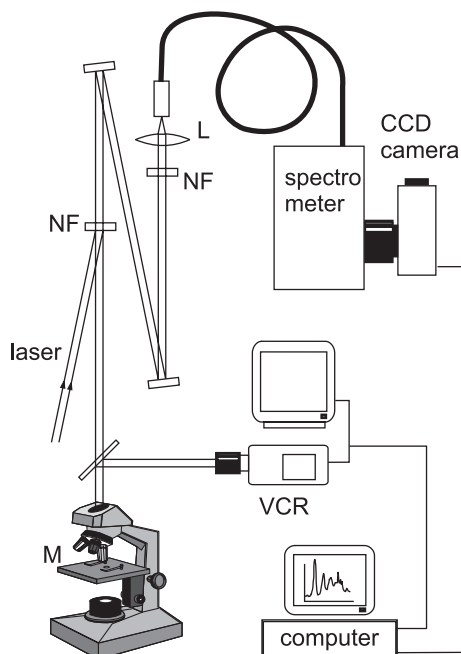


Figure 1 Confocal Raman microspectrometer. NF, notch filter; L, lens; M, microscope.

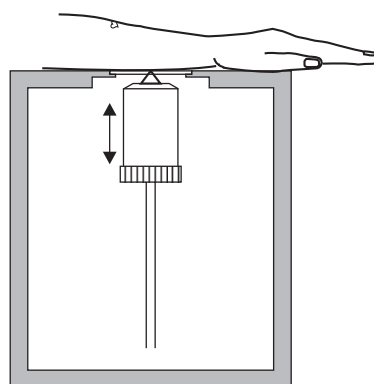


Figure 2 Inverted microscope used for *in vivo* measurements.

In vitro Raman spectroscopy

Samples were placed under a microscope (Leitz) interfaced to a confocal Raman microspectrometer that was built in-house (figure 1). A microscope objective (MIR Plan 80x /0.75, Olympus) was used to focus the laser light on the sample and to collect scattered light. The collected light was filtered through a holographic notch filter with an optical density of >6 (Kaiser Optical Systems, Inc., Ann Arbor, MI) and was focused through an NIR-coated achromat onto an optical fiber. The fiber (100 μm core diameter) was connected to an F/#2.1 spectrograph (holographic grating, 1200 lines/mm). The spectra were recorded with a back-illuminated, deep depletion CCD camera containing 1024 x 256 pixels (Princeton Instruments, Trenton, NJ) and cooled with liquid nitrogen to -70°C . A tunable titanium sapphire laser (model 3900S, Spectra-Physics, Mountain View, CA), pumped with an argon ion laser (model 2020, Spectra-Physics), was employed to illuminate the sample. The laser wavelength and power on the sample were 850 nm and 100 mW, respectively. A video image of the sample was used for accurate positioning of the laser spot on the sample. The spectra were corrected for the wavelength dependence of the setup's signal detection efficiency.^{21, 22} Wavenumber calibration of the spectra was carried out using the following compounds as the Raman calibration standards: 4-acetamidophenol, γ -caprolactone and succinic anhydride. The spectra of these compounds

were recorded on two FT-Raman instruments in different laboratories at 1 cm^{-1} resolution. Peak positions in these experiments were found to be in agreement within 1 cm^{-1} and were used for wavenumber calibration in the experiments described here.

The skin spectra were recorded from unstained tissue sections. Signal contributions of the substrate (quartz or glass) were subtracted. The spectra of human collagen type I and ceramide type III were measured in the dry state. Solutions of serine, pyrrolidone-5-carboxylic acid (PCA), citrulline, and glycine were prepared in a phosphate buffered solution at pH 5.5, which is the normal skin pH.²³ Urocanic acid was measured at pH 4 to facilitate solvation. The signal contribution of the buffer solution was measured separately, and subtracted from the spectra.

In vivo Raman spectroscopy

For the *in vivo* measurements, the microscope stage was replaced by a custom built unit that served essentially as an inverted microscope (figure 2). The skin region of interest was positioned onto a CaF_2 window, which was mounted horizontally in an aluminum stage. CaF_2 is an excellent material for sample support in Raman experiments because of its low scattering cross section and the presence of only one Raman band at 320 cm^{-1} . The laser light was focused in the skin through the CaF_2 window using a microscope objective (Plan Fluotar 63x /0.70, Leica). In this way movements of the skin relative to the microscope objective were minimized. By translating the objective vertically, the depth at which the laser was focused in the skin could be varied. A confocal detection scheme was employed. A useful measure for the axial resolution of the microspectrometer is the full width at half maximum (FWHM) of the depth response for planar objects. In the present (not yet fully optimized) setup the FWHM was up to $9\text{ }\mu\text{m}$. This depth response was determined by moving a thin silicon layer ($<1\text{ }\mu\text{m}$) through the laser focus along the optical axis while the Raman intensity of the intense silicon peak at 521 cm^{-1} was recorded as a function of the distance to the focal plane.

In vivo measurements were performed on three male volunteers (26-29 years of age). Measurements were performed at the volar aspect (i.e., the inner side) of the forearm, the dorsal side of the middle finger, the fingertip of the index finger, and the thenar (i.e., the ball of the palm). Before each measurement the skin was cleaned with a single wipe of tissue soaked in 97% ethanol.

Results

Figure 3 displays Raman spectra of the stratum corneum, epidermis, and dermis obtained *in vitro* from an unfixed and unstained skin section of $6\text{ }\mu\text{m}$ thickness. The spectra shown are averages of a number of measurements at different positions in a layer. No visual or spectral changes could be observed during the measurements, which would indicate degradation or heating of the sample. Note the similarity of the dermis spectrum with the spectrum of pure collagen (figure 3, lines C, D). Samples from three donors revealed interpersonal variation related to lipid contents.

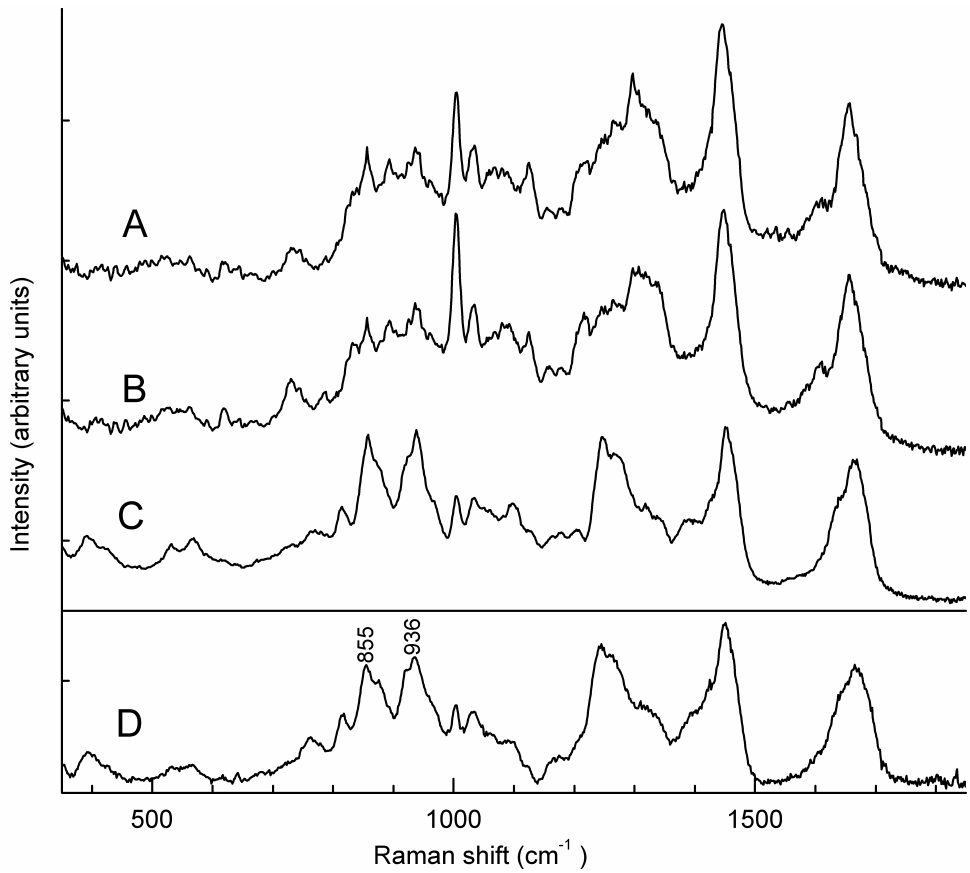


Figure 3 *In vitro* Raman spectra of different skin layers. (A) Stratum corneum, an average of six spectra; (B) epidermis, an average of four spectra; (C) dermis, an average of four spectra; (D) is human collagen type I. Objective 80 x /0.75. Excitation wavelength 850 nm, power 100 mW, measuring time 60 s. Note the resemblance of C and D.

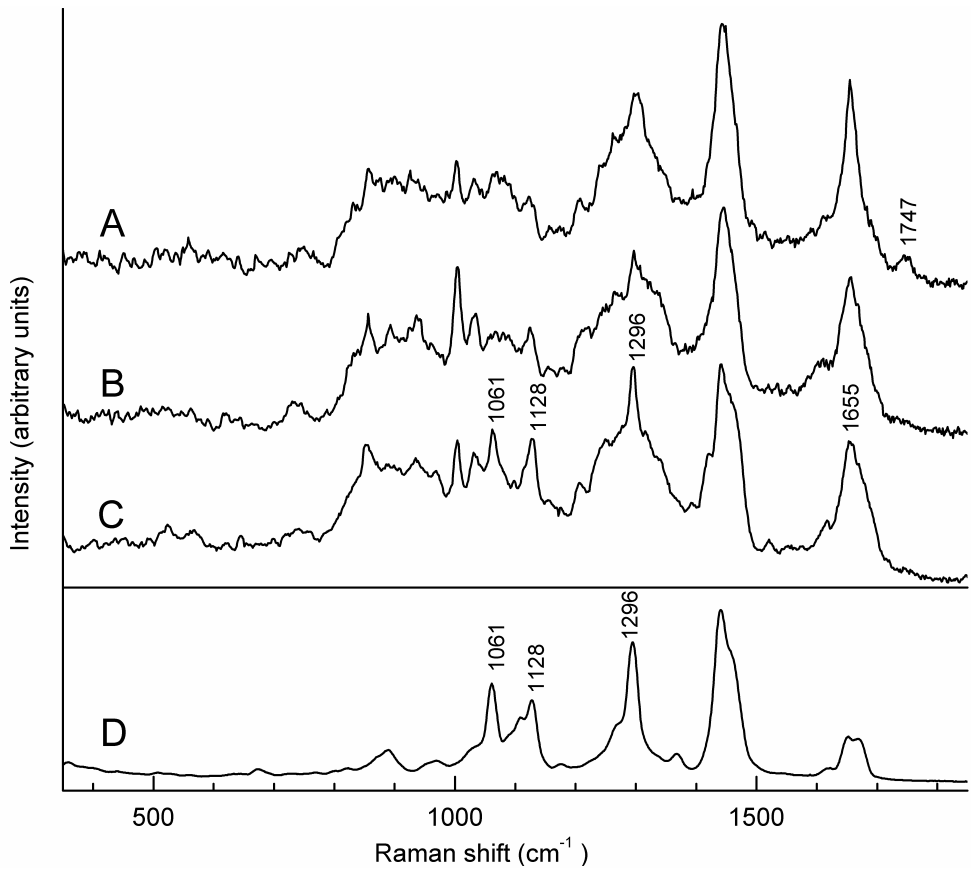


Figure 4 *In vitro* Raman spectra of the stratum corneum of three different donors. (A) Male abdominal skin obtained *post mortem*; (B, C) female breast biopsies; (D) pure ceramide.

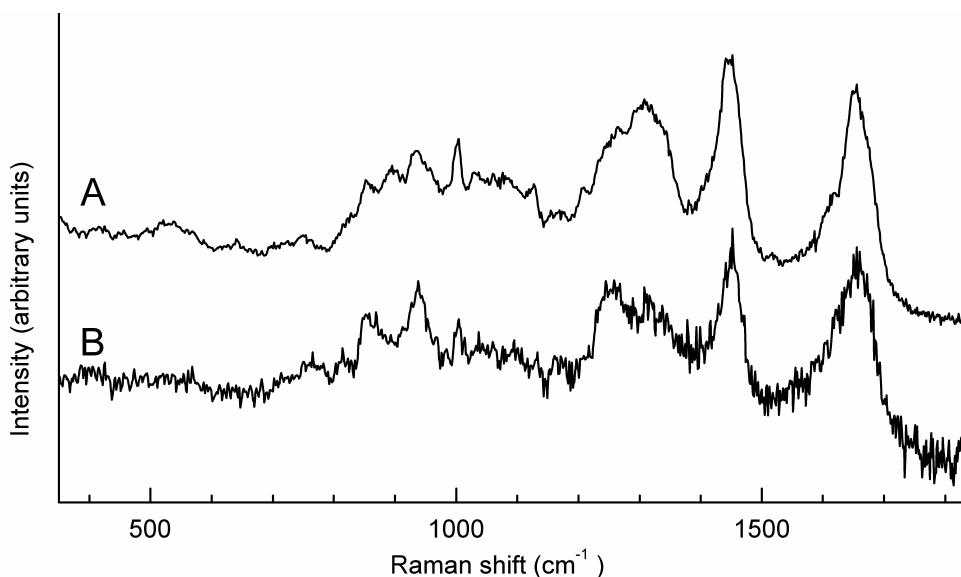


Figure 5 *In vivo* Raman spectra of different skin layers. (A) Stratum corneum at 0 μm depth; (B) dermis at ~ 85 μm depth. Objective 63 x /0.70. Excitation wavelength 850 nm, power 100 mW, measuring time 120 s.

This is demonstrated in figure 4, which shows the *in vitro* spectra of the stratum corneum of the different donors. *In vivo* Raman spectra were obtained from different skin layers and anatomical regions. Figure 5 displays Raman spectra of the volar aspect of the forearm. Spectrum A was measured at the skin surface, whereas spectrum B was measured with the laser focus ~ 85 μm below the surface. Raman spectra of the stratum corneum at different anatomical regions are shown in figure 6. The spectra were taken from the fingertip of the index finger, the thenar, the dorsal side of the middle finger, and the volar aspect of the forearm. This selection was based on the consideration that these regions were easily accessible with our present setup and that the thickness and functionality of the stratum corneum varies widely among these regions. For example, the stratum corneum at the volar aspect of the arm is very thin (~ 10 - 15 μm) whereas the stratum corneum of the fingertips is much thicker, owing to the high frictional forces it has to withstand.

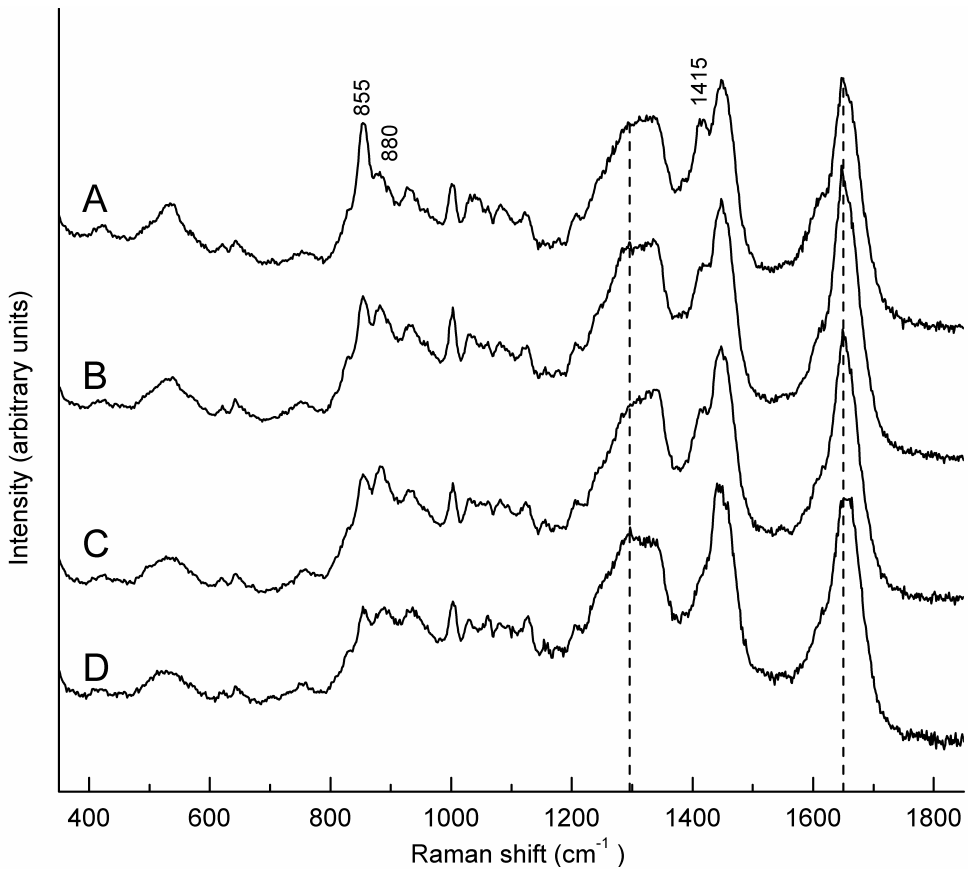


Figure 6 *In vivo* Raman spectra of stratum corneum at different anatomical regions, measured at the skin surface. The spectra are from a single person: (A) fingertip; (B) thenar; (C) dorsal surface of the middle finger; (D) volar aspect of the forearm. Spectrum A was measured in 180 s, all other spectra in 120 s. Objective 63 x /0.70. Excitation wavelength 850 nm, power 100 mW.

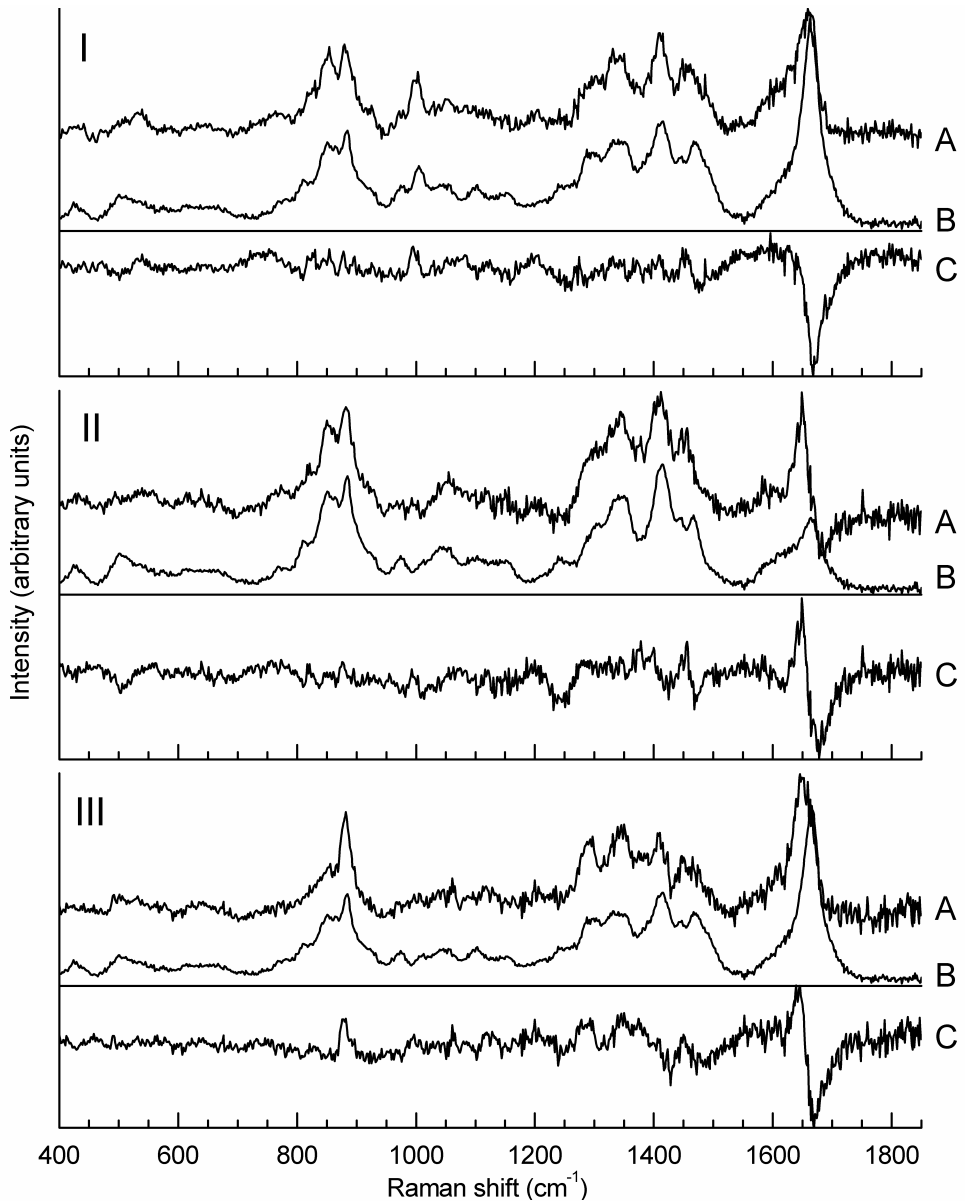


Figure 7 Difference spectra between the stratum corneum at the dorsal surface of the finger and the volar aspect of the forearm of subjects I, II and III. The difference spectra are marked A, the multiple regression fit with spectra of the major amino acid constituents of NMF are marked B, and the residuals are marked C. Spectra B are composed of the spectra of serine, PCA, glycine, citrulline, UCA and urea (see also Fig. 8). The residual spectra C are plotted on the same scale as A and B.

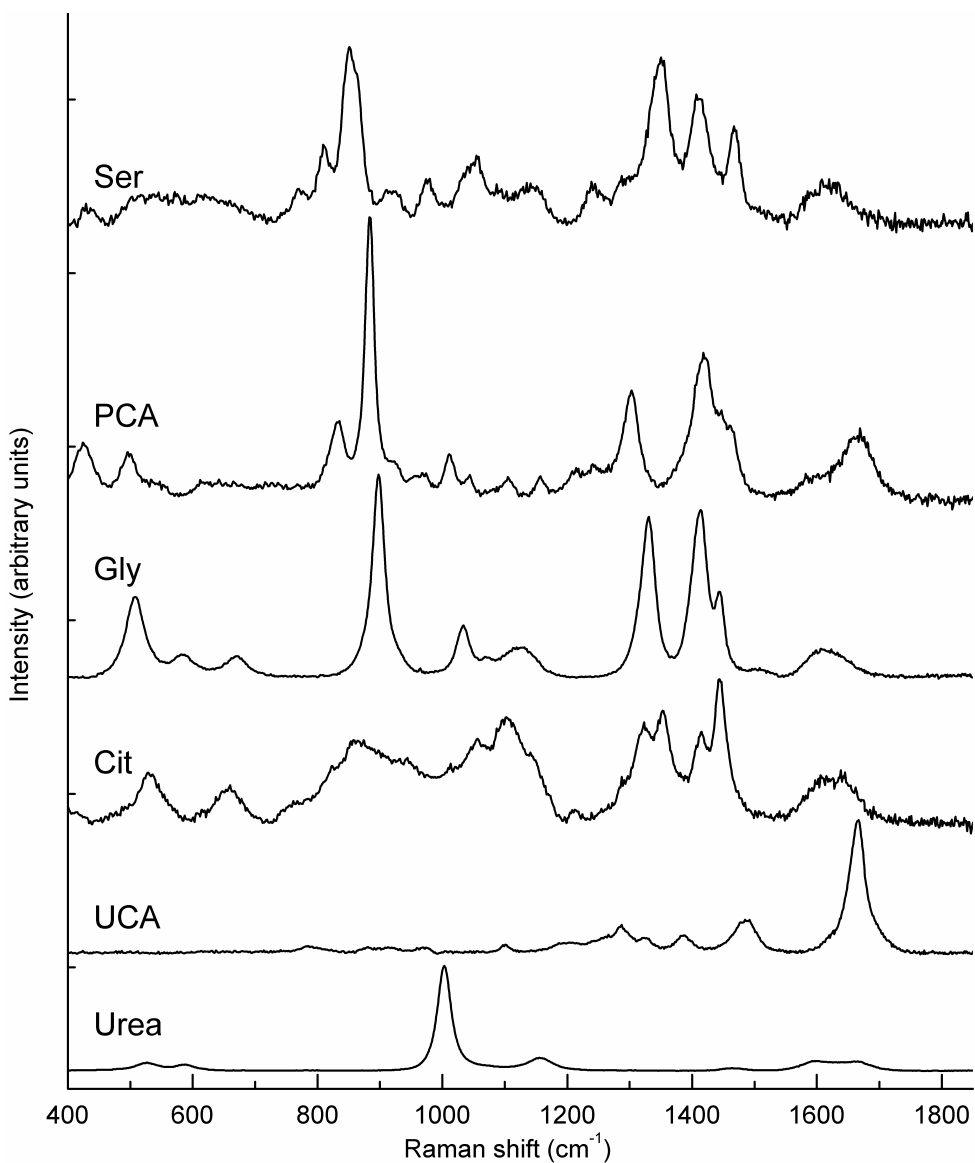


Figure 8 Raman spectra of the major amino acid constituents of NMF and urea. The spectra were measured in a phosphate buffer solution at pH 5.5 (pH 4 for UCA). Signal contributions from the buffer solution were subtracted.

Figure 7 displays the difference spectra calculated from the spectra obtained from the stratum corneum of the dorsal surface of the finger and of the volar aspect of the forearm for three individuals. For each individual, two to six recordings from each region were averaged. The difference spectra for the three individuals were calculated using multiple regression fits. In each multiple regression model, the spectrum from the dorsal surface of the finger was set as the dependent variable. The spectrum from the forearm was set as an

independent variable, together with spectra of ceramide type III (figure 4 D), serine (Ser), PCA, glycine (Gly), citrulline (Cit), UCA, and urea (figure 8). The amino acids and amino acid derivatives mentioned above have been reported to be the major constituents of human natural moisturizing factor (NMF).²⁴⁻²⁶ Table 1 presents an overview of the regression coefficients that were found, normalized with respect to the regression coefficients found for one individual (case 1). The signal contributions of ceramide were subtracted from the difference spectra shown in figure 7 to highlight the differences due to NMF constituents.

Table 1 Relative amounts of NMF compounds, ceramide and urea resulting from multiple regression fit.

	Case 1	Case 2	Case 3
Serine	1	0.81	0.90
PCA	1	1.04	0.93
Glycine	1	0.94	1.24
Citrulline	1	1.04	0.60
Urocanic acid	1	1.33	0.26
Urea	1	0.11	-0.38
Ceramide III	1	1.33	0.26

The factors are normalized to unit values of one person (case 1).

Discussion

Using a confocal detection scheme, rapid *in vitro* and *in vivo* acquisition of Raman spectra of skin is possible. The spectra show much detail and could be obtained with ample signal to noise. The excitation wavelength of 850 nm is sufficiently long to avoid interference from tissue fluorescence.

In vitro spectra of cross sections of human skin show clear differences between the different skin layers (figure 3). The Raman spectrum of the dermis almost completely consists of collagen signal. This is in accordance with the known fact that collagen makes up about 75% of the dry weight and 90% of the total protein content of the dermis.² Assignments of most of the Raman bands of collagen were presented by Frushour and Koenig.²⁷ Typical features in the collagen spectrum are two intense bands around 855 and 936 cm^{-1} . These bands originate from the amino acid side chain vibrations of proline and hydroxyproline, as well as from a $\nu(\text{C-C})$ vibration of the collagen backbone. Proline and hydroxyproline make up about one-fourth of the amino acids in collagen, which is much higher than in most other proteins. The dermis incorporates different types of collagen. About 80% of the total collagen in normal adult skin is type I, 15% is type III and 5% is types IV-VI.² Determination of collagen composition by means of Raman spectroscopy is a subject under investigation.

Most of the Raman bands in the stratum corneum spectrum (figure 3 A) are in agreement with results obtained from FT-Raman measurements on isolated stratum corneum.⁹⁻¹² The stratum corneum spectra are dominated by contributions from keratin and lipids. The position of the amide I band at 1655 cm^{-1} indicates that keratin in human stratum corneum adopts predominantly an α -helical conformation.^{18, 28} One of the most striking differences between the spectra of the stratum corneum and the underlying epidermis is the contribution of lipids, observed at 1061 , 1128 and 1296 cm^{-1} (figure 4). The first two bands were identified as originating from stratum corneum lipids by a method of extensive lipid extraction.¹⁸ All three bands are strong features in the Raman spectrum of ceramide (figure 4 D), which represents the most abundant class of stratum corneum lipids.^{6, 17} Therefore, it is likely that ceramide is the main source of the lipid signal contribution in the Raman spectrum of the stratum corneum.

Large differences in lipid content were observed between the stratum corneum of different individuals. This is illustrated in figure 4 that shows *in vitro* Raman spectra of the stratum corneum from three different donors, together with a spectrum of pure ceramide. The signal contribution of ceramide to spectrum C in figure 4 is remarkably high when compared to spectra A and B. Another interesting feature in spectrum C is the intensity of the bands at 1061 and 1128 cm^{-1} relative to the intensity at 1080 cm^{-1} . The former two are attributed to the all-trans conformation (gel phase) of the acyl backbone in lipids whereas the latter is due to mainly the gauche conformation (liquid crystal phase).²⁸ Apparently the acyl chains of ceramides in stratum corneum predominantly adopt the trans conformation. This observation illustrates the capability of Raman spectroscopy to provide information about the structure and composition of stratum corneum lipids. Spectrum A displays a small peak at 1747 cm^{-1} , which is absent from spectra B and C (figure 4). This peak is attributed to a $\nu(\text{C}=\text{O})$ ester vibration, which is abundantly present in triglycerides. Normally, triglycerides are not present in the stratum corneum. They are however, abundantly present in sebum and subcutaneous tissue. The presence of this peak in one of the stratum corneum spectra is therefore likely due to sebaceous or subcutaneous contamination, which might have occurred during excision of the tissue.

In vivo results

Figure 5 (spectrum A) is largely similar to the *in vitro* spectrum of the stratum corneum (figure 4). Some clear differences are observed in the $850\text{-}940\text{ cm}^{-1}$ region. The precise origin of these differences remains to be elucidated. Spectrum B was obtained after translating the microscope objective $50\text{ }\mu\text{m}$ toward the skin surface. The actual location of the laser focus is determined by the displacement and the numerical aperture of the objective, as well as by the refractive indices of CaF_2 and the stratum corneum (both ~ 1.4). It can be calculated²⁹ that in this case the laser focus was located at approximately $85\text{ }\mu\text{m}$ below the skin surface. The spectrum closely resembles the spectrum of collagen, which is the dominant protein in the dermis. Therefore, it can be concluded that the Raman signal originates predominantly from the dermis, which is also evident from a comparison with the *in vitro* spectrum of the dermis (figure 3C). When compared to the spectrum of the stratum corneum, the dermis spectrum has a strongly decreased signal to noise ratio due to

scattering in the highly turbid skin tissue. Nevertheless, these results clearly illustrate that different skin layers can be studied separately by means of in vivo Raman microspectroscopy. Remarkable differences were observed between spectra of the stratum corneum obtained from different anatomical regions. *In vivo* spectra of the stratum corneum of volar forearm, fingertip of the index finger, dorsal side of the middle finger and thenar are presented in figure 6. The spectra display differences in the amide I region (1640-1680 cm^{-1}), the amide III region (1240-1300 cm^{-1}), the intensity of the shoulder located at 1415 cm^{-1} , and in the intensity of the bands at 855 and 880 cm^{-1} . These spectral differences point out the existence of regional variations in the molecular composition of the stratum corneum. Part of the spectral differences can be explained by variations in the amount of NMF. This very efficient humectant is found exclusively in the stratum corneum and can make up as much as 10% of the dry weight of the keratinocytes. It comprises a highly water soluble and hygroscopic mixture of free amino acids, derivatives of amino acids, and salts. The major constituents are serine, PCA and glycine and to a lesser extend UCA, and citrulline.²⁴⁻²⁶ Spectral differences can also be attributed to variation in lipid content (ceramide) and urea, which is present in sweat. Raman spectra of all these compounds are displayed in figure 8. Figure 7 shows that they can account for many of the spectral differences between the stratum corneum of the dorsal surface of the finger and the volar aspect of the forearm of three subjects. Further studies are needed to elucidate the origin of the remaining spectral differences shown in the residual spectra. The spectra of PCA, serine and glycine were the dominant factors in the multiple regression fits. Their normalized regressions were approximately the same for the three cases studied. This and the fact that these three compounds are the major constituents of NMF led us to interpret these results as evidence for the existence of differences between NMF content of the stratum corneum at different anatomical locations. The importance of this result lies in the fact that it was obtained in a completely noninvasive manner in contrast to previous studies of NMF.

Conclusion

Confocal Raman microspectroscopy was used *in vitro* and *in vivo* to obtain qualitative information about (variations in) molecular composition and molecular structure of different skin layers. Future work will concentrate on quantification of molecular compounds in the skin. The results presented here illustrate that valuable information about the lipid and NMF content of stratum corneum can be obtained in a straightforward, noninvasive and rapid manner. Therefore, we expect that Raman spectroscopy will develop into a powerful method for *in vivo* skin characterization with many applications in pathologic, pharmaceutical and cosmetic research.

Acknowledgments

The authors wish to thank Alex KleinJan, Department of Otorhinolaryngology, for providing some of the skin samples.

References

1. G. F. Odland, "Structure of the skin", in *Physiology, Biochemistry and molecular Biology of the Skin*, ed. by L. A. Goldsmith, Oxford University Press, New York, 1991, pp. 3-62.
2. H. R. Jakubovic and A. B. Ackerman, "Structure and function of skin: development, morphology, and physiology", in *Dermatology*, ed. by S. L. Moschella, and H. J. Hurley, W. B. Saunders company, Philadelphia, 1992, pp. 3-87.
3. G. J. Puppels and J. Greve, "Whole cell studies and tissue characterization by Raman spectroscopy", in *Biomedical Applications of Spectroscopy*, ed. by R. J. H. Clark, and R. E. Hester, John Wiley & Sons; Ltd., Chichester, 1996, pp. 1-42.
4. M. Gniadecka, H. C. Wulf, O. F. Nielsen, D. H. Christensen, and J. Hercogova, "Distinctive molecular abnormalities in benign and malignant skin lesions: Studies by Raman spectroscopy", *Photochem Photobiol.* **66**, 418-423, (1997).
5. M. Gniadecka, H. C. Wulf, N. Nymark Mortensen, O. Feurskov Nielsen, and D. H. Christensen, "Diagnosis of basal cell carcinoma by Raman spectroscopy", *J Raman Spectrosc.* **28**, 125-130, (1997).
6. P. W. Wertz and D. T. Downing, "Epidermal lipids", in *Physiology, Biochemistry and molecular Biology of the Skin*, ed. by L. A. Goldsmith, Oxford University Press, New York, 1991, pp. 205-236.
7. J. A. Bouwstra, M. A. Salomons-de Vries, B. A. I. van den Bergh, and G. S. Gooris, "Changes in lipid organisation of the skin barrier by N-alkyl-azocycloheptanones: A visualisation and X-ray diffraction study", *Int J Pharm.* **144**, 81-90, (1997).
8. D. A. Van Hal, E. Jeremiasse, H. E. Junginger, F. Spies, and J. A. Bouwstra, "Structure of fully hydrated human stratum corneum: a freeze-fracture electron microscopy study", *J Invest Dermatol.* **106**, 89-95, (1996).
9. A. C. Williams, H. G. M. Edwards, and B. W. Barry, "Fourier transform Raman spectroscopy. A novel application for examining human stratum corneum", *Int J Pharm.* **81**, R11-14, (1992).
10. B. W. Barry, H. G. M. Edwards, and A. C. Williams, "Fourier Transform Raman and infrared vibrational study of human skin: assignment of spectral bands", *J Raman Spectrosc.* **23**, 641-645, (1992).
11. H. G. M. Edwards, D. W. Farwell, A. C. Williams, B. W. Barry, and F. Rull, "Novel spectroscopic deconvolution procedure for complex biological systems: vibrational components in the FT-Raman spectra of ice-man and contemporary skin", *J Chem Soc Faraday Trans.* **91**, 3883-3887, (1995).
12. A. C. Williams, B. W. Barry, H. G. M. Edwards, and D. W. Farwell, "A critical comparison of some Raman spectroscopic techniques for studies of human stratum corneum", *Pharm Res.* **10**, 1642-1647, (1993).
13. A. C. Williams, B. W. Barry, and H. G. M. Edwards, "Comparison of Fourier transform Raman spectra of mammalian and reptilian skin", *Analyst*, **119**, 563-565, (1994).
14. A. C. Williams, H. G. M. Edwards, and B. W. Barry, "Raman spectra of human keratotic biopolymers: skin, callus, hair and nail", *J Raman Spectrosc.* **25**, 95-98, (1994).
15. B. W. Barry, A. C. Williams, and H. G. M. Edwards, "Fourier transform Raman and IR spectra of snake skin", *Spectrochim Acta, Part A*, **49**, 801-807, (1993).
16. H. G. M. Edwards, D. W. Farwell, A. C. Williams, and B. W. Barry, "Raman spectroscopic studies of the skins of the Sahara sand viper, the carpet python and the American black rat snake", *Spectrochim Acta, Part A*, **49**, 913-919, (1993).

17. M. Wegener, R. Neubert, W. Rettig, and S. Wartewig, "Structure of stratum corneum lipids characterized by FT-Raman spectroscopy and DSC I. ceramides", *Int J Pharm.* **128**, 203-213, (1996).
18. A. N. C. Anigbogu, A. C. Williams, B. W. Barry, and H. G. M. Edwards, "Fourier transform Raman spectroscopy of interactions between the penetration enhancer dimethyl sulfoxide and human stratum corneum", *Int J Pharm.* **125**, 265-282, (1995).
19. R. O. Potts, D. B. Guzek, R. R. Harris, and J. E. McKie, "A noninvasive, in vivo technique to quantitatively measure water concentration of the stratum corneum using attenuated total-reflectance infrared spectroscopy", *Arch Dermatol Res.* **277**, 489-495, (1985).
20. G. W. Lucassen, G. N. A. van Veen, and J. A. J. Jansen, "Band analysis of hydrated human skin stratum corneum ATR-FTIR spectra in vivo", *J Biomed Optics.* **3**, 267-280, (1998).
21. M. G. Shim and B. C. Wilson, "Development of an *in vivo* Raman spectroscopic system for diagnostic applications", *J Raman Spectrosc.* **28**, 131-142, (1997).
22. G. J. Puppels, W. Colier, J. H. F. Olminkhof, C. Otto, F. F. M. de Mul, and J. Greve, "Description and performance of a highly sensitive confocal Raman spectrometer", *J Raman Spectrosc.* **22**, 217-225, (1991).
23. O. Braun-Falco and H. C. Korting, "Normal pH value of human skin", *Hautarzt*, **37**, 126-129, (1986).
24. A. V. Rawlings, I. R. Scott, C. R. Harding, and P. A. Bowser, "Stratum corneum moisturization at the molecular level", *J Invest Dermatol.* **103**, 731-741, (1994).
25. I. Horii, K. Kawasaki, J. Koyama, Y. Nakayama, K. Nakajima, K. Okazaki, and M. Seiji, "Histidine-rich protein as a possible origin of free amino acids of stratum corneum", *J Dermatol.* **10**, 25-33, (1983).
26. J. Tabachnick and J. H. LaBadie, "Studies on the biochemistry of epidermis. IV. The free amino acids, ammonia, urea, and pyrrolidone carboxylic acid content of conventional and germ-free albino guinea pig epidermis", *J Invest. Dermatol.* **54**, 24-31, (1970).
27. B. G. Frushour and J. L. Koenig, "Raman scattering of collagen, gelatin, and elastin", *Biopolymers*, **14**, 379-391, (1975).
28. A. T. Tu, *Raman Spectroscopy in Biology*, John Wiley & Sons; Ltd., New York, 1982.
29. T. D. Visser, J. L. Oud, and G. J. Brakenhoff, "Refractive index and axial distance measurements in 3-D microscopy", *Optik*, **90**, 17-19, (1992).

In vivo confocal Raman microspectroscopy of the skin: noninvasive determination of molecular concentration profiles

Journal of Investigative Dermatology
2001, 116(3): 434-442

Chapter

3

P. J. Caspers
G. W. Lucassen
E. A. Carter
H. A. Bruining
G. J. Puppels

Abstract

Confocal Raman spectroscopy is introduced as a noninvasive *in vivo* optical method to measure molecular concentration profiles in the skin. It is shown how it can be applied to determine the water concentration in the stratum corneum as a function of distance to the skin surface, with a depth resolution of 5 μm . The resulting *in vivo* concentration profiles are in qualitative and quantitative agreement with published data, obtained by *in vitro* X-ray microanalysis of skin samples.^{1,2} Semiquantitative concentration profiles were determined for the major constituents of natural moisturizing factor (serine, glycine, pyrrolidone-5-carboxylic acid, arginine, ornithine, citrulline, alanine, histidine, urocanic acid) and for the sweat constituents lactate and urea. A detailed description is given of the signal analysis methodology that enables the extraction of this information from the skin Raman spectra. No other noninvasive *in vivo* method exists, that enables an analysis of skin molecular composition as a function of distance to the skin surface with similar detail and spatial resolution. Therefore, it may be expected that *in vivo* confocal Raman spectroscopy will find many applications in basic and applied dermatological research.

Introduction

Driven by medical, pharmaceutical and cosmetic research questions a large number of methods have been developed to obtain information about the presence and concentration of molecular compounds in the skin. Many of these methods are *ex vivo* methods, which require material to be removed from the skin and analyzed *in vitro*. A drawback of these *ex vivo* methods is that they are, to a greater or lesser extent, invasive. They alter the system under investigation either by extraction of compounds from the skin or by physical disruption of cell layers.

A widespread *ex vivo* method is tape stripping, whereby cell layers are removed from the stratum corneum with adhesive tape. Sequential tape stripping has been employed in various studies to obtain information about the depth distribution of molecular compounds in the stratum corneum.³⁻⁸ Rawlings and coworkers have developed a tape-stripping procedure that allowed measurement of the concentration of natural moisturizing factor (NMF) at different depths in the stratum corneum.⁹ In a number of studies extraction techniques have been employed to determine concentration levels of free amino acids in the stratum corneum.¹⁰⁻¹³

A limited number of *in vivo* methods have been developed to study the skin. Tagami and coworkers described a noninvasive high frequency electrical impedance method, which evaluates skin surface hydration *in vivo*.¹⁴ This technique enables indirect detection of changes in skin hydration, but not direct quantitative measurements of water content, and the information is not obtained from a well-defined location within the skin. Infrared (IR) spectroscopy has been used for *in vivo* studies of stratum corneum-hydration and permeability.^{7, 15-18} However, due to the strong absorption of mid- and far-infrared radiation by water, the penetration depth in a naturally hydrated tissue such as the skin is limited to a few microns. Therefore in an *in vivo* IR-spectroscopic experiment only the outermost layer of the stratum corneum is sampled.

Raman spectroscopy, in contrast, can be applied to obtain information regarding the molecular composition of the skin down to several hundred micrometers below the skin surface. Raman spectroscopy is a vibrational spectroscopy, similar to infrared spectroscopy, but based on inelastic light scattering rather than absorption of light. In a Raman experiment the sample under investigation is illuminated by monochromatic laser light. Interactions between the incident photons and molecules in the sample result in scattering of light. In a Raman scattering event a sharply defined amount of energy is transferred from the photon to the molecule, in which a vibrational mode is excited. It follows that a small fraction of the scattered light (the Raman spectrum) is found at wavelengths longer than that of the incident light. The exact energy needed to excite a molecular vibration depends on the masses of the atoms that are involved in the vibration and the type of chemical bonds between these atoms and may be influenced by molecular structure, molecular interactions, and the chemical microenvironment of the molecule. This and the fact that molecules may have a great number of independent vibrational modes ($3N-6$ for a molecule consisting of N atoms), many of which may be excited by a Raman scattering event, means that a Raman spectrum is highly molecule specific. Therefore the positions, relative

intensities and shapes of the bands in a Raman spectrum carry detailed information about the molecular composition of a sample and about molecular structures and interactions present.¹⁹

Raman spectroscopy is widely used in biological studies, varying from investigations of purified compounds to studies at the level of single cells (reviews by Carey, 1982; Tu, 1982; Parker, 1983; Puppels, 1999).²⁰⁻²³ More recently Raman spectroscopic investigations have been initiated, aimed at tissue characterization and pathological tissue classification; many of these targeting the skin.²⁴⁻²⁸ First *in vivo* (Fourier-transform) Raman spectra of skin were published by Schrader *et al* (1997), Shim and Wilson (1997), and Williams (1993). Recently, Schallreuter and coworkers published results of *in vivo* Raman studies in which the concentrations of phenylalanine and hydrogen peroxide were measured in the skin.^{29; 30} However, in all these studies there was little or no control over the actual tissue volume that was being sampled. Recently, Caspers *et al* (1998) introduced *in vivo* confocal Raman spectroscopy as a method to gain control over the actual skin layer from which Raman signal is collected.

The stratum corneum is the skin's outermost layer and the main protective barrier against water loss, microorganisms and toxic agents. A detailed knowledge of the concentration and distribution of water and free amino acids in the stratum corneum is of importance for a better understanding of the properties of this layer. Water greatly affects physical properties of the stratum corneum, such as permeability and flexibility, and is also thought to regulate the activity of specific hydrolytic enzymes that are important for normal desquamation of corneocytes at the skin surface.³¹ Hydration of the stratum corneum, which is exposed to the relatively dry environment, is maintained by natural moisturizing factor (NMF). NMF is a highly hygroscopic and water-soluble mixture of amino acids, derivatives of amino acids and specific salts and is found exclusively in the stratum corneum.⁹ It is produced in the lower part of the stratum corneum by enzymatic degradation of the protein filaggrin.^{32; 33}

In this paper we present confocal Raman microspectroscopy as a noninvasive *in vivo* optical method for obtaining detailed information about the molecular composition of the skin and for determining molecular concentration gradients in the skin. Water concentration profiles were determined for the stratum corneum, as well as semiquantitative concentration profiles of constituents of NMF and sweat.

Materials and Methods

Sample preparation

Preparation of washed and delipidized ex vivo stratum corneum samples Sheets of human stratum corneum were obtained from the upper back and shoulders of a male volunteer (37 years of age) suffering from a mild sunburn. Water-soluble compounds and lipids were extracted by washing the stratum corneum samples in ultra-pure water for 60 minutes, followed by soaking in chloroform/methanol (2:1, v:v) for 48 hours. Finally the

samples were washed again in water to remove possible water-soluble compounds that had not been released before lipid extraction.

Preparation of solutions Chemicals were purchased from Sigma-Aldrich Chemie (Zwijndrecht, The Netherlands) and used without further purification. Protein solutions in water were prepared of pepsin (33 kDa), urease (480 kDa), lysozyme (14 kDa) and bovine serum albumin (68 kDa), in 20% concentrations (mass-%, for bovine serum albumin 20% and 40% were used). Solutions of pyrrolidone carboxylic acid (PCA, 0.26 M), arginine (Arg, 0.19 M), ornithine (Orn, 0.46 M), citrulline (Cit, 0.19 M), serine (Ser, 0.72 M), proline (Pro, 0.37 M), glycine (Gly, 0.96 M), histidine (His, 0.21 M) and alanine (Ala, 0.45 M) were prepared in ultra pure water at pH 5.5. Solutions of urocanic acid (UCA, 0.013 M) were prepared at pH 4.5 and pH 6.5. These compounds represent the main free amino acids and amino acid derivatives that constitute natural moisturizing factor. Also solutions of the sweat constituents lactate (1.14 M) and urea (0.90 M) were prepared in pure water at pH 5.5.

Instrumentation

In vitro Raman experiments described in this paper (measurements on amino acid solutions and on stratum corneum samples) were carried out on a custom built near infrared Raman microspectrometer, that has been described in detail elsewhere.^{28; 34} *In vivo* Raman experiments on skin were carried out on a dedicated inverted confocal Raman microspectrometer that was developed in our laboratory (figure 1). Raman spectra of the skin of hand and arm were obtained by placing the hand or arm on a CaF₂ window in a metal stage. A laser beam from a tunable titanium-sapphire laser (model 3900S, Spectra Physics, Mountain View, CA) pumped by an Argon-ion laser (model 2020, Spectra Physics, Mountain View, CA) is focused in the skin by a microscope objective (Leica PL Fluotar 63x0.7 corr) located under the CaF₂-window. Light that is scattered by the tissue is collected by the same objective and focused onto an optical fiber connected to the spectrograph. The core of this optical fiber (100 μm diameter) acts as a confocal pinhole, which rejects signal coming from out-of-focus regions of the skin.^{35; 23} The microscope objective is mounted on a precision translation table. This enables the distance between the objective and the skin surface to be adjusted in order to focus the laser light at a selected depth below the skin surface. Raman spectra were thus obtained from different, well-defined depths, at a depth resolution of 5 μm . The depth resolution was measured as follows: The Raman signal of oil was recorded, as the laser focus was scanned across a CaF₂ - oil interface. The step response function thus obtained was differentiated to obtain the impulse response of the system (i.e. the response of the system that would be obtained if it were scanned through an infinitesimally thin plane with Raman scatterers). The bandwidth (full-width-at-half-maximum) of this impulse response is a measure for the depth resolution. For both excitation wavelengths used in this study (730 and 850 nm) the depth resolution was 5 μm . Due to the fact that the hand or arm rests on the metal stage and is in contact with the CaF₂-window, artifacts caused by unwanted vertical movement of the skin during the measurements are avoided.

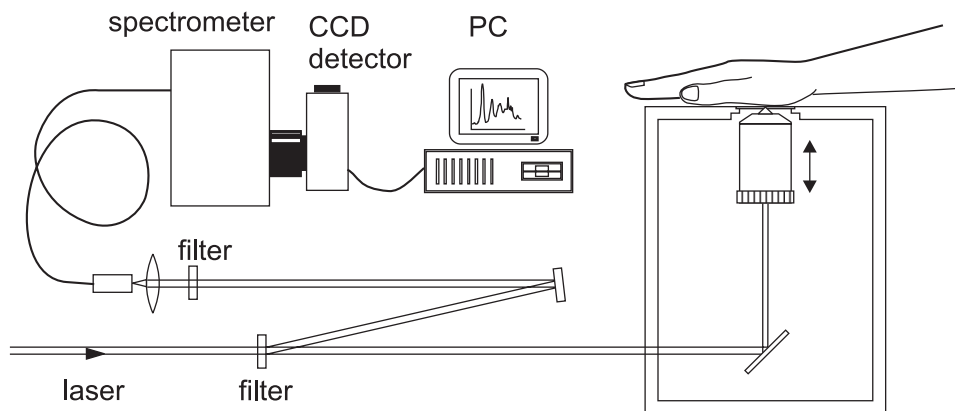


Figure 1. Confocal Raman setup for *in vivo* experiments. Laser light from a titanium-sapphire laser is transmitted by a short-pass filter and focused in the skin by a microscope objective. Raman scattered light is collected by the same objective, reflected by the short-pass filter, filtered by a laser rejection filter (either a notch filter or a color glass filter) and focused onto the core of an optical fiber. The fiber guides the light into a multichannel spectrometer equipped with a CCD camera.

No changes in Raman spectra occurred during prolonged measurements at the same focusing depth (30 spectra for up to 6 min), and repeated scans through the skin resulted in identical molecular concentration profiles. It is estimated therefore that such vertical movements are limited to 1-2 μm ; i.e. well below the depth resolution of the setup.

Near-infrared (NIR) laser light is used in order to minimize the excitation of tissue-autofluorescence, which severely hampers Raman experiments in which visible laser light is used.^{36, 37} On the other hand the quantum efficiency of charge coupled device detectors, which are the detectors of choice in multichannel Raman spectroscopy rapidly decreases above 1000 nm. This puts an upper limit to the NIR-excitation wavelengths that can be employed. Therefore different laser excitation wavelengths were used for measurements in the so-called fingerprint region (400-1850 cm^{-1} , excitation wavelength 850 nm, Raman signal detected between about 880 and 1000 nm) and for measurements in the high wavenumber region (2500-3800 cm^{-1} , excitation wavelength 730 nm, Raman signal detected between about 890 and 1010 nm).

Data acquisition

Determination of concentration profiles of water and NMF. *In vivo* Raman spectra were recorded of the thenar and the volar aspect of the arm of six healthy individuals (three male, three female; between 23 and 37 years of age). The spectra were measured at a range of depths below the skin surface, along a line perpendicular to the skin. Raman profiles of the thenar, where the thickness of the stratum corneum is of the order of 100 μm , were recorded with depth increments of 5 and 10 μm . Profiles of the arm (stratum corneum thickness 10-15 μm) were recorded with depth increments of 2 μm . By using depth increments of 2 μm the optical depth resolution of 5 μm (i.e. the dimension of the measuring volume in the direction perpendicular to the skin surface) is in fact over sam-

pled by more than a factor of 2. In this way the resolution of the Raman scans is determined only by the optical properties of the system and not degraded by the step size of the depth increments. Measurement time was 30 s per spectrum in the 400-1850 cm^{-1} spectral region and 3 s per spectrum in the 2500-3800 cm^{-1} region. The laser power on the skin was 100 mW in all experiments. Other than removal of superficial dirt and excessive sebum with a tissue soaked in ethanol, no pre-treatment of the skin was performed.

Data analysis

Wavenumber calibration and sensitivity correction

Raman-standards with accurately known peak frequencies were used for wavenumber calibration of the Raman spectra. Recorded Raman intensities were corrected for the wavelength dependence of the detection efficiency of the setup using the emission spectrum of a calibrated tungsten band lamp. A detailed description of these procedures is given elsewhere.³⁴

Determination of water concentration

The ratio of the intensities of the Raman bands at 3390 cm^{-1} and 2935 cm^{-1} can be used to determine the water to protein ratio in tissue, as was successfully demonstrated by Huizinga and coworkers in their work on eye lenses³⁸ and more recently by Bauer and coworkers in studies of the cornea.³⁹ We have used this method to determine the water concentration in the skin. Water to protein ratios in the stratum corneum were calculated as the ratio between the Raman signal intensity of water (due to OH stretching vibrations) integrated from 3350 to 3550 cm^{-1} and that of protein (due to CH_3 stretching vibrations) integrated from 2910 to 2965 cm^{-1} . These spectral ranges were chosen so as to maximize signal-to-noise and to avoid overlap between the N-H vibration of protein⁴⁰ at 3329 cm^{-1} and the water Raman signal. This is illustrated in figure 2, which shows Raman spectra of pure water and of freeze-dried stratum corneum. A straight baseline between the spectrum points at 2500 and 3800 cm^{-1} was subtracted from the *in vivo* skin spectra in order to correct for the influence of slight variations in background (fluorescence) signal. Water content was calculated from the water/protein ratio using the following equations:

$$\frac{W}{P} = \frac{m_w}{m_p} \cdot R \quad (1)$$

$$\text{water content (\%)} = \frac{m_w}{m_w + m_p} = \frac{\frac{W}{P}}{\frac{W}{P} + R} \cdot 100\% \quad (2)$$

where m_w and m_p are the water and protein masses in the sampling volume, W is the integrated Raman signal of water, P is the integrated Raman signal of protein and R is a proportionality constant, describing the ratio between the Raman signals of water and protein of a 50% solution. The water content is expressed in grams of water per 100 g of wet tissue (water + dry mass).

Raman spectra of various solutions of protein in water (40% and 20% solutions of bovine serum albumin and 20% solutions of pepsin, lysozyme, and urease) were used to obtain an estimate of the proportionality constant R . Equation (2) was then used to convert ratios of water/protein Raman signal (W/P) to absolute water content in weight percentage. The proportionality constant R was found to vary with the type of protein used: $R = 2.0 \pm 15\%$. (Attempts to use keratin, for a calibration along this line failed. Keratin is water insoluble, so that inhomogeneous mixtures of protein and water were obtained which resulted in strongly varying and therefore unreliable values for R . Calibration experiments with hydrated delipidized stratum corneum samples failed for the same reason. Also here sample inhomogeneity caused the ratio between water signal intensity and protein signal intensity to vary strongly as a function of exact measurement location, whereas only one overall water-protein ratio can be determined for a sample by weighing it before and after hydration).

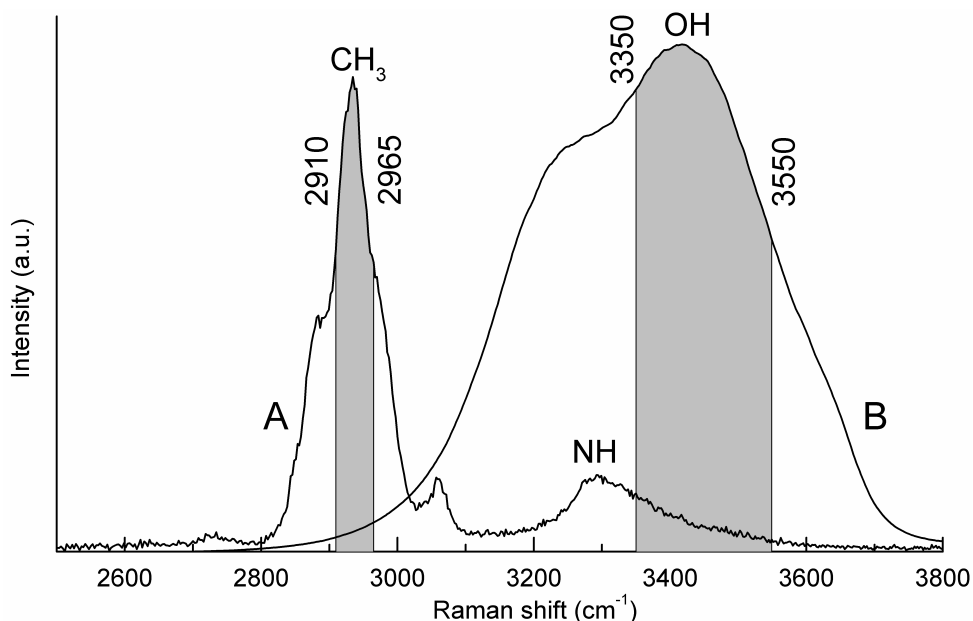


Figure 2. Raman spectra of water and dry stratum corneum. (A) Raman spectrum of freeze-dried stratum corneum. (B) Raman spectrum of water. The gray areas highlight the spectral intervals that are used in the calculation of water content in the skin.

Error estimation for Raman spectroscopic determination of water concentration

The absolute error ΔR in R and the absolute error $\Delta W/P$ in the ratio W/P were used to obtain an estimation of the error in absolute water content as determined by Raman spectroscopy according to expression 3.

$$\frac{\Delta\left(\frac{m_w}{m_w + m_p}\right)}{\left(\frac{m_w}{m_w + m_p}\right)} = \frac{\Delta\left(\frac{W}{P}\right)}{\left(\frac{W}{P}\right)} + \frac{\Delta\left(\frac{W}{P}\right)}{\left(\frac{W}{P}\right) + R} + \frac{\Delta R}{\left(\frac{W}{P}\right) + R} \quad (3)$$

The first two terms on the right hand side of expression 3 represent random errors, the third term represents a systematic error introduced by the error in the determination of the proportionality constant R . The error ΔR in the value of R that was obtained for the four calibration proteins, was 15%. The error $\Delta W/P$ in the W/P -ratio for a specific protein solution, as determined from independently prepared and measured samples, was $\leq 4\%$.

Determination of the concentration of free amino acids

Raman spectra obtained at different depths below the skin surface were found to show consistent differences in the 400-1850 cm^{-1} spectral interval. Multiple least squares fitting procedures were used to analyze these spectral differences. Both a qualitative analysis and a semiquantitative analysis were made. The qualitative analysis served to identify the molecular components of the skin that give rise to these spectral differences. The semiquantitative analysis yielded information about the semiquantitative concentrations of these components as a function of depth below the skin surface.

Qualitative analysis In a previous study we identified differences in the relative concentration of NMF and sweat constituents as the source of differences in skin spectra obtained at different locations of the body.^{28; 34} This led us to consider variations in the concentrations of NMF and sweat constituents as a possible source of the observed differences in this study. A set of *in vitro* Raman spectra of solutions of the dominant constituents of NMF (PCA, Arg, Orn, Cit, Ser, Pro, Gly, His, Ala, and UCA).^{10, 12; 13; 32} was collected. Also included in this set were spectra of solutions of the sweat compounds lactate and urea and spectra of ceramide 3 and of water. The spectrum of UCA was found to be strongly pH-dependent within the acidity range that may be encountered in the skin (pH 4.5-7). Because skin pH varies from person to person and changes as a function of depth,^{4, 41} UCA-spectra were obtained at pH 4.5 and pH 6.5 and included in the set of fit spectra. It was verified that the UCA spectrum at intermediate pH is a linear combination of these two spectra. The intensities of the spectra of the solutions of NMF and sweat components were normalized with respect to the concentration of the respective solutions.

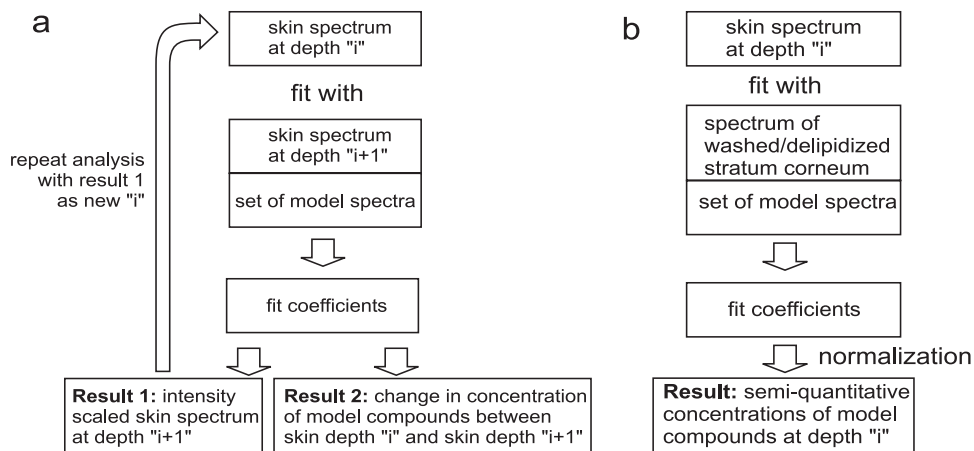


Figure 3. Schematic representation of the fit methods. (a) Flow chart of the method used to qualitatively analyze the changes in Raman spectra as a function of distance to the skin surface. (b) Flow chart of the method used for semiquantitative determination of the concentration of skin constituents as a function of distance to the skin surface.

Hereafter this set of spectra will be referred to as “model set” or “model spectra”. The qualitative analysis then proceeded as follows (illustrated in figure 3a). The *in vivo* Raman spectrum obtained at the skin surface (i.e. the spectrum obtained at depth “0”) was fitted with the model set, and the *in vivo* skin spectrum that was obtained at the next depth increment (depth “1”). The results of this analysis are fit coefficients for each of the model spectra, and a fit coefficient for the *in vivo* skin spectrum obtained at depth “1”. The fit coefficients for the model spectra reflect the changes in concentration of the NMF and sweat constituents between the two locations in the skin. However, the absolute Raman signal intensity of *in vivo* skin spectra decreased with increasing distance to the skin surface. In order to enable a direct comparison of relative changes in concentration at different depths in the skin, the absolute intensities of the *in vivo* skin spectra were normalized. This was done by multiplying the skin spectrum at depth “1” by the fit coefficient that was obtained for this spectrum.

The procedure described above was then repeated with the intensity normalized skin spectrum obtained at depth “1” and the skin spectrum obtained at depth “2”, in order to analyze of the changes in molecular composition between depth “1” and depth “2”. In this way changes in molecular composition at successive distances to the skin surface were analyzed, until the spectrum measured furthest below the skin surface had been used in the analysis.

Semiquantitative analysis The qualitative analysis described above only analyzes the changes in the concentrations of molecular compounds between two locations in the skin. In order to obtain a semiquantitative determination of the concentrations of NMF and sweat constituents as a function of distance to the skin surface, the fitting procedure described above was slightly altered (illustrated in figure 3b). Instead of using an *in vivo*

skin spectrum, an *in vitro* spectrum of a washed/delipidized stratum corneum sample was included in the set of fit spectra. Therefore, each individual *in vivo* skin spectrum was modeled with a fixed set of fit spectra, consisting of the model set and the spectrum of washed/delipidized stratum corneum. The fit coefficients for the model spectra, that were thus obtained, were normalized with respect to the fit coefficient of the spectrum of the washed/delipidized SC-sample. In this way one obtains a measure for the concentrations of NMF and sweat constituents relative to the keratin concentration (keratin being present only in the SC-sample and being its major component). This semiquantitative measure was used to monitor changes in the concentrations of NMF and sweat constituents as a function of distance below the skin surface.

In both the qualitative and the semiquantitative analysis the fit procedures used the spectral interval 400-1500 cm^{-1} . The reason for excluding the amide I band around 1650 cm^{-1} was that its bandwidth and position were found to vary. These changes, which are probably due to changes in protein secondary structure and protein-water interactions, cannot be modeled by the set of spectra used in the fit procedure. Nevertheless the least-squares algorithm would try to fit these spectral changes, using the available set of spectra. This was found to worsen the fit result in the 400-1500 cm^{-1} spectral interval and to significantly influence the fit coefficients of urocanic acid, which possesses an intense band at 1650 cm^{-1} .

The model set contained 15 spectra. In some spectral intervals a degree of spectral overlap exists between spectra of the model set. Therefore, it was verified that the model set is an independent set of spectra, which is a prerequisite for the fits to yield reliable results. Two tests were performed. First it was attempted to fit each individual spectrum of the model set by all other spectra of the model set. This was not possible. For each of the model spectra a very poor fit was obtained, judged by the large Raman features in the fit residuals (i.e. the features of the spectrum being fitted, that cannot be accounted for by the set of fit spectra). Second, for each of the compounds in the model set an independently measured spectrum was fitted with the complete model set. It was verified that only the spectrum of that compound, as included in the model set, contributed to the fit (i.e. had a fit contribution > 99%). Together the results of these tests show that the model set forms indeed a sufficiently independent set of spectra for the purposes of this study.

Estimation of errors in the fit results

An independent set of fit spectra will yield unique fit results. However, the presence of noise in the spectra may affect the fit results. Therefore an estimate was made of the influence of noise on the semiquantitative fit results. For this purpose noise was added to the *in vivo* skin spectra to artificially decrease the signal-to-noise ratio by a factor 2, and a new set of fit coefficients was calculated according to the semiquantitative fit procedure described above. For each of the *in vivo* skin spectra this procedure was repeated 100 times. The standard deviation thus obtained for each of the fit coefficients was used as an estimate for the error in the fit-coefficients.

Results

The experimental results presented in this section reflect a total of 30 experiments in which multiple Raman depth scans were made through the stratum corneum of the thenar and the volar aspect of the arm of a total six healthy volunteers (three male, three female; between 23 and 37 years of age).

Water concentration profiling

Figure 4 shows a series of *in vivo* Raman spectra obtained from the stratum corneum of the thenar (palm of the hand) at a range of depths below the skin surface. A first-order polynomial was subtracted from each spectrum. The spectra were normalized to the CH stretching band ($I_{2910-2965}$), which originates from the stratum corneum proteins. The OH stretching modes of water are visible as a broad spectral band centered around 3450 cm^{-1} . The distances to the skin surface are indicated in the figure. The spectra clearly illustrate that the ratio between the water signal and the protein signal varies strongly as a function of distance to the skin surface.

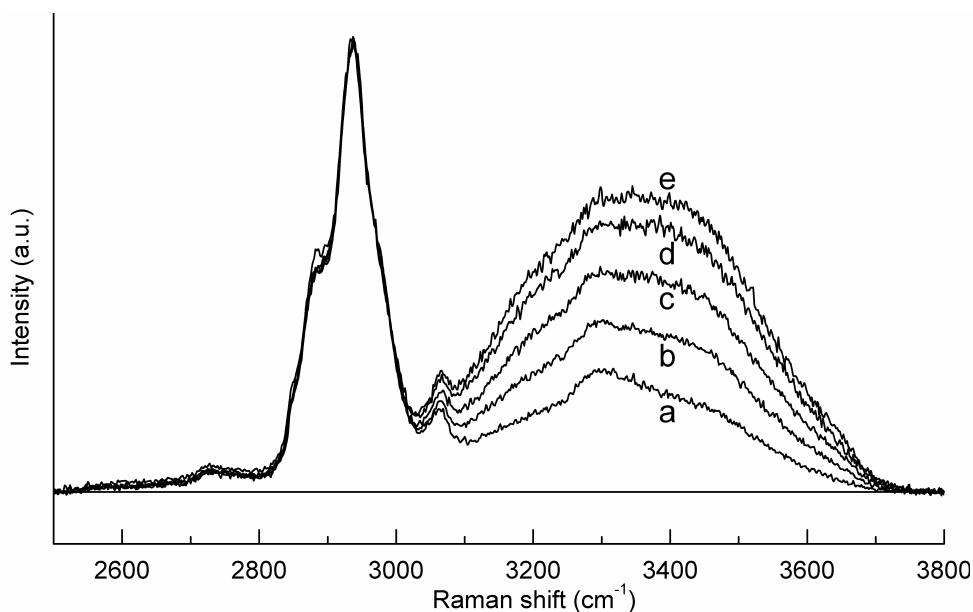


Figure 4. *In vivo* Raman spectra of the stratum corneum in the spectral interval $2500\text{--}3800\text{ cm}^{-1}$. Illustration of the spectral changes due to differences in water content. The spectra were obtained at the thenar, at different depths below the skin surface. Distance to skin surface: (a) $0\text{ }\mu\text{m}$, (b) $75\text{ }\mu\text{m}$, (c) $80\text{ }\mu\text{m}$, (d) $85\text{ }\mu\text{m}$, (e) $90\text{ }\mu\text{m}$. The spectra were normalized on the intensity of the protein signal ($2910\text{--}2965\text{ cm}^{-1}$). Signal collection time for each spectrum: 3 s, excitation wavelength: 730 nm, laser power on the skin: 100 mW.

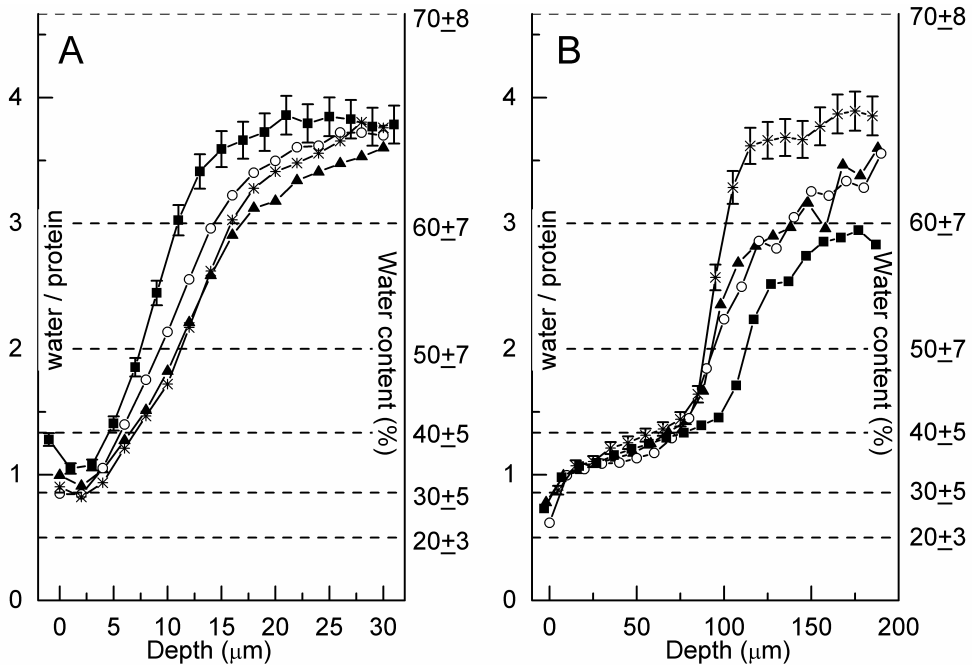


Figure 5. *In vivo* water concentration profiles of the stratum corneum. (A) Four water concentration profiles, calculated from Raman measurements on the volar aspect of the forearm. Different symbols were used for profiles obtained for different measurement locations. (B) Four water concentration profiles based on Raman measurements on the thenar. Different symbols demarcate different measurement locations. Signal collection time: 3 s per data point. The left hand ordinate is the ratio between the Raman signal intensities of water and protein ($I_{3350-3550}/I_{2910-2965}$). The right hand ordinate represents the absolute water content in mass-% (grams of water per 100 g of wet tissue), as calculated from expression 2. Note that this is a non-linear scale. The error bars and error margins are explained in the text.

In vivo water concentration profiles are displayed in figure 5. Figure 5A shows four *in vivo* depth profiles for the volar aspect of the forearm. Figure 5B shows four *in vivo* profiles for the thenar. Each profile is from a different location on the thenar or arm, revealing significant local variations in the shape of the water concentration profiles. However, repeated recordings at one location, scanning either from or to the skin surface, resulted in highly reproducible profiles (results not shown). The left-hand ordinate in figure 5 (A, B) represents the Raman signal intensity ratio ($I_{\text{water}}/I_{\text{protein}}$). The error bars plotted on the top trace represent the 4% random error margin in the determination of this intensity ratio (see *Data analysis*). The right hand ordinate represents absolute water concentration in grams of water per 100 grams of wet tissue, as calculated from expression (2). The errors in the absolute water concentration are indicated along the right hand ordinate. These are systematic errors as calculated from expression (3).

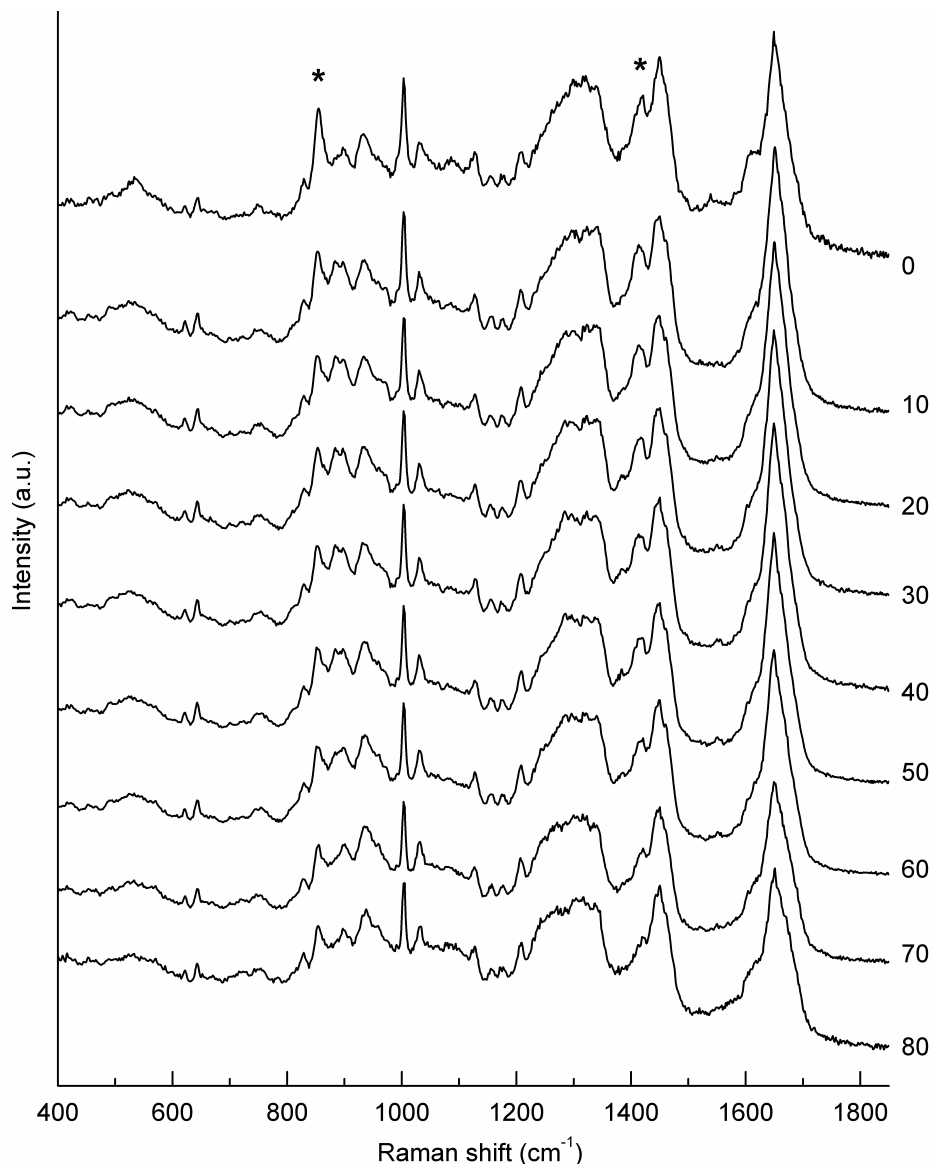


Figure 6. *In vivo* Raman spectra of the stratum corneum of the thenar in the 400-1850 cm^{-1} spectral interval. Raman spectra were recorded of the stratum corneum of the thenar at a range of depths, starting at the skin surface down to 80 μm below the skin surface. Numbers to the right of the spectra indicate this depth in μm . The spectra are intensity normalized (see *Data Analysis* for details on the normalization procedure) and offset along the ordinate for clarity of presentation. Signal collection time: 30 s per spectrum.

NMF

Similar to the measurements described above Raman depth scans were made in the 400-1850 cm^{-1} spectral interval. Figure 6 shows a series of *in vivo* Raman spectra obtained at a range of depths in the stratum corneum of the thenar. Since the absolute signal intensity of the spectra decreased with depth (increments of 10 μm), the intensities of the spectra were normalized as described in *Data analysis*. Although the signal collection time for each spectrum was only 30 s, the quality of the spectra is high and the spectra show many clear spectral features. Several spectral variations can be discerned, two of which are marked by an asterisk to guide the eye.

Inspection of the differences between consecutive spectra revealed two regions where significant changes in stratum corneum molecular composition occur, namely between the skin surface and 10 μm below, and between 60 and 70 μm below the skin surface (figure 7). Only minor changes were observed between consecutive spectra in the depth range from 10 to 60 μm below the skin surface.

A qualitative analysis of the origin of these spectral changes was carried out by a multiple regression fitting procedure, using a set of model spectra, which consisted of spectra of solutions of NMF and sweat constituents, and spectra of ceramide and water. The results of this analysis are displayed in figure 7. The spectral interval 400-1850 cm^{-1} is shown. In the fitting calculations only the 400-1500 cm^{-1} interval was used, as explained in *Data analysis*. In this 400-1500 cm^{-1} spectral interval, no clear remaining spectral features are visible in the fit residuals, indicating that virtually all of the changes in molecular composition that are reflected in the Raman spectra have been accounted for.

Analysis of the spectral changes between the skin surface and 10 μm below the surface yielded large fit-contributions from the sweat constituents lactate and urea, as well as fit-contributions from NMF constituents. In contrast, analysis of the spectral differences between 60 and 70 μm below the skin surface showed only fit-contributions from NMF constituents.

If a difference in NMF-concentration is the origin of the spectral differences between 60 and 70 μm below the skin surface, then the relative contributions to the fit of each of the amino acid (derivative) spectra should reflect the composition of NMF. We therefore repeated the qualitative analysis for five independent *in vivo* Raman experiments and for each experiment we determined the relative fit contributions of the dominant NMF constituents, expressed in mole percent. Figure 8 shows a comparison between this Raman analysis and published reports on the composition of NMF (*in vitro* determinations based on various methods).^{10, 12; 13}

The qualitative analysis of the differences in the Raman spectra obtained from different distances to the skin surface, enabled identification of the molecular compounds that vary in concentration. However, a different analysis is needed to quantify these variations in concentration as a function of distance to the skin surface.

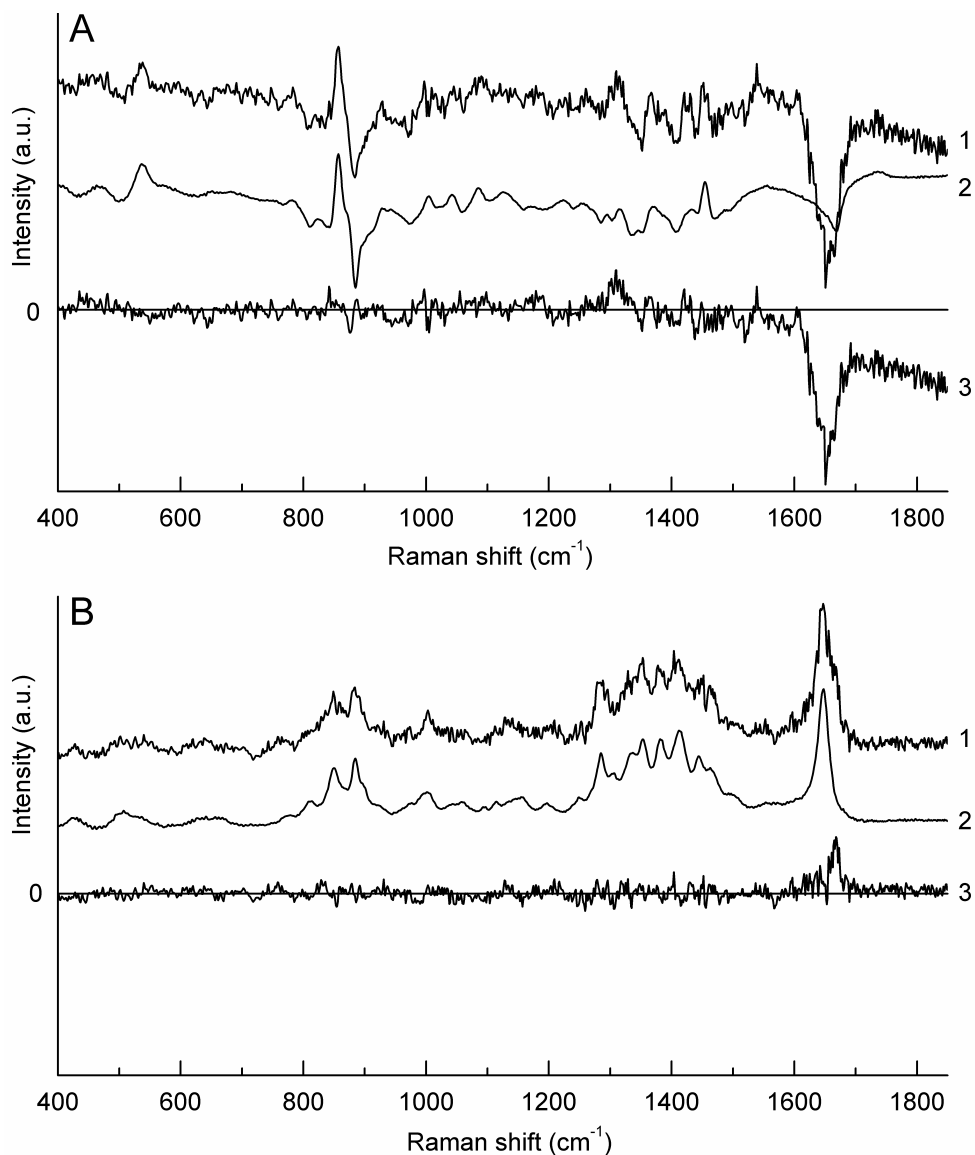


Figure 7. Analysis of the differences in Raman spectra obtained at different depths below the skin surface by means of the qualitative least-squares fit procedure with a set of model spectra of NMF and sweat constituents. A: (1) difference between the Raman spectra obtained at the skin surface and 10 μm below the skin surface (0 μm -10 μm); (2) fit result; (3) residual (curve 1 - curve 2). **B:** (1) difference between the Raman spectra obtained at 60 μm below the skin surface and 70 μm below the skin surface (60 μm - 70 μm); (2) fit result; (3) residual (curve 1 - curve 2). The spectra are all plotted on the same scale. Details of the fit procedure are given in *Data Analysis*.

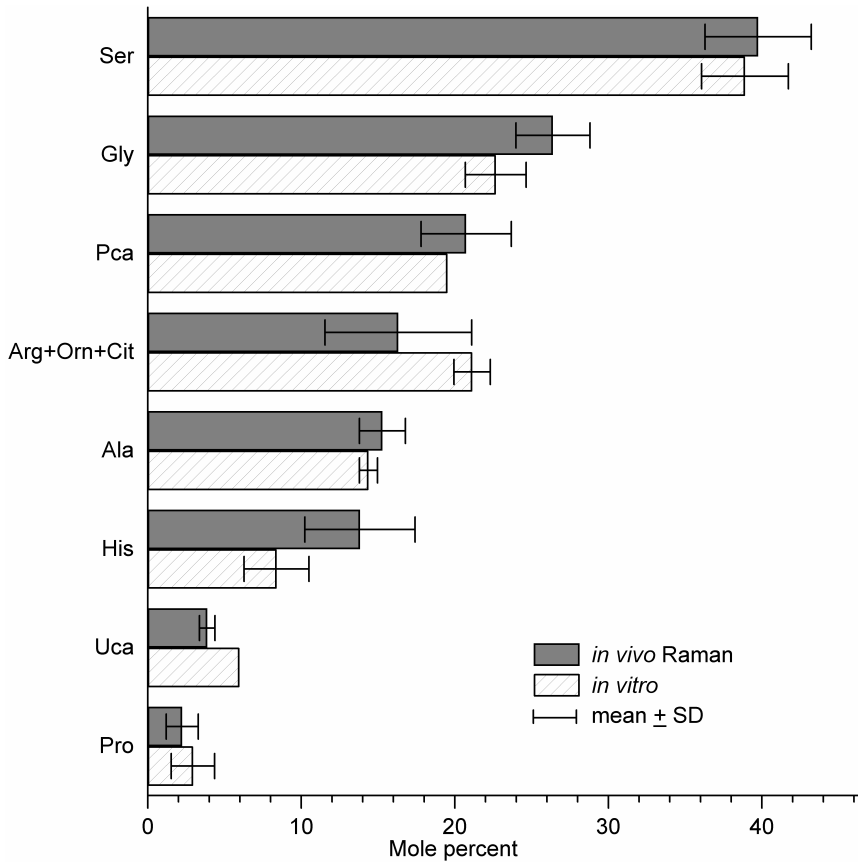


Figure 8. Comparison of the composition of human NMF as determined by *in vivo* Raman spectroscopy and results of previously published *in vitro* studies. The bar plot shows the molar fractions of the predominant NMF-constituents as determined by *in vivo* Raman spectroscopy (solid bars) and by 3 *in vitro* methods (hatched bars). The fractions of Arg, Orn and Cit have been combined (Arg is the precursor of Orn, which is the precursor of Cit). All concentrations have been normalized such, that the total sum of Ser, Ala, Arg, Orn, Cit, Gly, Pro is 100 mol-%. The concentrations of PCA, UCA and His were not included in this normalization, because none of the *in vitro* studies in this comparison provides values for both PCA and UCA (being the precursor of UCA, His was also excluded). The Raman results are based on qualitative analysis (as described in *Data Analysis*) of the differences in Raman spectra obtained at different distances from the skin surface. The mean molar fractions and standard deviations shown in the figure are based on the analysis of 5 independent sets of Raman data. *In vitro* methods: Tabachnick and LaBadie (1970)¹³, amino acid analysis of skin scrapings of the trunk and extremities; Pratzel and Fries (1977)¹², amino acid analysis of stratum corneum that was removed from the buttocks by tape stripping; Koyama *et al* (1984)¹⁰, amino acid analysis of water soluble compounds extracted with a water filled glass cup from various body regions.

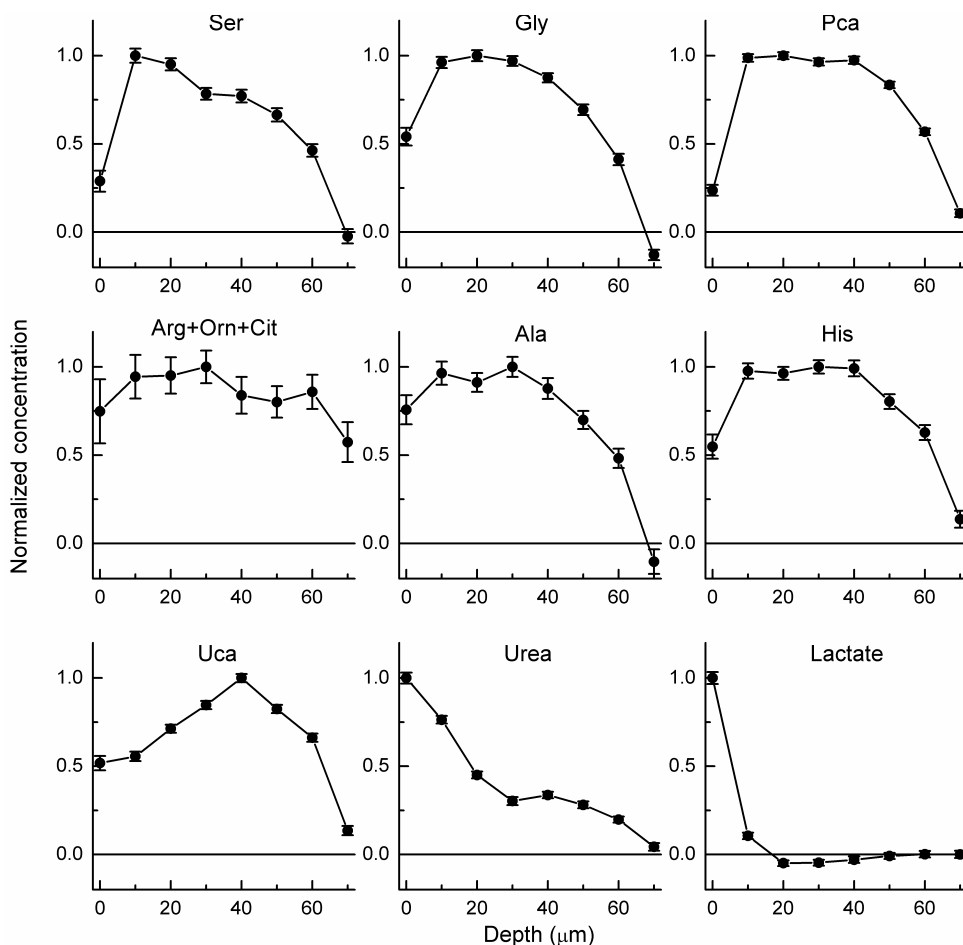


Figure 9. Semiquantitative *in vivo* concentration profiles of NMF and sweat constituents in the SC of the thenar as determined by Raman spectroscopy. The concentration profiles have been determined from the Raman spectra displayed in Fig. 6 by application of the fit procedure described in *Semiquantitative Analysis in Data Analysis*. Each profile has been normalized to its maximum concentration. Error bars represent the uncertainty in the fit results as explained in *Estimation of errors in the fit results in Data Analysis*.

For semiquantitative determination of molecular concentration profiles a fit procedure was applied in which each individual *in vivo* spectrum was modeled by a set of spectra representing all main skin constituents (see *Data analysis*). A spectrum of washed/delipidized stratum corneum was used to represent the keratin fraction in skin. Fit residuals were only slightly larger than in the qualitative analysis described above (results not shown). In this way for each *in vivo* spectrum a complete set of fit coefficients was obtained (one for each of the spectra of the model set). These fit-coefficients were normalized to the fit-coefficient of washed/delipidized stratum corneum. With the assumption that the keratin concentration is relatively constant throughout the stratum corneum, the fit-coefficients

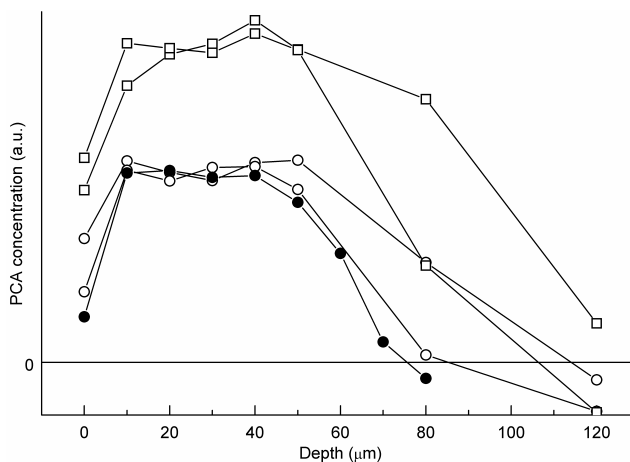


Figure 10. Semiquantitative concentration profiles of PCA as determined by Raman spectroscopy. Concentration profiles were measured in the stratum corneum of the thenar of two volunteers. Subject A (squares) male, 30 y; subject B (circles) female, 30 y. Open and solid symbols refer to experiments on two different days.

provide semiquantitative measures of the concentrations of NMF and sweat constituents as a function of distance to the skin surface. Figure 9 shows the concentration profiles of the dominant NMF and sweat constituents, as determined by semiquantitative analysis of the measurements shown in figure 6. The error bars represent the uncertainty (standard deviation) due to noise in the *in vivo* spectra (see *Data analysis*). Figure 10 shows the concentration profiles of PCA, one of the major NMF constituents, as determined from five series of Raman measurements. Spectra were obtained at different locations of the thenar for two subjects (one male, one female). A clear difference is observed in the relative concentrations of PCA between these subjects (i.e. the concentration of PCA relative to that of keratin).

Discussion

The *in vivo* water concentration profiles of the stratum corneum of the arm as determined by Raman spectroscopy (figure 5a) are very similar to *in vitro* results obtained by X-ray microanalysis.^{1,2} These *in vitro* results show a continuous rise in water concentration in the stratum corneum from 15-25% at the skin surface to about 40% at the boundary between stratum corneum and stratum granulosum. This was followed by a steep rise to a constant level of about 70% in the viable cells. Our results obtained with Raman spectroscopy show a somewhat higher water content of about $30\% \pm 5\%$ at the skin surface, continuously increasing to about $65\% \pm 8\%$ at a depth of about 15 μm . If we assume, in accordance with Warner *et al* (1988) and von Zglinicki *et al* (1993), that the boundary between the stratum corneum and the stratum granulosum is located near the high end of the steep water concentration gradient, it follows from figure 5a that the stratum corneum thickness at the volar aspect of the arm is 10-15 μm . This is in agreement with known

literature values.⁴² The stratum corneum is much thicker at the thenar than at the volar aspect of the arm. Also the water profiles obtained from the thenar (figure 5b) are qualitatively and quantitatively distinct from the water profiles of the arm (figure 5a). In contrast to the arm, where the water concentration increases throughout the stratum corneum, the stratum corneum of the thenar shows only little variation in water concentration. However, a steep water gradient exists at about 80-120 μm below the skin surface, with an increase in water content from 40 (± 5) to about 60 (± 7)%. The *in vitro* results of Warner and coworkers showed a similar water discontinuity at the SC-SG boundary in the skin of the lower leg. If we again assume that this discontinuity demarcates the boundary between the flat stratum corneum cells and the water-rich cells of the viable epidermis, the Raman results imply a stratum corneum thickness at the thenar of 90-110 μm . The results of the *in vivo* Raman experiments on the arm (figure 5a) also suggest the presence of such a discontinuity. The present depth resolution of 5 μm of our setup precludes a definitive conclusion, however.

Absolute determination of water concentration by Raman spectroscopy suffers from a relatively large uncertainty caused by the relative error of 15% in the calibration constant R , which links Raman intensities to molecular concentrations (see *Data analysis*). We are investigating ways to obtain a better absolute calibration. However in many applications the determination of relative differences in water concentration is of interest, rather than the absolute water concentration. These relative differences can be determined with a much higher accuracy than the absolute water content (figure 5), because in this case only the experimental (random) errors in the determination of Raman intensities in the CH stretching region and in the water band play a role.

NMF is produced in the lower part of the stratum corneum and this would be expected to give rise to a noticeable increase in the concentration of free amino acids in this region. Therefore, it seemed likely that this would be reflected in the Raman spectra. As shown in figure 7b, the differences between the Raman spectra obtained at 60 and 70 μm below the skin surface can be almost completely accounted for by differences in the concentration of NMF-constituents. Moreover, the relative concentrations of the NMF constituents that were determined from the fitting procedure compare well to published reports on the NMF composition as determined by various *in vitro* methods (figure 8). This indicates that the changes in molecular composition observed at a depth of 60-70 μm are indeed due to a difference in the concentration of NMF-constituents.

According to Rawlings *et al* (1994) a zone of stable filaggrin exists in the lowermost part of the stratum corneum where the epidermal water barrier is formed. The conversion of filaggrin to NMF would take place above this zone, i.e. closer to the skin surface. This is consistent with our observations. The concentration profiles (figure 9) actually show that for most NMF constituents the concentration approaches zero at 70 μm below the skin surface. Between 70 and 50 μm the concentrations increase sharply and from 50 to 10 μm below the skin surface the concentrations remain constant. This suggests that, for this particular depth series, the conversion from filaggrin to NMF takes place between 50 and 70 μm below the skin surface. Sweat is excreted at the skin surface. This is reflected in the

concentration profiles of the sweat constituents lactate and urea, which have their maximum at the skin surface and drop rapidly below the surface.

If we combine the water concentration profiles (as in figure 5b) and the NMF concentration profiles (as in figure 9) the following overall picture emerges: In the stratum corneum of the thenar the zone of stable filaggrin is located between about 110 and 70 μm below the skin surface. Between 80 and 50 μm below the surface filaggrin is converted to NMF and between 50 and 10 μm no further changes take place. The concentration of NMF drops in the uppermost part of the stratum corneum.

At depths of about 80 μm or more below the skin surface the results of the quantitative analysis, which was used to determine concentration profiles, became less reliable as the residuals of the fits increased strongly. It points out that the set of fit spectra, used to model the *in vivo* spectra, does not suffice to adequately represent the actual molecular composition of the stratum corneum at depths greater than about 80 μm . This is in accordance with the fact that at this depth the zone of stable filaggrin is reached.

The concentration profiles of PCA, as determined at different locations of the thenar (figure 10), show that some variation exists in the depth at which filaggrin is converted to NMF. However, throughout the larger part of the stratum corneum (between 10-50 μm) the concentration profiles for a single subject are remarkably similar, whereas a clear difference is observed between the two subjects. These results may indicate the possibility to detect inter-personal variations in the NMF content of the stratum corneum.

Conclusions

In vivo confocal Raman microspectroscopy is a novel technique for noninvasive spatially resolved determination of molecular concentration profiles. We have demonstrated that water concentration profiles across the stratum corneum can be measured *in vivo*, both in thin and in thick stratum corneum (arm and thenar). Presently an automated depth scanning Raman instrument is being developed, which will enable the recording of a complete water concentration profile within a total signal collection time of 30-60 seconds or less. It was shown that variations in the concentration of NMF significantly contribute to the differences in Raman spectra obtained at different depths in the stratum corneum and that NMF-concentration profiles determined *in vivo* by Raman spectroscopy are in agreement with published results of *in vitro* studies.

The fact that the technique is completely noninvasive makes it uniquely suitable for studies in which changes in molecular concentrations or molecular concentration profiles are induced, e.g. by topical application of chemicals or drugs, hydration/dehydration as a result of chemical or physical challenges, or as a result of disease processes and treatments. It may therefore be expected that future confocal Raman microspectroscopic studies will generate important data related to skin physiology and pathology.

References

1. Warner, R. R., M. C. Myers, and D. A. Taylor. 1988. Electron probe analysis of human skin: determination of the water concentration profile. *J Invest Dermatol.* 90:218-24.
2. von Zglinicki, T., M. Lindberg, G. M. Roomans, and B. Forslind. 1993. Water and ion distribution profiles in human skin. *Acta Derm Venereol.* 73:340-3.
3. Kalia, Y. N., F. Pirot, R. O. Potts, and R. H. Guy. 1998. Ion mobility across human stratum corneum in vivo. *J Pharm Sci.* 87:1508-11.
4. Berardesca, E., F. Pirot, M. Singh, and H. Maibach. 1998. Differences in stratum corneum pH gradient when comparing white Caucasian and black African-American skin. *Br J Dermatol.* 139:855-7.
5. Pilgram, G. S., A. M. Van Pelt, F. Spies, J. A. Bouwstra, and H. K. Koerten. 1998. Cryo-electron diffraction as a tool to study local variations in the lipid organization of human stratum corneum. *J Microsc.* 189:71-8.
6. Higo, N., A. Naik, D. B. Bommannan, R. O. Potts, and R. H. Guy. 1993. Validation of reflectance infrared spectroscopy as a quantitative method to measure percutaneous absorption in vivo. *Pharm Res.* 10:1500-6.
7. Bommannan, D., R. O. Potts, and R. H. Guy. 1990. Examination of stratum corneum barrier function in vivo by infrared spectroscopy. *J Invest Dermatol.* 95:403-8.
8. van der Molen, R. G., F. Spies, J. M. van 't Noordende, E. Boelsma, A. M. Mommaas, and H. K. Koerten. 1997. Tape stripping of human stratum corneum yields cell layers that originate from various depths because of furrows in the skin. *Arch Dermatol Res.* 289:514-8.
9. Rawlings, A. V., I. R. Scott, C. R. Harding, and P. A. Bowser. 1994. Stratum corneum moisturization at the molecular level. *J Invest Dermatol.* 103:731-741.
10. Koyama, J., I. Horii, K. Kawasaki, Y. Nakayama, Y. Morikawa, and T. Mitsui. 1984. Free amino acids of stratum corneum as a biochemical marker to evaluate dry skin. *J Soc Cosmet Chem.* 35:183-195.
11. Meyer, W., H. M. Poehling, and K. Neurand. 1991. Intraepidermal distribution of free amino acids in porcine skin. *J Dermatol Sci.* 2:383-92.
12. Pratzel, H., and P. Fries. 1977. Modification of relative amount of free amino acids in the stratum corneum of human epidermis by special factors of the environment. I. The influence of UV-irradiation (author's transl). *Arch Dermatol Res.* 259:157-60.
13. Tabachnick, J., and J. H. LaBadie. 1970. Studies on the biochemistry of epidermis. IV. The free amino acids, ammonia, urea, and pyrrolidone carboxylic acid content of conventional and germ-free albino guinea pig epidermia. *J Invest Dermatol.* 54:24-31.
14. Tagami, H., M. Ohi, K. Iwatsuki, Y. Kanamaru, M. Yamada, and B. Ichijo. 1980. Evaluation of the skin surface hydration in vivo by electrical measurement. *J Invest Dermatol.* 75:500-7.
15. Wichrowski, K., G. Sore, and A. Khaïat. 1995. Use of infrared spectroscopy for in vivo measurement of the stratum corneum moisturization after application of cosmetic preparations. *Int J Cos Sci.* 17:1-11.
16. Pirot, F., Y. N. Kalia, A. L. Stinchcomb, G. Keating, A. Bunge, and R. H. Guy. 1997. Characterization of the permeability barrier of human skin in vivo. *Proc Natl Acad Sci U S A.* 94:1562-7.
17. Potts, R. O., D. B. Guzek, R. R. Harris, and J. E. McKie. 1985. A noninvasive, in vivo technique to quantitatively measure water concentration of the stratum corneum using attenuated total-reflectance infrared spectroscopy. *Arch Dermatol Res.* 277:489-495.

18. Lucassen, G. W., G. N. A. Van Veen, and J. A. J. Jansen. 1998. Band analysis of hydrated human skin stratum corneum ATR-FTIR spectra *in vivo*. *J Biomed Opt.* 3:267-280.
19. Koningstein, J. A. 1971. Introduction to the theory of the Raman effect. D. Reidel Publishing Company, Dordrecht.
20. Tu, A. T. 1982. Raman Spectroscopy in Biology. John Wiley & Sons Ltd, New York.
21. Carey, P. R. 1982. Biochemical applications of Raman and Resonance Raman spectroscopies. Academic Press, New York.
22. Parker, F. S. 1983. Application of infrared, Raman and resonance Raman spectroscopy in biochemistry. Plenum Press, New York.
23. Puppels, G. J. 1999. Confocal Raman microspectroscopy. *In* Fluorescent and luminescent probes for biological activity. W. Mason, editor. Academic Press, London. 377-406.
24. Barry, B. W., H. G. M. Edwards, and A. C. Williams. 1992. Fourier Transform Raman and infrared vibrational study of human skin: assignment of spectral bands. *J Raman Spectroscopy.* 23:641-645.
25. Gniadecka, M., O. F. Nielsen, S. Wessel, M. Heidenheim, D. H. Christensen, and H. C. Wulf. 1998. Water and protein structure in photoaged and chronically aged skin. *J Invest Dermatol.* 111:1129-33.
26. Schrader, B., B. Dippel, S. Fendel, S. Keller, T. Löchte, M. Riedl, R. Schulte, and E. Tatsch. 1997. NIR FT Raman spectroscopy - a new tool in medical diagnosis. *J Mol Struct.* 408/409:23-31.
27. Shim, M. G., and B. C. Wilson. 1997. Development of an *in vivo* Raman spectroscopic system for diagnostic applications. *J Raman Spectroscopy.* 28:131-142.
28. Caspers, P. J., G. W. Lucassen, R. Wolthuis, H. A. Bruining, and G. J. Puppels. 1998. *In vitro* and *in vivo* Raman spectroscopy of human skin. *Biospectroscopy.* 4:S31-39.
29. Schallreuter, K. U., J. Moore, J. M. Wood, W. D. Beazley, D. C. Gaze, D. J. Tobin, H. S. Marshall, A. Panske, E. Panzig, and N. A. Hibberts. 1999. *In vivo* and *in vitro* evidence for hydrogen peroxide (H₂O₂) accumulation in the epidermis of patients with vitiligo and its successful removal by a UVB-activated pseudocatalase [In Process Citation]. *J Invest Dermatol Symp Proc.* 4:91-6.
30. Schallreuter, K. U., M. Zschiesche, J. Moore, A. Panske, N. A. Hibberts, F. H. Herrmann, H. R. Metelmann, and J. Sawatzki. 1998. *In vivo* evidence for compromised phenylalanine metabolism in vitiligo. *Biochem Biophys Res Commun.* 243:395-9.
31. Rawlings, A., C. Harding, A. Watkinson, J. Banks, C. Ackerman, and R. Sabin. 1995. The effect of glycerol and humidity on desmosome degradation in stratum corneum. *Arch Dermatol Res.* 287:457-64.
32. Scott, I. R., C. R. Harding, and J. G. Barrett. 1982. Histidine-rich protein of the keratohyalin granules. Source of the free amino acids, urocanic acid and pyrrolidone carboxylic acid in the stratum corneum. *Biochim Biophys Acta.* 719:110-7.
33. Dale, B. A., K. A. Resing, and P. V. Haydock. 1990. Filaggrins. *In* Cell and molecular biology of intermediate filaments. R. D. Goldman and P. M. Steinert, editors. Plenum, New York. 393-412.
34. Wolthuis, R., T. C. Bakker Schut, P. J. Caspers, H. P. J. Buschman, T. J. Roemer, H. A. Bruining, and G. J. Puppels. 1999. Raman spectroscopic methods for *in vitro* and *in vivo* tissue characterization. *In* Fluorescent and luminescent probes for biological activity. W. Mason, editor. Academic Press, London. 433-455.

35. Puppels, G. J., W. Colier, J. H. F. Olminkhof, C. Otto, F. F. M. de Mul, and J. Greve. 1991. Description and performance of a highly sensitive confocal Raman spectrometer. *J Raman Spectroscopy*. 22:217-225.
36. de Faria, D. L. A., and M. A. de Souza. 1999. Raman spectra of human skin and nail excited in the visible region. *J Raman Spectroscopy*. 30:169-171.
37. Frank, C. J., D. C. B. Redd, T. S. Gansler, and R. L. McCreery. 1994. Characterization of human breast biopsy specimens with near-IR Raman spectroscopy. *Analytical Chemistry*. 66:319-326.
38. Huizinga, A., A. C. Bot, F. F. de Mul, G. F. Vrensen, and J. Greve. 1989. Local variation in absolute water content of human and rabbit eye lenses measured by Raman microspectroscopy. *Exp Eye Res*. 48:487-96.
39. Bauer, N. J., J. P. Wicksted, F. H. Jongsma, W. F. March, F. Hendrikse, and M. Motamedi. 1998. Noninvasive assessment of the hydration gradient across the cornea using confocal Raman spectroscopy. *Invest Ophthalmol Vis Sci*. 39:831-5.
40. Leikin, S., V. A. Parsegian, W. Yang, and G. E. Walrafen. 1997. Raman spectral evidence for hydration forces between collagen triple helices. *Proc Natl Acad Sci U S A*. 94:11312-7.
41. Oehman, H., and A. Vahlquist. 1998. The pH gradient over the stratum corneum differs in X-linked recessive and autosomal dominant ichthyosis: A clue to the molecular origin of the "acid skin mantle"? *J Invest Dermatol*. 111:674-677.
42. Holbrook, K. A., and G. F. Odland. 1974. Regional differences in the thickness (cell layers) of the human stratum corneum: an ultrastructural analysis. *J Invest Dermatol*. 62:415-22.

**Automated depth-scanning confocal
Raman microspectrometer for rapid in vivo
determination of water concentration
profiles in human skin**

Journal of Raman Spectroscopy
2000, 31: 813-818

Chapter

4

P.J. Caspers
G.W. Lucassen
H.A. Bruining
G.J. Puppels

Abstract

An automated confocal Raman microspectrometer for rapid measurement of molecular concentration profiles in the skin is described. It permits the successive collection of Raman spectra at a range of depths below skin surface. The axial resolution of the confocal Raman microspectrometer is $5.1 \pm 0.2\mu\text{m}$. The setup was applied to determine water concentration profiles of the stratum corneum and to determine changes therein as a result of hydration of the skin.

Introduction

The skin is composed of two major tissue layers and various sub-layers, all of which have different molecular compositions and morphologies (see figure 1). The deeper skin layer is the dermis. It has a thickness of 1-4 mm and is comprised mainly of collagen and water. The superficial skin layer is a stratified epithelium called the epidermis. The principal cells of the epidermis, keratinocytes, originate in the basal layer, at the boundary between the dermis and the epidermis and move towards the skin surface in a process of maturation and differentiation.

Once the cells reach the outer epidermis, they form the outermost skin layer, the stratum corneum. The stratum corneum consists of flattened, enucleate cells (corneocytes). These contain a large amount of the protein keratin, which makes up about 80% of the dry weight of the stratum corneum.¹ The stratum corneum is only about 15 μm thick on most parts of the body.^{2, 3} Nonetheless, it forms the body's main protective barrier against epidermal water loss. A number of skin problems, ranging from dryness or flakiness to dehydration and hypothermia in neonates, are related to an impaired stratum corneum barrier (see reviews⁴⁻⁶). Another important barrier function of the stratum corneum is to prevent microorganisms and chemical agents from entering the body. However, this also poses a major problem for transdermal drug administration.

Water is known to play an important role in the stratum corneum barrier function. Water acts as a plasticizer, keeping the stratum corneum supple and preventing cracking due to mechanical stress. Moreover, it is thought to regulate the activity of specific hydrolytic enzymes that are important for normal desquamation of corneocytes at the skin surface.^{4, 7} It is clear, therefore, that the possibility of analyzing the water content of the stratum corneum *in vivo* would be of great help in addressing many biological, medical and cosmetic research questions.

A limited number of *in vivo* techniques have been developed to study hydration and water permeability of the stratum corneum. Measurement of electrical impedance of the skin is widely used to evaluate changes in skin hydration.⁸ Other techniques include attenuated total reflectance infrared spectroscopy,⁹ nuclear magnetic resonance imaging¹⁰ and measurement of transepidermal water loss, which is the most common method to study water permeability.¹¹ However, these *in vivo* methods have in common that they provide little depth information about the water distribution in the stratum corneum. Therefore, at present, knowledge about water concentration in the skin and changes in water concentration throughout skin layers comes from invasive or *ex vivo* studies and theoretical models.^{12, 13}

Raman spectroscopy has been applied in a number of *in vitro* skin studies, addressing various issues such as transdermal drug delivery, and the characterization and classification of pathological conditions.¹⁴⁻¹⁸ *In vivo* Fourier transform (FT)-Raman spectroscopy was employed to characterize the changes in molecular composition of the skin caused by vitiligo.^{19, 20} However, in some of these studies isolation procedures involving harsh denaturing conditions were employed to prepare samples of specific tissue layers. In other *in vitro* studies employing fresh skin biopsies and in the *in vivo* FT-Raman studies the actual measuring volume of the Raman setup was not well defined, so that it is unclear how

much signal each of the different cell layers contributed to the recorded Raman spectra. We recently described an *in vivo* confocal Raman microspectrometer, which enables one to obtain Raman signals from skin tissue at various depths below skin surface.^{21, 22} Here we describe and characterize an automated version of this setup and show how it can be used to monitor changes in stratum corneum water concentration profiles due to hydration.

Materials and Methods

A detailed description of the *in vivo* confocal Raman microspectrometer that was developed in our laboratory is given elsewhere.²² Briefly, NIR laser light (here with a wavelength of 720 nm) is focused in the skin at a well defined distance from the skin surface by a microscope objective (Leica PL Fluotar 63 x 0.7). The arm or hand of a volunteer rests on an aluminum table, which contains a small, thin fused silica or CaF₂ window (figure 1). In this way the distance between the microscope objective and the interface between the window material and the skin surface is well defined and not affected by movement artifacts.

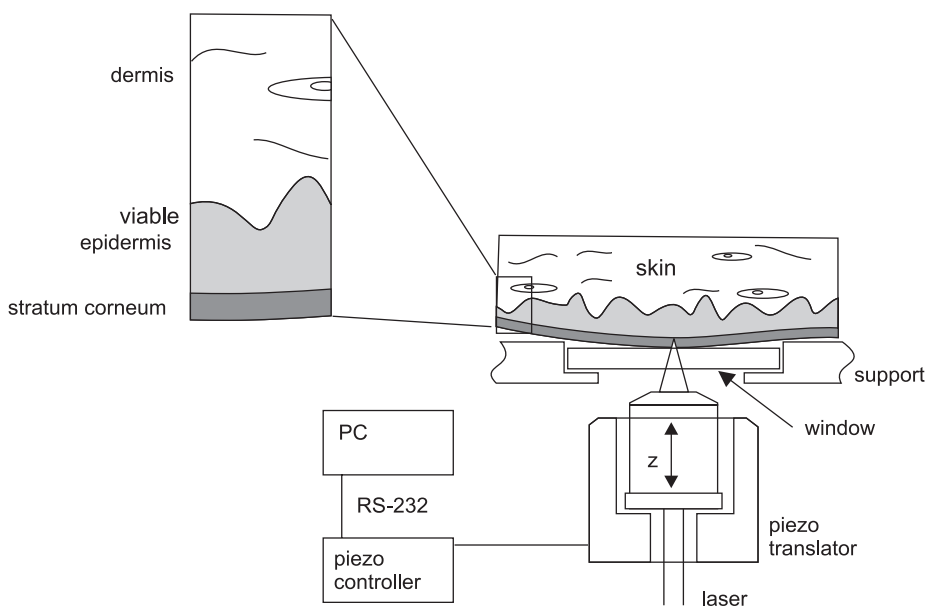


Figure 1 Schematic of the setup for automated *in vivo* confocal Raman measurements of the skin. The laser light is focused at a selected depth (or range of depths) below the skin surface, which is in contact with a fused silica window. The microscope objective is mounted on a computer controlled piezo translator to enable rapid and accurate vertical positioning. The inset shows a magnification of the various skin layers. At the volar aspect of the forearm the thickness of the viable epidermis is about 30 μm and the thickness of the stratum corneum about 13 μm .^{2,3}

Light that is scattered by the tissue is collected by the same microscope objective. After suppression of the intensity of the scattered laser light by a dielectric high pass filter it is focused onto an optical fiber connected to the spectrograph. The core of this optical fiber (100 μm diameter) acts as a confocal pinhole that rejects signal coming from out-of-focus regions of the skin.^{23, 24} This setup was adapted to allow the rapid automated determination of molecular concentration profiles. To this end, the microscope objective was mounted in a PIFOC piezo flexure nanopositioner, equipped with a LVDT sensor (Linear Variable Differential Transformer) and operating in closed loop (Physik Instrumente, Waldbronn, Germany). The use of this piezo positioner results in rapid and highly accurate axial positioning of the laser focus. The PIFOC provides zero stiction/friction travel over a 350 μm range, with high linearity (typically 0.1%, closed loop) and full range repeatability of about 60 nm. The controller of the PIFOC was operated from a personal computer, which permits fully automated recordings at predefined depths below the skin surface. Communication between the PC and the PIFOC controller was established in WinSpec macro language (Princeton Instruments Benelux Office, Groenekan, The Netherlands), using the RS-232 protocol. WinSpec was provided with the Princeton Instruments CCD detector as a control and data acquisition software package.

Calibration and sensitivity correction

Previously we reported the use of Raman standards for wavenumber calibration in the 400-1850 cm^{-1} spectral interval.^{22, 25, 26} However, these Raman standards do not provide enough Raman bands in the high wavenumber region (about 2500-3800 cm^{-1}) to make this method suitable for calibration. For this reason we used the lines of a neon-argon lamp for calibration of the wavenumber axis in absolute wavenumbers. The 3056.4 cm^{-1} band of naphthalene was then used to accurately determine the laser excitation wavelength and to transform the absolute wavenumber axis to relative wavenumbers. The estimated accuracy of the relative wavenumber axis is 2 cm^{-1} . This is sufficient for the present application, which makes use of signal intensities integrated over more than 50 cm^{-1} . For applications that require a better wavenumber accuracy, e.g. for band fitting of the OH stretch modes of water, the accuracy may be improved by using several Raman lines for the transformation from absolute to relative wavenumbers. All Raman spectra were corrected for the wavelength dependent detection efficiency of the setup, using a calibrated tungsten band-lamp.²⁵

Axial resolution

Maize oil was placed on the fused silica window of the setup (thickness 0.2 mm) and a series of Raman spectra was measured at 0.5 μm depth increments, starting with the laser focused at 20 μm below the fused silica-oil interface. The step response of the setup was calculated by integrating the Raman oil signal from 2800 to 3050 cm^{-1} and plotting this integrated intensity as a function of position of the laser focus. The step response function was smoothed (three points running average) and differentiated, which yields the impulse response. This impulse response can be regarded as the relative Raman signal intensity

obtained from an infinitesimal thin planar source as a function of its distance to the focal plane of the setup. The axial resolution was defined as the full width at half maximum (FWHM) of this impulse response.

Calibration of the water content

The water content in tissue can be determined from the ratio of Raman intensities of the OH stretch vibration of water at 3390 cm^{-1} and the CH_3 stretch of protein at 2935 cm^{-1} . This method has been used before to determine the water content in eye lenses²⁷ and corneas.²⁸ For determination of water/protein ratios in the skin we used the ratio of the integrated intensities of water ($3350\text{--}3550\text{ cm}^{-1}$) and protein ($2910\text{--}2965\text{ cm}^{-1}$), in order to maximize the signal-to-noise ratio and to avoid overlap of the water signal with the NH vibration of protein at 3329 cm^{-1} . A simple method was used to correct for signal contributions due to a usually small fluorescent background. A straight line, drawn through the spectrum points at 2600 cm^{-1} and 3800 cm^{-1} was used as the baseline for the water/protein ratio calculation explained above. The procedure is illustrated in figure 2.

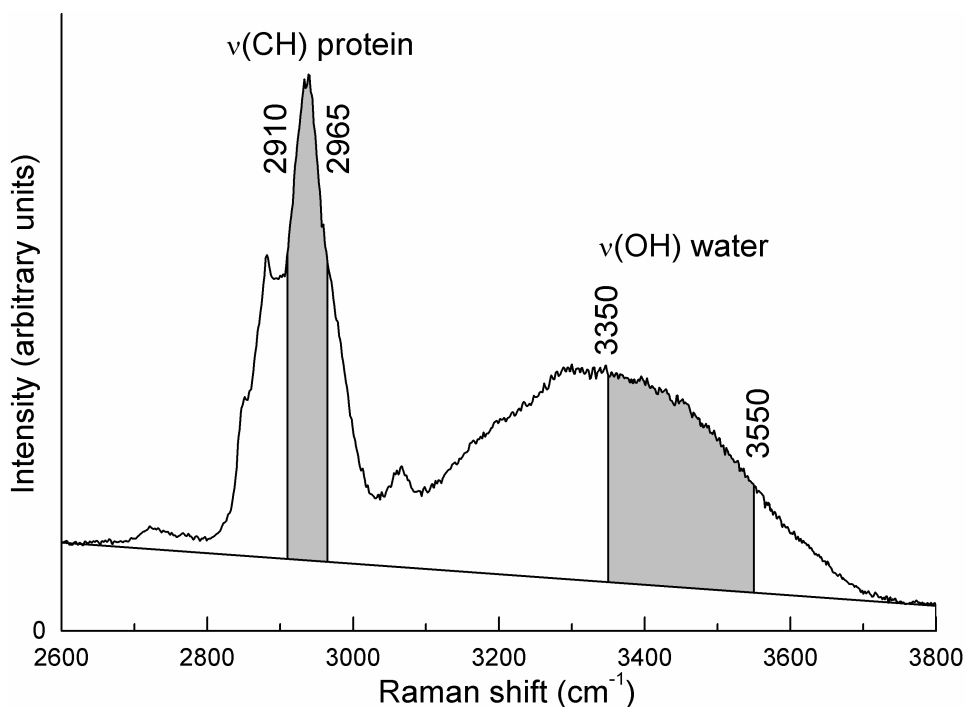


Figure 2 *In vivo* Raman spectrum of the stratum corneum obtained at the volar aspect of the arm. The water protein ratio is calculated as the ratio between the integrated signal intensities of the gray areas (see text for details). Experimental conditions: Signal collection time: 3 s, laser power: 100 mW, excitation wavelength: 720 nm.

Solutions of known concentrations of bovine serum albumin (BSA) in water were used for calibration in mass percentage or grams of water per 100 g (wet weight) of tissue. Raman spectra were measured of solutions of 20-40% albumin in water (wet weight percentages), of solid albumin, and of water. The limited solubility of albumin precluded the use of solutions containing more than 40 wt%.

Skin hydration experiments

Hydration experiments were carried out on four volunteers (two male, aged 28 and 30 years; two female, aged 21 and 30 years) on the volar aspect of the forearm. Representative results obtained with two of the volunteers (one male, aged 30 years; one female, aged 21 years) are shown in this paper. Water concentration profiles were obtained by measuring Raman spectra at a range of depths below the skin surface with 2 μm depth increments. The signal collection time was 5 s per spectrum. This was increased to 10 s at depths more than ~ 20 μm below the skin surface, owing to the decreased signal intensity at greater depths. The intensity of the protein signal (2910-2965 cm^{-1}) was used to determine the precise location of the interface between the fused-silica window and the skin. If the focal plane is located at this junction, half of the measuring volume is in the skin. Therefore, the location of the skin surface was defined as the position of 50% of the maximum protein signal.

Before hydration, several water concentration profiles were measured at different spots of the arm. The skin was then hydrated for 45 min through the application of a wet bandage, which was covered with Parafilm. Recording of water profiles of hydrated skin was initiated directly after removal of the bandage.

Results and Discussion

Setup

In the original setup the microscope objective was mounted on a manually operated translation stage. In order to record a series of measurements at a range of depths below the skin surface, the microscope objective had to be repositioned manually between consecutive measurements. This meant that the duration of the experiment was determined by the repositioning of the objective, rather than by the actual exposure time. Especially when water concentrations are being determined one may expect hydration levels of the skin to be influenced by occlusion in the course of the experiment due to the skin being in contact with the window. Therefore, the manual translation stage was replaced by a computer controlled piezo-positioner (see *Materials and Methods* for details). This allows fast, computer controlled, high-precision adjustment of the microscope objective and completely automated measurements. In this way the duration of a series of measurements is determined by the signal collection time and detector read-out time only.

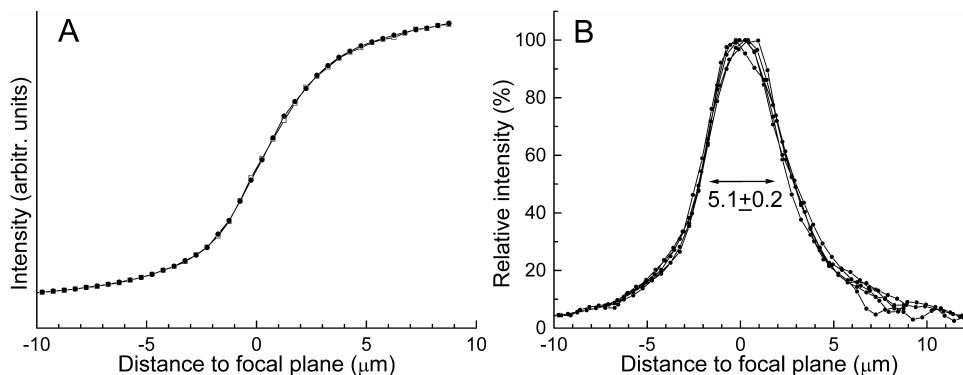


Figure 3 Determination of the axial resolution of the Raman setup. (A) Step response at a fused silica-oil interface, showing the integrated Raman signal intensity of oil (2800-3050 cm^{-1} spectral interval) as a function of the distance between the fused silica-oil interface and the focal plane. The step response was determined for two scanning directions. (B) Derivatives of 5 step response curves of a fused silica-oil interface, measured at 3 different days. The average FWHM is $5.1 \pm 0.2 \mu\text{m}$. Experimental conditions: microscope objective: 63x; NA 0.70; scan-step size: $0.5 \mu\text{m}$; signal collection time per spectrum: 3 s; laser power: 100 mW; excitation wavelength: 720 nm.

Axial and lateral resolutions determine the volume from which Raman signal is collected. In the present work only axial resolution is of interest. In confocal microscopy the axial resolution is often determined by measuring the signal response of a point object, e.g. moving a mirror through the laser focus and detecting the reflected light that passes the pinhole.²⁹ For optical sectioning in a tissue, a more appropriate method is to determine the response of a thin planar object. Here such an object was simulated by an interface between two materials. Figure 3A shows two step response curves of the setup for a fused silica-oil interface, measured in opposite directions, i.e. scanning through the interface in the direction from fused silica towards oil and vice versa. Clearly, the curves are nearly identical and free of hysteresis. Figure 3B shows the derivatives of the step response curves for oil, measured on three different days. The curves are normalized to maximum intensity and centered horizontally. The axial resolution of the confocal setup, defined as the width of the response curve (see figure 3B) at 50% of the maximum signal (FWHM), is $5.1 \pm 0.2 \mu\text{m}$. The axial resolution depends on a number of parameters, including the numerical aperture of the microscope objective, the laser and Raman wavelengths, the magnification of the image on the confocal pinhole (in this case the core of the optical fiber) and optical aberrations due to refractive index mismatches at the air-quartz and quartz-skin boundaries.²⁹ Studies using *in vivo* confocal imaging microscopy of skin have reported axial resolutions of about 1-3 μm .^{3,30} It is reasonable, therefore, to expect that the axial resolution of the present Raman setup can still be improved if needed, e.g. by employing a higher numerical aperture (NA) objective and by improving the refractive index match between the window material and the skin surface.

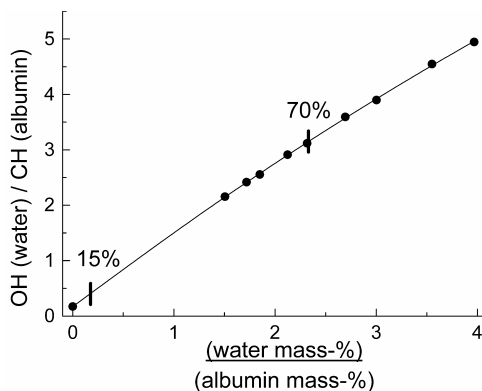


Figure 4 Plot of the intensity ratio $I_{\text{OH, water}} / I_{\text{CH, albumin}}$ as a function of the mass-ratio water/albumin for a range of concentrated albumin solutions. The line represents a second-order polynomial least-squares fit through the data points. The bars at 15% and 70% mark the physiological water concentration range in skin.

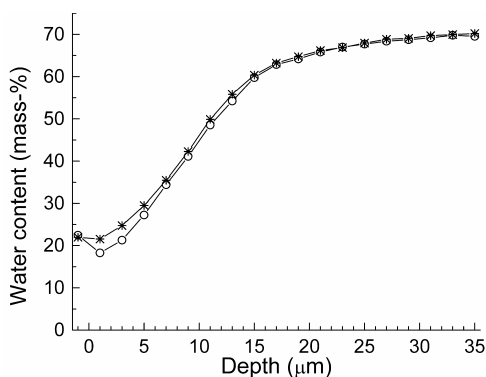


Figure 5 Consecutive *in vivo* water concentration profiles of the stratum corneum measured at one spot on the volar aspect of the arm: (o) from the skin surface towards the viable epidermis, (*) from the viable epidermis to the skin surface. Experimental conditions: signal collection time: 3 s per data point; step size: 2 μm ; laser power: 100 mW; excitation wavelength: 720 nm.

Hydration experiments

The ratio of the Raman signal intensities of the CH stretching band (I_{CH} : 2910-2965 cm^{-1}) and the OH stretching band (I_{OH} : 3350-3550 cm^{-1}) was used to obtain a measure of the water concentration in the stratum corneum. The dry weight of the stratum corneum is largely determined by protein (80%).¹ In order to determine absolute water concentrations the $I_{\text{CH}}/I_{\text{OH}}$ ratio was calibrated by recording Raman spectra of albumin solutions of known concentrations. In figure 4 the ratio $I_{\text{OH}}/I_{\text{CH}}$ is plotted as a function of the water/protein mass-ratio. Although a linear relationship would be expected, some non-linearity is evident. This is because a tail of the water signal overlaps with the protein sig-

nal, the effects of which become evident at higher water concentrations. Therefore, a second-order polynomial was fitted to the data points in figure 4 and used to transform Raman intensity ratios into absolute water concentrations in skin.

The determination of absolute water concentrations in skin can perhaps be improved by using multiple least-squares fitting or band fitting methods. This would also give the interesting opportunity to use the shape of the water spectrum in the OH stretching region to obtain information about the ratio between bound and free water.³¹⁻³³

Figure 5 shows two consecutive water concentration profiles that were calculated from *in vivo* Raman spectra obtained at the volar aspect of the arm. The two profiles are the result of two consecutive Raman scans in opposite directions, i.e. from the skin surface into the skin and back. The differences between the profiles are very small. This illustrates that the influence of skin hydration caused by occlusion is small, within the time that was needed to complete the automated sequence (less than 3 min). In the experiments described here, relatively long signal integration times were used. In principle the signal integration time can be reduced to 1-2 s per spectrum instead of the 5-10 s used here. The signal-to-noise ratio of the spectra will be reduced but since in the determination of the water concentration the Raman signal is integrated over large wavenumber intervals, this does not affect the results. It is therefore possible to determine water concentration profiles for the stratum corneum in about 30 s. Figure 6 shows representative *in vivo* water concentration profiles for normal and hydrated stratum corneum of the arm, obtained from two of a total of four volunteers. The water concentration is low in the stratum corneum (15-30%) and increases rapidly across the boundary between the stratum corneum and the viable epidermis (located at 10-15 μm below the skin surface) where it reaches a concentration of about 70%. A more detailed discussion of the water concentration profile in non-hydrated stratum corneum will be given elsewhere.²¹ The results for non-hydrated skin are in good agreement (both qualitatively and quantitatively) with *in vitro* results obtained by X-ray microanalysis of thin tissue sections.^{34, 35}

The water concentration profiles of hydrated skin (figure 6C and 6D) clearly show a higher water content in the stratum corneum. However, in the viable cells of the epidermis (about 15-20 μm below the surface) the water content reaches a constant value of about 70%, as in non-hydrated skin. The profiles in figure 6 were obtained from different spots on the arm and therefore reflect local variations in the water distribution. Especially hydrated stratum corneum reveals local structures with higher and lower water content, such as the local maximum about 10 μm below the skin surface. Further interpretation of the origin of these local structures will benefit from a combination of Raman spectroscopy with an imaging technique. We are currently investigating the feasibility to combine *in vivo* Raman spectroscopy with confocal video reflectance microscopy.³

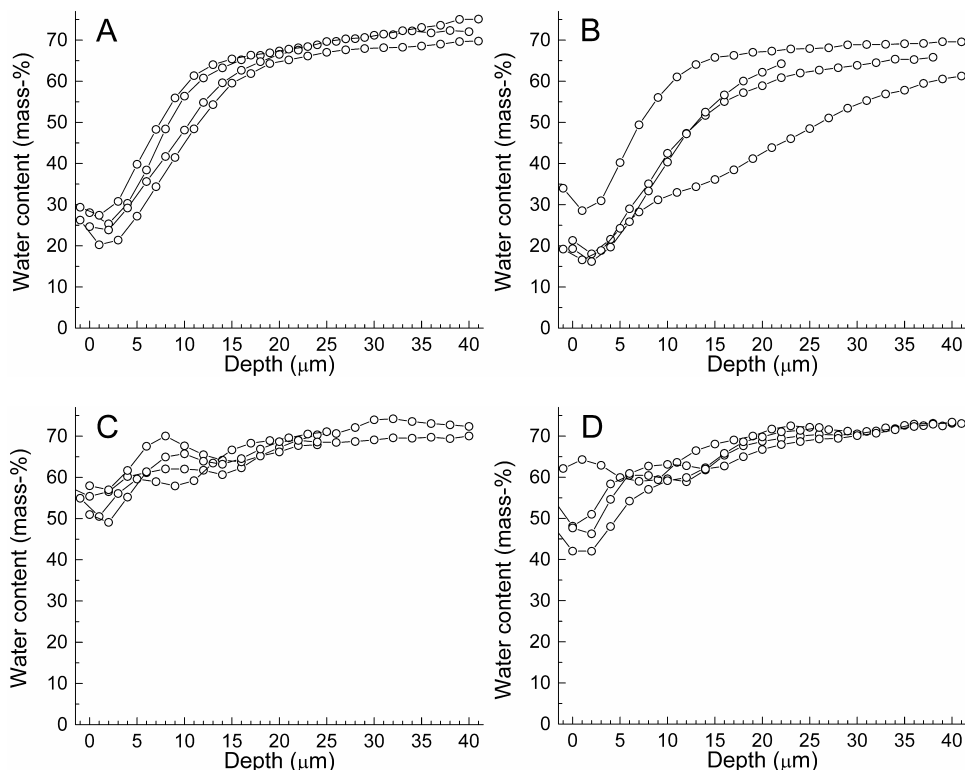


Figure 6 *In vivo* water concentration profiles of hydrated and non-hydrated skin of healthy volunteers. Each curve was measured at a different position on the volar aspect of the arm: (A) man (aged 30 years), before hydration; (B) woman (aged 21 years), before hydration; (C) man, after hydration; (D) woman, after hydration. Experimental conditions: exposure time: 5 s per data point, 10 s at depths greater than 20 μm ; scan-step size: 2 μm ; laser power: 100 mW; excitation wavelength: 720 nm.

Conclusions

An automated *in vivo* confocal Raman microspectrometer was described and characterized that allows rapid, spatially resolved, determination of the water content in the skin. We have demonstrated this by determining water concentration profiles for the stratum corneum of the arm, before and after hydration of the skin.

In vivo confocal Raman microspectroscopy has the unique advantage of noninvasive, spatially resolved depth profiling of skin hydration. Therefore, this technique offers great possibilities for a range of medical, cosmetic and pharmaceutical studies, e.g. addressing the interaction between water and other skin compounds (leading to part of the water molecules being present in bound form), interpersonal variations in skin hydration, the influence of various environmental challenges (season, climate) and the influence of aging. It can also be applied to monitor effects of hydrating compounds and cosmetics to the skin.

References

1. Steinert, P. M., and I. M. Freedberg. 1991. Molecular and cellular biology of keratins. *In* Physiology, biochemistry and molecular biology of the skin. L. A. Goldsmith, editor. Oxford University Press, New York. 113-147.
2. Holbrook, K. A., and G. F. Odland. 1974. Regional differences in the thickness (cell layers) of the human stratum corneum: an ultrastructural analysis. *J Invest Dermatol.* 62:415-22.
3. Corcuff, P., and J. L. Leveque. 1993. In vivo vision of the human skin with the tandem scanning microscope [see comments]. *Dermatology.* 186:50-4.
4. Rawlings, A. V., I. R. Scott, C. R. Harding, and P. A. Bowser. 1994. Stratum corneum moisturization at the molecular level. *J Invest Dermatol.* 103:731-741.
5. Wertz, P. W., and D. T. Downing. 1991. Epidermal lipids. *In* Physiology, Biochemistry and molecular Biology of the Skin. L. A. Goldsmith, editor. Oxford University Press, New York. 205-236.
6. Lavrijsen, A. P., J. A. Bouwstra, G. S. Gooris, A. Weerheim, H. E. Bodde, and M. Ponc. 1995. Reduced skin barrier function parallels abnormal stratum corneum lipid organization in patients with lamellar ichthyosis. *J Invest Dermatol.* 105:619-624.
7. Rawlings, A., C. Harding, A. Watkinson, J. Banks, C. Ackerman, and R. Sabin. 1995. The effect of glycerol and humidity on desmosome degradation in stratum corneum. *Arch Dermatol Res.* 287:457-64.
8. Tagami, H., M. Ohi, K. Iwatsuki, Y. Kanamaru, M. Yamada, and B. Ichijo. 1980. Evaluation of the skin surface hydration in vivo by electrical measurement. *J Invest Dermatol.* 75:500-7.
9. Potts, R. O., D. B. Guzek, R. R. Harris, and J. E. McKie. 1985. A noninvasive, in vivo technique to quantitatively measure water concentration of the stratum corneum using attenuated total-reflectance infrared spectroscopy. *Arch Dermatol Res.* 277:489-495.
10. Querleux, B., S. Richard, J. Bittoun, O. Jolivet, I. Idy-Peretti, R. Bazin, and J. L. Leveque. 1994. In vivo hydration profile in skin layers by high-resolution magnetic resonance imaging. *Skin Pharmacol.* 7:210-6.
11. Barel, A. O., and P. Clarys. 1995. Comparison of methods for measurement of transepidermal water loss. *In* Non-invasive methods and the skin. J. Serup and G. B. E. Jemec, editors. CRC Press, Boca Raton. 179-184.
12. Stockdale, M. 1978. Water diffusion coefficients versus water activity in stratum corneum: a correlation and its implications. *J Soc Cosmet Chem.* 29:625-639.
13. Elsner, P., E. Berardesca, and H. I. Maibach. 1994. Bioengineering of the skin: Water and the stratum corneum. *In* Dermatology: Clinical and basic science. H. I. Maibach, editor. CRC Press, Ann Arbor.
14. Anigbogu, A. N. C., A. C. Williams, B. W. Barry, and H. G. M. Edwards. 1995. Fourier transform Raman spectroscopy of interactions between the penetration enhancer dimethyl sulfoxide and human stratum corneum. *Int J Pharm.* 125:265-282.
15. Gniadecka, M., H. C. Wulf, O. Faurskov Nielsen, D. H. Christensen, and J. Hercogova. 1997. Distinctive molecular abnormalities in benign and malignant skin lesions: Studies by Raman spectroscopy. *Photochem Photobiol.* 66:418-423.

16. Gniadecka, M., H. C. Wulf, N. Nymark Mortensen, O. Feurskov Nielsen, and D. H. Christensen. 1997. Diagnosis of basal cell carcinoma by Raman spectroscopy. *J Raman Spectroscopy*. 28:125-130.
17. Schrader, B., B. Dippel, S. Fendel, S. Keller, T. Löchte, M. Riedl, R. Schulte, and E. Tatsch. 1997. NIR FT Raman spectroscopy - a new tool in medical diagnosis. *J Mol Struct*. 408/409:23-31.
18. Wessel, S., M. Gniadecka, G. B. Jemec, and H. C. Wulf. 1999. Hydration of human nails investigated by NIR-FT-Raman spectroscopy. *Biochim Biophys Acta*. 1433:210-6.
19. Schallreuter, K. U., J. Moore, J. M. Wood, W. D. Beazley, D. C. Gaze, D. J. Tobin, H. S. Marshall, A. Panske, E. Panzig, and N. A. Hibberts. 1999. In vivo and in vitro evidence for hydrogen peroxide (H₂O₂) accumulation in the epidermis of patients with vitiligo and its successful removal by a UVB-activated pseudocatalase [In Process Citation]. *J Invest Dermatol Symp Proc*. 4:91-6.
20. Schallreuter, K. U., M. Zschesche, J. Moore, A. Panske, N. A. Hibberts, F. H. Herrmann, H. R. Metelmann, and J. Sawatzki. 1998. In vivo evidence for compromised phenylalanine metabolism in vitiligo. *Biochem Biophys Res Commun*. 243:395-9.
21. Caspers, P. J., G. W. Lucassen, E. A. Carter, H. A. Bruining, and G. J. Puppels. 2001. In vivo confocal Raman microspectroscopy of the skin: noninvasive determination of molecular concentration profiles. *J Invest Dermatol*. 116:434-442.
22. Caspers, P. J., G. W. Lucassen, R. Wolthuis, H. A. Bruining, and G. J. Puppels. 1998. In vitro and in vivo Raman spectroscopy of human skin. *Biospectroscopy*. 4:S31-39.
23. Puppels, G. J. 1999. Confocal Raman microspectroscopy. In *Fluorescent and luminescent probes for biological activity*. W. Mason, editor. Academic Press, London. 377-406.
24. Puppels, G. J., W. Colier, J. H. F. Olminkhof, C. Otto, F. F. M. de Mul, and J. Greve. 1991. Description and performance of a highly sensitive confocal Raman spectrometer. *J Raman Spectroscopy*. 22:217-225.
25. Wolthuis, R., T. Bakker Schut, P. Caspers, H. Buschman, T. Roemer, H. Bruining, and G. Puppels. 1999. Raman spectroscopic methods for in vitro and in vivo tissue characterization. In *Fluorescent and luminescent probes for biological activity*. W. Mason, editor. Academic Press, London. 433-455.
26. McCreery, R. L. 1996. . In *Modern techniques in Raman spectroscopy*. J. J. Laserna, editor. John Wiley & Sons, Chichester. 41-72.
27. Huizinga, A., A. C. Bot, F. F. de Mul, G. F. Vrensen, and J. Greve. 1989. Local variation in absolute water content of human and rabbit eye lenses measured by Raman microspectroscopy. *Exp Eye Res*. 48:487-96.
28. Bauer, N. J., J. P. Wicksted, F. H. Jongsma, W. F. March, F. Hendrikse, and M. Motamedi. 1998. Noninvasive assessment of the hydration gradient across the cornea using confocal Raman spectroscopy. *Invest Ophthalmol Vis Sci*. 39:831-5.
29. Sheppard, C. J., M. Gu, K. Brian, and H. Zhou. 1994. Influence of spherical aberration on axial imaging of confocal reflection microscopy. *Applied Optics*. 33:616-624.
30. Rajadhyaksha, M., M. Grossman, D. Esterowitz, R. H. Webb, and R. R. Anderson. 1995. In vivo confocal scanning laser microscopy of human skin: melanin provides strong contrast. *J Invest Dermatol*. 104:946-52.

31. Gniadecka, M., O. Faurskov Nielsen, D. H. Christensen, and H. C. Wulf. 1998. Structure of water, proteins, and lipids in intact human skin, hair, and nail. *J Invest Dermatol.* 110:393-8.
32. Scherer, J. R., M. K. Go, and S. Kint. 1973. Raman spectra and structure of water in dimethyl sulfoxide. *J Phys Chem.* 77:2108-2117.
33. Leikin, S., V. A. Parsegian, W. Yang, and G. E. Walrafen. 1997. Raman spectral evidence for hydration forces between collagen triple helices. *Proc Natl Acad Sci US A.* 94:11312-7.
34. von Zglinicki, T., M. Lindberg, G. M. Roomans, and B. Forslind. 1993. Water and ion distribution profiles in human skin. *Acta Derm Venereol.* 73:340-3.
35. Warner, R. R., M. C. Myers, and D. A. Taylor. 1988. Electron probe analysis of human skin: determination of the water concentration profile. *J Invest Dermatol.* 90:218-24.

Monitoring the penetration enhancer dimethyl sulfoxide in human stratum corneum in vivo by confocal Raman spectroscopy

Pharmaceutical Research
2002, 19(10): 1577-1580
Short Communications

Chapter

5

P.J. Caspers
A.C. Williams
E.A. Carter
H.G.M. Edwards
B.W. Barry
H.A. Bruining
G.J. Puppels

Introduction

The stratum corneum (SC) barrier typically consists of layers of corneocytes embedded in a lipid continuum that regulates barrier function. The lipid domain, containing ceramides, cholesterol and free fatty acids, provides the major pathway for most drugs permeating across the SC.¹

Penetration enhancers diminish the SC barrier function. The classic enhancer is dimethyl sulfoxide (DMSO).² Its mechanisms of action remain unclear although DMSO disrupts lipid organization and may displace protein-bound water.³

Here we use confocal Raman spectroscopy to probe molecular interactions between a finite (depleting) dose of DMSO and SC, as functions of depth and time, providing novel information about residence time and location of DMSO in human SC *in vivo*.

Materials and Methods

A confocal Raman microspectrometer, described elsewhere,⁴⁻⁶ acquired data with a depth resolution (for planes) of 5 μm .⁶ A palm was positioned on an aluminium stage containing a CaF_2 window; this served as a reference plate to determine skin surface position and prevent movement artifacts. Spectra were calibrated and corrected for the instrument response.⁷

Raman spectra from a male and female were recorded from the ball of palm (30 seconds with 100 mW laser power on the skin). Sites were briefly cleaned with 97% ethanol.

Spectra from untreated SC were collected then 4 μL of 80% v/v DMSO in a 5% v/v propylene glycol:water solution was placed within a template. After ambient drying, the template was removed and the skin surface was rinsed with pure water. A fresh template located the marked application site during spectral collection. The first spectra were obtained approximately 15 min after DMSO application. Next day the area was briefly cleaned and spectra were collected from the palm surface inwards in 10 μm increments to 120 μm .

Results and Discussion

When investigating skin distribution of chemicals it is necessary to establish which tissue layer, SC or viable epidermis (VE), is sampled. Thus depth profiles from untreated SC identified indicators for when the laser no longer probed the SC but sampled the VE.

Depth profile of untreated palmar SC

Figure 1 presents spectra from within untreated palmar SC (not scaled but offset for clarity). Intensity differences with depth are notable; the skin surface (0 μm) provides a much lower intensity than from 10 μm , since at the surface only half of the measuring volume probes skin and the remainder locates in the CaF_2 window. Remaining spectra decrease in intensity as the laser focuses deeper into the skin, partly due to elastic light scattering, which strengthens with increasing light path. The spectrum 120 μm below the surface is

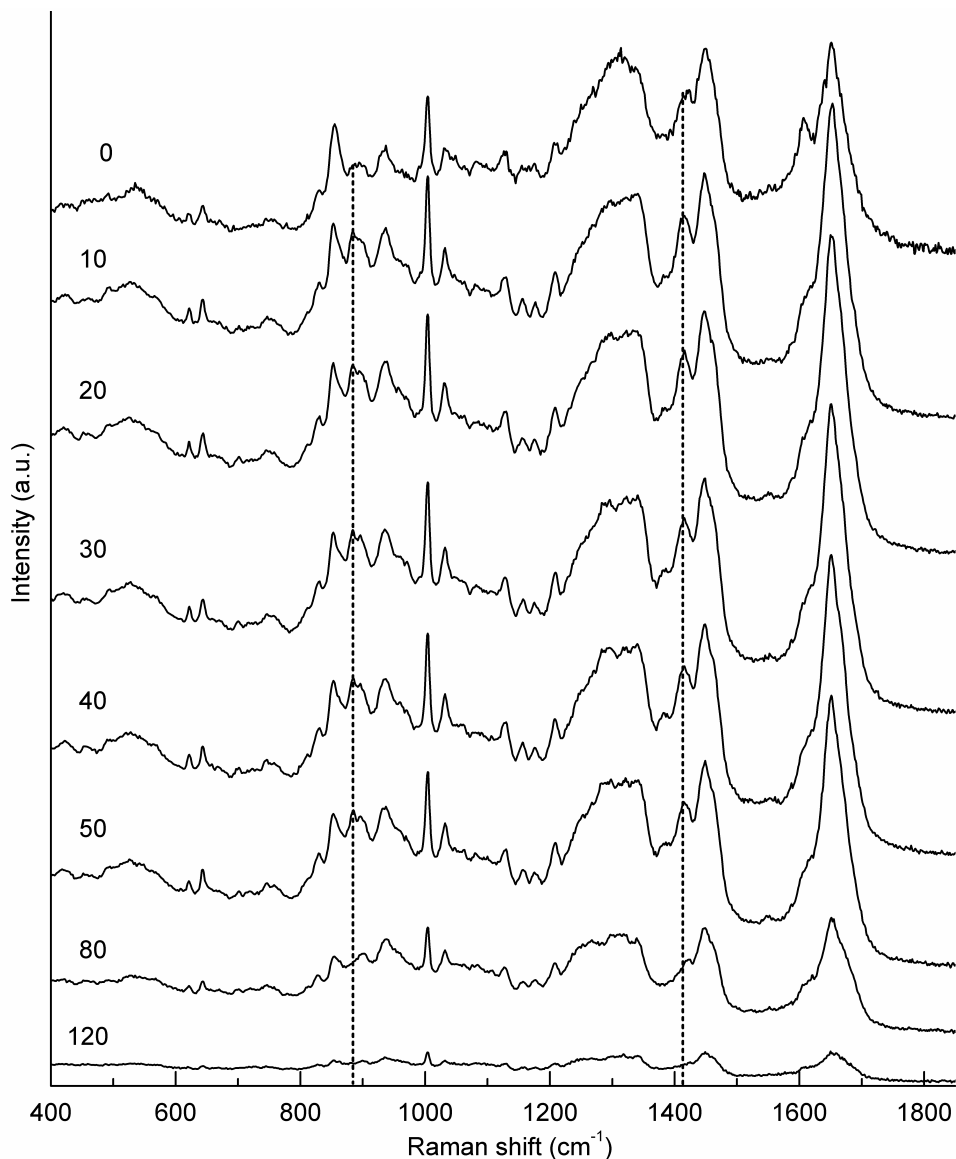


Figure 1. *In vivo* Raman depth profile of untreated palm (0 – 120 μm). Spectra are to scale and offset along intensity axis for clarity. The dashed lines indicate some vibrational modes originating from the natural moisturizing factor.

markedly less intense compared with that at 80 μm , consistent with the scatter coefficient being higher in viable epidermis than in the SC. Another factor affecting signal intensity is increased water concentration in lower regions of the SC, effectively reducing the signal contribution of lipids and proteins.^{6,7}

Spectral intensity decreases may indicate that VE is assessed instead of denser SC, but overall signal intensity does not designate clearly the skin layers. Chemically based markers were therefore used to distinguish between SC and VE. Natural moisturizing factor (NMF) is a mixture of amino acids, their derivatives and salts produced in the lower SC. The concentration of these constituents change markedly just above the SC/stratum granulosum boundary.⁵

We determined NMF-to-protein signal ratios⁵ as a function of palm skin depth, to identify spectral markers useful for distinguishing between SC and VE (figure 2). NMF concentration drops rapidly between about 60 and 80 μm below the surface. Since NMF is in the SC only, this implies that palm SC has a thickness of about 80 μm . NMF vibrations at 1415 cm^{-1} (mainly from glycine, serine and alanine) and 885 cm^{-1} (from pyrrolidone-5-carboxylic acid) are usually well resolved with *in vivo* Raman spectra of the SC. For example (figure 1, arrowed), these vibrations are clear down to 50 μm , but disappear between 80 and 120 μm , indicating that here NMF is absent and the SC is no longer sampled. Thus NMF presence can be verified from vibrations at 1415 and 885 cm^{-1} , and hence these provide convenient markers to distinguish between SC and VE. However, we have determined NMF concentration profiles to distinguish unambiguously between skin layers.

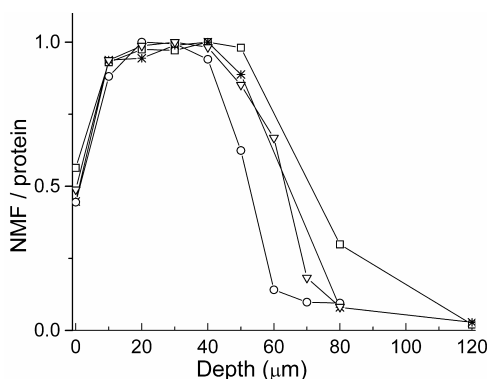


Figure 2. Concentration profiles of natural moisturizing factor (NMF) in palmar stratum corneum, normalized to maximum concentration. The left-hand ordinate represents ratio between the Raman signal intensity of NMF and of keratin.

Depth profile of palmar SC treated with DMSO

80% v/v DMSO in 5% v/v PG/water (application mixture) possesses distinctive characteristic bands, notably a strong doublet at 671 and 702 cm^{-1} , assigned to symmetric and asymmetric $\nu(\text{CSC})$ modes respectively, and a broad 1030/1048 cm^{-1} band assigned to $\nu(\text{S}=\text{O})$ stretching.

Figure 3 illustrates data of DMSO in palmar SC collected 15 to 20 min after application. Compared with application mixture, DMSO in the SC shows major shifts in several vibration positions; the $\nu(\text{S}=\text{O})$ feature shifts to 1017 cm^{-1} and the 671/702 cm^{-1} $\nu(\text{CSC})$ doublet presents at 677/711 cm^{-1} .

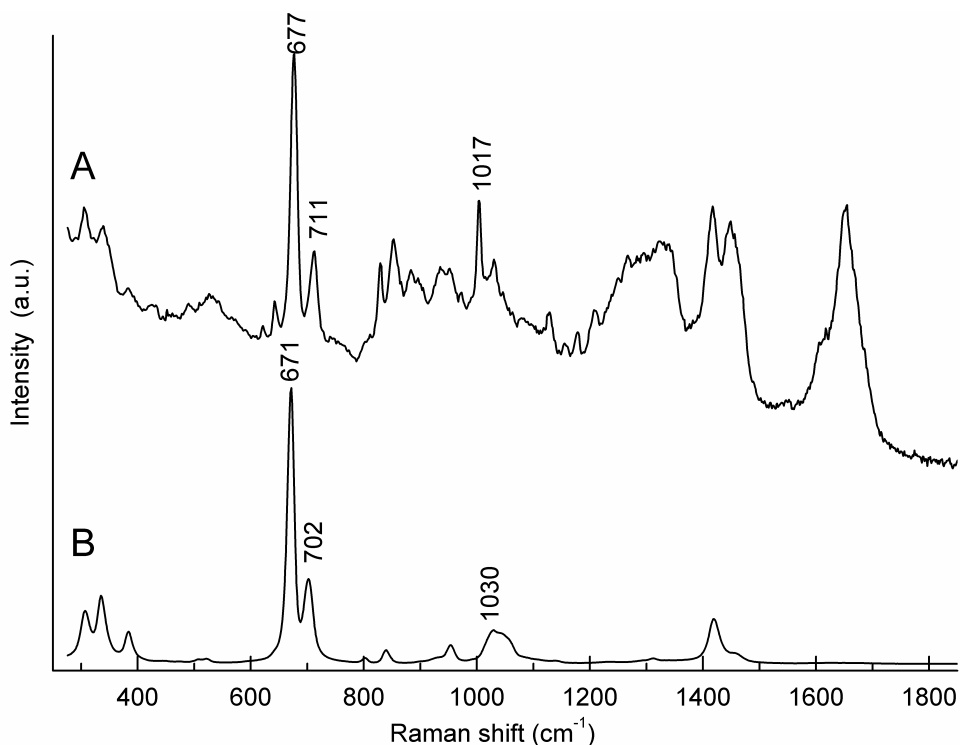


Figure 3. (A) Raman spectrum of palmar stratum corneum treated with dimethyl sulfoxide (DMSO), 17 min after application. Recording depth is 20 μm below the skin surface; (B) Raman spectrum of DMSO application mixture (80% v/v DMSO in 5% v/v PG/water).

DMSO complexes with water through dipole-dipole and hydrogen bonding interactions that are stronger than those formed between water molecules.⁸ DMSO also associates with polar portions of lipids and replaces water molecules as hydrogen bond acceptor, thereby associating with the N-H and C=O protein moieties. Significant, reproducible wavenumber shifts (figure 3) indicate DMSO interaction with one or more of these skin components.

Raman microscopic depth-profiling studied DMSO-treated palm SC over 72 hours. The DMSO vibrations dominated spectra obtained 15-20 min and 3½ h after treatment, and were strongest at the palm surface and to 30 μm deep. After 72 h, the only DMSO vibration discerned was the very strong $\nu(\text{CSC})$ mode at 677 cm^{-1} , appearing as a relatively weak signal in the SC. These depth profiles indicated that some of the DMSO remained in the SC for at least up to 72 h.

To examine the distribution of DMSO through the SC *in vivo* with time, we measured areas of $\delta(\text{CH}_2)$ vibration at 1450 cm^{-1} (integrated signal intensity of 1430-1470 cm^{-1} interval) from SC proteins and the $\nu(\text{CSC})$ band of DMSO at 677 cm^{-1} (integrated signal intensity of 661-691 cm^{-1} interval); area ratios of the DMSO/protein bands (A_{677}/A_{1450})

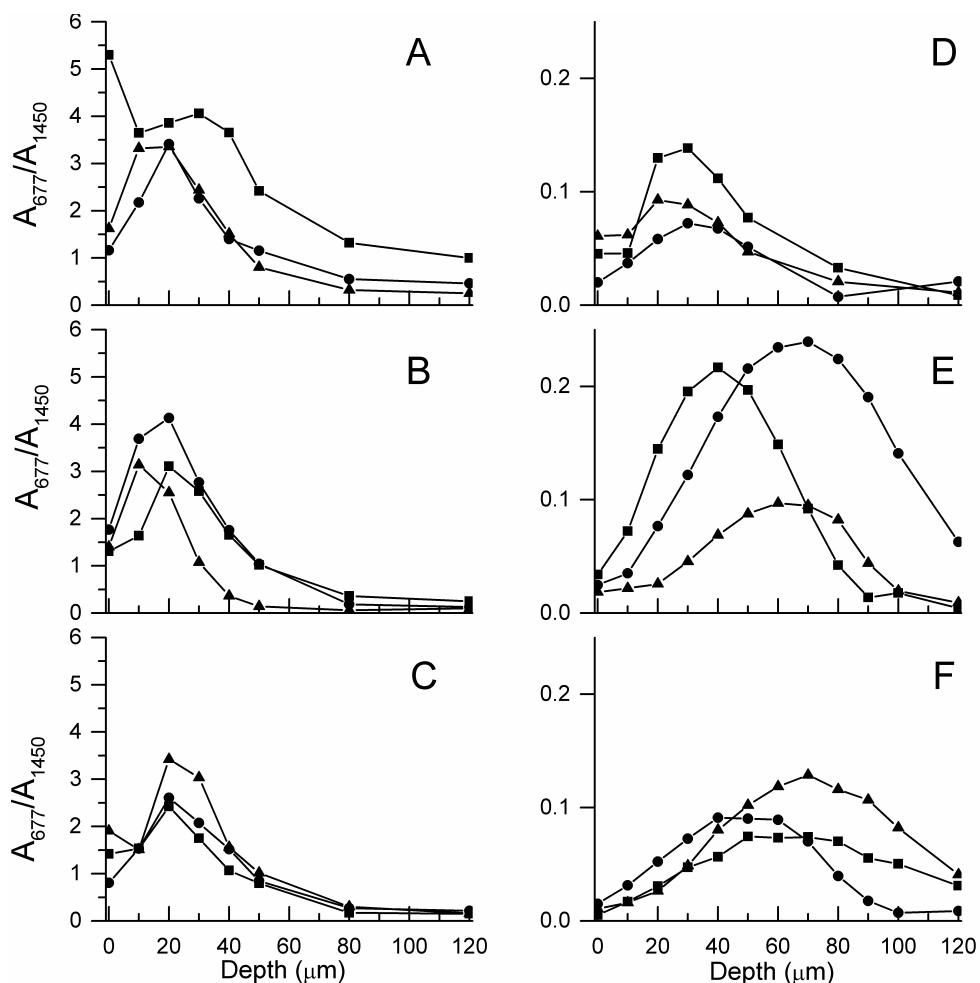


Figure 4. Dimethyl sulfoxide (DMSO) distribution throughout palmar stratum corneum. Ratio of DMSO/protein band areas (A_{677}/A_{1450}) versus depth. (A) 15–45 minutes; (B) 150–170 minutes; (C) ~4 h; (D) ~22 h; (E) ~48 h; (F) ~72 h post application.

were plotted against skin depth (figures 4A to F). Figure 4A presents ratios for depth profiles obtained 15 to 20 (squares), 31 to 36 (circles) and 39 to 45 min (triangles) after DMSO application. The first data set demonstrates that DMSO distributed throughout the SC and that a small fraction may be present in VE; 120 μm NMF vibrations were absent, confirming that this spectrum was from VE.

Subsequent data, collected 30 to 45 min after dosing, showed different DMSO distributions. The DMSO/protein ratio had decreased significantly, i.e. there was considerably less DMSO present. In contrast to the earliest data, the enhancer was now largely confined to the outer 10 to 20 μm with very little detected at deeper layers, or in VE.

Data collected up to 4 hours post application (figure 4A to C) showed gradual permeation of DMSO through the SC. Intensity of the DMSO peak relative to that of the endogenous

protein remained essentially invariant, but it was evident that the sulfoxide was detected at increasing depths with time.

At 22 hours post-application (figure 4D) enhancer intensity relative to the protein modes dramatically decreased. This reduced intensity element of the enhancer progressed to increasing depths within the SC with time; there were still detectable levels of DMSO within the tissue up to 72 hours post dose (figure 4F).

One interpretation of figure 4 is that three mechanisms operate during DMSO permeation; initial rapid shunt route permeation (i.e. via hair follicles and/or sweat ducts) followed by pseudo steady-state transport across the bulk of the skin with the minor 72 hours fraction attributed to highly bound enhancer. However, the spectral data do not support such a scheme. Firstly, the laser sampling diameter is approximately 2 μm , thus it is unlikely that spectra will be recorded reproducibly from DMSO in a follicle or a sweat duct. Secondly, a very small dose of DMSO was applied to the skin (4 μL of 80% DMSO solution) and hence steady-state conditions would not arise. Finally, the positions of the vibrational modes from DMSO in the SC were invariant; there was no evidence that the residual 72 hr fraction was any more "bound" than that detected 15 minutes after dosing.

Thus, it appears likely that the profiles in figure 4 arise simply from percutaneous absorption of a finite dose. Though clearly the enhancer interacts with SC components ('binding'), most small polar molecules traverse the tissue rapidly whereas a "tail" remains that permeates over an extended time.

Recently, FT-Raman spectroscopy probed DMSO effects on hydrated SC following one-hour treatment *in vitro*,⁹ DMSO progressively modified keratin from an α -helical to a β -pleated sheet conformation. SC lipids were also affected; at concentrations enhancing drug flux, DMSO modified lipids from the predominant all *trans* gel phase to a *trans-gauche* liquid crystalline phase. Here, the *in vivo* Raman spectra of DMSO-treated SC obtained were examined for changes that might indicate DMSO interaction with SC lipids and/or a conformational change of keratin. DMSO amounts applied were very small and there was no compelling evidence that it modified SC components. However, the Full Width at Half Height value of the amide I band for the surface spectrum in figure 3 was 92 cm^{-1} , markedly different to $58 \pm 14 \text{ cm}^{-1}$ for spectra of untreated SC. This measurement reflects changes in protein molecular environment which, together with a positional shift of this amide I band, implies that DMSO molecules may hydrogen bond directly to the protein C=O and N-H moieties.

Conclusions

Permeation of DMSO in human skin was studied *in vivo* using confocal Raman microspectroscopy. DMSO distribution in the SC was monitored with depth and time. As expected, most of the dose permeated through the SC within 20 minutes. Surprisingly, some remained within the tissue for hours and a small fraction was detected for days, decreasing steadily with time. Differences in DMSO vibrational modes provided evidence for interactions with water and possibly other polar tissue moieties. Changes in the amide I region were recorded from the skin surface, but firm conclusions regarding conformational changes of keratin due to DMSO interaction could not be drawn.

This study demonstrated a unique capability to monitor, *in vivo* and noninvasively, molecular permeation through human skin. Such investigations have major implications for design and evaluation of topical and transdermal formulations and for clinical evaluation of many therapeutic agents.

Acknowledgements

The authors acknowledge the British Council and NWO (Netherlands) for grant award support.

References

1. Barry, B. W. 1983. *Dermatological Formulations, Percutaneous Absorption*. Marcel Dekker, Inc., New York.
2. Szmant, H. H. 1971. Chemistry of DMSO. *In Dimethyl Sulfoxide*. Basic Concepts of DMSO. S. W. Jacob, E. E. Rosenbaum, and D. C. Wood, editors. Marcel Dekker, Inc., New York. 1-98.
3. Barry, B. W. 1987. Mode of action of penetration enhancers in human skin. *J Control Rel.* 6:85-97.
4. Caspers, P. J., G. W. Lucassen, R. Wolthuis, H. A. Bruining, and G. J. Puppels. 1998. *In vitro* and *in vivo* Raman spectroscopy of human skin. *Biospectroscopy*. 4:S31-39.
5. Caspers, P. J., G. W. Lucassen, E. A. Carter, H. A. Bruining, and G. J. Puppels. 2001. *In vivo* confocal Raman microspectroscopy of the skin: noninvasive determination of molecular concentration profiles. *J Invest Dermatol.* 116:434-442.
6. Caspers, P. J., G. W. Lucassen, H. A. Bruining, and G. J. Puppels. 2000. Automated depth-scanning confocal Raman microspectrometer for rapid *in vivo* determination of water concentration profiles in human skin. *J Raman Spectrosc.* 31:813-818.
7. Wolthuis, R., T. C. Bakker Schut, P. J. Caspers, H. P. J. Buschman, T. J. Roemer, H. A. Bruining, and G. J. Puppels. 1999. Raman spectroscopic methods for *in vitro* and *in vivo* tissue characterization. *In Fluorescent and luminescent probes for biological activity*. W. Mason, editor. Academic Press, London. 433-455.
8. Cowie, J. M. G., and P. M. Toporowski. 1961. Association in the binary liquid system, dimethyl sulfoxide-water. *Can J Chem.* 39:2240-2243.
9. Anigbogu, A. N. C., A. C. Williams, B. W. Barry, and H. G. M. Edwards. 1995. Fourier transform Raman spectroscopy of interactions between the penetration enhancer dimethyl sulfoxide and human stratum corneum. *Int J Pharm.* 125:265-282.

**Combined in vivo confocal Raman
spectroscopy and confocal microscopy of
human skin**

Biophysical Journal
2003, 85:572-580

Chapter

6

P.J. Caspers
G.W. Lucassen
G.J. Puppels

Abstract

In vivo confocal Raman spectroscopy is a noninvasive optical method to obtain detailed information about the molecular composition of the skin with high spatial resolution. *In vivo* confocal scanning laser microscopy is an imaging modality that provides optical sections of the skin without physically dissecting the tissue. A combination of both techniques in a single instrument is described. This combination allows the skin morphology to be visualized and (sub-surface) structures in the skin to be targeted for Raman measurements. Novel results are presented that show detailed *in vivo* concentration profiles of water and of natural moisturizing factor for the stratum corneum that are directly related to the skin architecture by *in vivo* cross sectional images of the skin. Targeting of skin structures is demonstrated by recording *in vivo* Raman spectra of sweat ducts and sebaceous glands *in situ*. *In vivo* measurements on dermal capillaries yielded high quality Raman spectra of blood in a completely noninvasive manner. From the results of this exploratory study we conclude that the technique presented has great potential for fundamental skin research, pharmacology (percutaneous transport), clinical dermatology, and cosmetic research, as well as for noninvasive analysis of blood analytes, including glucose.

Introduction

The human skin is layered. Conventionally the skin is described as divided in two major layers. The inner layer, the dermis, is between 1 and 4 mm thick. It consists mainly of connective tissue composed of collagen fibers. Other dermal structures include nerves, blood vessels, lymph vessels, muscles, and gland units. The outer layer, the epidermis, is typically about 40 μm thick, but it can be much thicker on load bearing areas such as palms and soles. The epidermis can be divided in various sub layers. The principal cells of the epidermis are keratinocytes. These cells originate in the lower epidermis by division of basal cells in the basal layer. As the keratinocytes mature, they move upward towards the skin surface, thereby changing shape and molecular composition. Finally, the viable keratinocytes undergo a rapid, terminal transition into a cornified layer of dead, flattened cells, called the stratum corneum (SC).^{1,2} This outermost skin layer has a thickness of 10–15 μm on most areas of the body, except for the palms and the soles, where the SC can be more than ten times thicker. Despite its normally minute thickness, the SC provides a highly efficient barrier for water and protection against microbial and chemical assault. The major constituent of the SC is keratin, which accounts for about 80% of its dry weight.³

Optical microscopic techniques offer unique possibilities for noninvasive skin research and skin characterization at high spatial resolution. Examples of such techniques are Optical Coherence Tomography (OCT), two-photon fluorescence, and *in vivo* confocal scanning laser microscopy (CSLM). OCT takes advantage of the short temporal coherence of a broadband light source to reject multiple scattered light. The spatial resolution in the axial direction is $\sim 10\text{--}20$ μm , which is close to the thickness of the stratum corneum^{4,5} although more recently, depth resolutions better than 5 μm have been reported.^{6–8} Two-photon fluorescence microscopy uses two-photon excitation of endogenous chromophores in the tissue, which results in imaging with a high spatial resolution.^{9–11}

In vivo confocal microscopy enables real-time imaging of living tissue at high resolution and high contrast, without physically dissecting the tissue. The first *in vivo* confocal microscopic images of human skin were obtained with a tandem scanning confocal microscope. A mercury lamp was employed as light source and a Nipkow disk as scanning device.¹² Subsequently, confocal scanning laser microscopy (CSLM) has been developed, offering the advantage of precise wavelength selectivity and high illumination power.¹³ *In vivo* CSLM can be used to study the morphology of living skin for basic and clinical research. Confocal images show cellular and nuclear structure in the epidermis, collagen fibers in the dermis and circulating blood cells in dermal capillaries, as well as structures such as sebaceous glands, hair and hair follicles, and sweat ducts. Different skin layers (stratum corneum, viable epidermis, dermis) can be clearly identified. *In vivo* confocal microscopy is a potential tool in the clinic for imaging skin lesions and their margins prior to biopsy, and for diagnosis of lesions.¹⁴

These imaging techniques are methods to study skin morphology. *In vivo* confocal Raman spectroscopy provides detailed information about the molecular composition of the skin. Raman spectroscopy is widely used to study biological samples and, more recently, also

to study the skin.^{15, 16} Application in clinical dermatology has been probed in studies of vitiligo,¹⁷ atopic and psoriatic skin¹⁸ and basal cell carcinoma.¹⁹ We have introduced *in vivo* confocal Raman spectroscopy as a method to obtain depth-resolved information about the molecular composition of the skin.²⁰ The axial resolution of 5 μm (full width at half maximum) enabled the determination of *in vivo* concentration profiles of constituents of natural moisturizing factor (free amino acids and amino acid derivatives), sweat (lactate and urea) and of water in the SC.²¹⁻²³

In this paper we demonstrate that Raman spectroscopy for *in vivo* skin research can be further extended by combining the technique with CSLM. In this way, precise targeting of a (sub-surface) skin structure for Raman measurements is enabled. In addition, molecular concentration profiles, as determined by Raman spectroscopy, can be directly related to skin architecture in particular the skin layers.

Materials and Methods

Instrumentation

Figure 1 depicts the combined CSLM/Raman system. The system is based on a custom-built confocal Raman microspectrometer dedicated to *in vivo* examination of the skin,^{22, 23} and a confocal scanning laser microscope (type VivaScope 1000, Lucid Inc., Rochester, NY). The confocal Raman system employs a tunable titanium-sapphire laser (model 3900S, Spectra-Physics, Mountain View, CA) pumped by an Argon-ion laser (model 2020, Spectra-Physics). The spectra were recorded using a custom-designed F/2.1 spectrograph with 6 cm^{-1} spectral resolution and a liquid-nitrogen cooled, deep depletion Charge Coupled Device (CCD) camera with a chip size of 1024 x 256 pixels (Princeton Instruments, Trenton, NJ). A 30x numerical aperture (NA) 0.90 water immersion microscope objective with cover glass correction was used (Lomo, Vermont Optechs, Charlotte, VT) to focus the laser light from both the Raman laser and the CSLM laser. The objective was mounted in a fast and accurate piezoelectric focusing drive, accurate to less than 0.1 μm when operating in closed-loop (position-controlled) mode (Physik Instrumente, Waldbronn, Germany). Focusing of the microscope objective and adjustment of the power of the laser diode of the CSLM were controlled by a Personal Computer. This PC was also used to digitize and store the confocal images produced by the VivaScope. The operating software was custom-developed (Philips Research, Eindhoven, The Netherlands). A second PC was used to record the Raman spectra.

The laser beam of the CSLM was focused to a diffraction-limited spot, which was continuously scanned in two dimensions across the focal plane. The maximum field of view was 500 x 500 μm , using a 30x objective. The laser beam for Raman excitation was focused to a static diffraction limited spot in the center of the focal plane. The CSLM and the Raman system were optically coupled using a custom-designed filter inserted in the light path just above the microscope objective (see figure 1A). An anti-reflection coated window is placed above the filter in order to correct for the parallel beam displacement caused by refraction at the filter surfaces (see figure 1B).

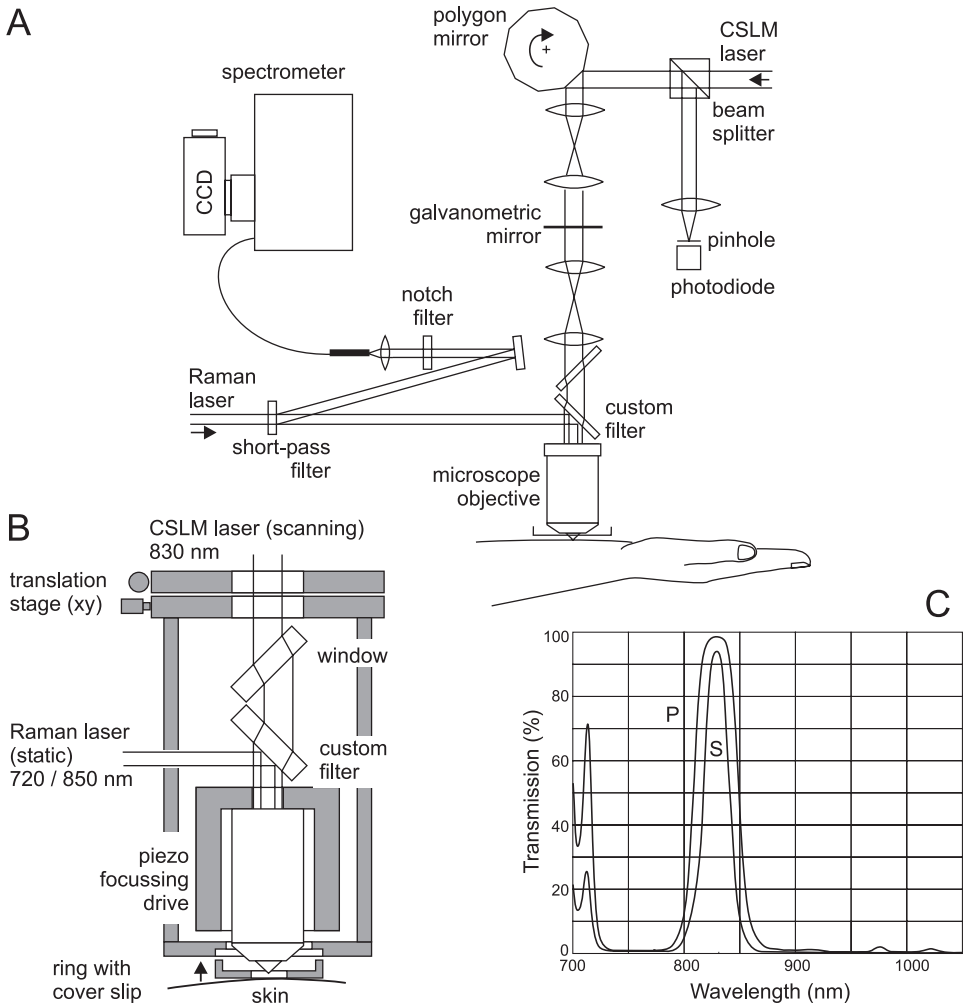


Figure 1. Combined confocal scanning laser microscope and Confocal Raman spectrometer for *in vivo* study of the skin. **(A)** Schematic overview of the setup. Light from the Raman laser (720 nm and 850 nm) was transmitted by a short-pass filter and reflected by a custom-designed filter (transmission curve shown in Fig. 1C), which partially reflected light at wavelengths 720 nm and 850 nm and completely reflected Raman scattered light with wavelengths >850 nm. The light was then focused to a diffraction-limited spot by a microscope objective. Scattered light was collected by the same objective and reflected by the custom filter and by the short-pass filter. The scattered light was filtered by a laser rejection filter and focused onto the 100 μm core of an optical fiber, using an $f = 149$ mm achromat. The core of the optical fiber served as a confocal pinhole, rejecting out-of-focus light. The output of the fiber was connected to a spectrograph. Laser light from the CSLM, produced by an 830 nm diode laser, was transmitted by the custom filter and focused by the microscope objective to a diffraction limited spot, which was scanned across the focal plane; **(B)** Detailed view of the coupling between the CSLM and the Raman system; **(C)** Transmission curve of the coupling filter between the CSLM and the Raman spectrometer for parallel (P) and normal (S) polarization. Angle of incidence: 45° .

The coupling filter was designed to transmit the imaging laser beam of the CSLM (830 nm) and to reflect the Raman signal at wavelengths >850 nm. As described below, Raman measurements were performed using either 720 nm or 850 nm laser excitation. At both wavelengths, the filter transmitted a fraction of the laser light that was scattered by the skin (see figure 1C). In this way the location of the focus of the Raman laser appears in the CSLM-image. When the surface of a cover glass was imaged, the focus of the Raman laser appeared as a small, bright spot. The position of this spot was marked with a digital cross-hair in the video image. This was done because the focus of the Raman laser, while imaging the skin, was generally less bright and often difficult to distinguish from contrasting structures of the skin. With the cross-hair in place, the location of the focal point of the Raman laser was unambiguously marked, accurately indicating the location from which a Raman spectrum is obtained.

The standard operating procedure of the CSLM was applied, in which a cover glass was mounted in a metal ring that was stuck to the skin with double-sided tape. The metal ring was then attached to the microscope and could be moved laterally with a xy -translation stage. In this way a target of interest in the skin could be positioned in the focused laser beam for Raman spectroscopic evaluation. Since the skin was in contact with the cover glass, the distance between the microscope objective and the skin surface could be accurately controlled. Unintentional vertical motion of the skin could be limited to $\sim 2 \mu\text{m}$.²³ Cover glasses were made of CaF_2 , because of its weak Raman signal in the spectral region of interest. Demineralized water between the cover glass and the skin surface was used to improve refractive index matching. This is of particular importance for the quality of the confocal images of the skin. Without water, a thin layer of air exists between cover glass and skin, resulting in large changes in the refractive index at the cover glass-air-skin interface. This would strongly degrade the image quality.¹⁴ The refresh rate of the CSLM images was 14 frames/s.

It was experimentally verified that the origin of the Raman signal was located within $2 \mu\text{m}$ of the focal plane of the CSLM. For this purpose polystyrene beads of $1 \mu\text{m}$ diameter were stuck to the cover glass of the CSLM and the surface of the cover glass was brought into the focal plane of the CSLM. A bead was positioned in the focused Raman laser by moving the cover glass laterally. Once the bead was in focus, the intensity of its Raman signal was monitored while the bead was moved through the focal plane in the axial direction. In this way it was determined that the maximum Raman signal was obtained when the bead was within $2 \mu\text{m}$ of the focal plane of the CSLM. This is well within the current axial resolution of the confocal Raman spectrometer in the combined system ($9 \mu\text{m}$). The axial resolution, defined as the Full Width at Half Maximum (FWHM) of the response curve of an infinitesimal thin plane, was determined from the derivative of a measured step response curve across an oil- CaF_2 interface. Details of this method have been described elsewhere.²² In the current set-up we used the standard microscope objective that was provided with the VivaScope (30x NA 0.9 water immersion). The combination of magnification and NA of the microscope objective, the focal length of the lens in front of the signal collection fiber, and the core diameter of this fiber (see figure 1A) was not fully

optimized. Therefore, the axial resolution for the Raman measurements was worse than the 5 μm resolution achieved in previous studies.²²

In all *in vivo* experiments the depth, or distance to the skin surface, was determined from the displacement of the piezoelectric drive relative to the zero position, at which the focal plane was at the skin surface. No attempt was made to correct for a focus shift in the axial direction due to refractive index differences between water, the cover glass, and skin.¹⁴

Experiments

In vivo experiments were carried out on the volar aspect of the arm and on the palm of the hand of healthy volunteers. The skin was not pre-treated in any way. Approval for these experiments was obtained from the Medical Ethics Review Board of the Erasmus MC, University Medical Center Rotterdam.

In vivo concentration profiles of water and constituents of sweat and natural moisturizing factor (NMF) were determined as follows. Raman spectra were recorded from a range of depths across the SC of the palm, from the skin surface down to the viable epidermis. Depth increments were typically 10 μm . A corresponding set of CLSM images was used to visualize the boundary between the SC and the viable epidermis. Images were recorded at depth intervals of 1 μm . The images were stored on disk and processed afterwards to obtain an *in vivo* cross sectional image of the SC and part of the viable epidermis.

For determination of water concentrations in the SC, a laser wavelength of 720 nm was used for Raman excitation. Raman spectra were recorded at 1 s per spectrum in the wavenumber region from 2000 to 4000 cm^{-1} . From these Raman spectra, water concentration profiles were determined. The water concentration in mass percentage was calculated using the intensity ratio between the Raman bands of water (3350-3550 cm^{-1}) and protein (2910-2965 cm^{-1}). The details of this procedure are described elsewhere.^{23; 22}

For the determination of concentration profiles of NMF and sweat constituents, Raman spectra were recorded in the spectral region from 400-2000 cm^{-1} ("fingerprint region"). The excitation wavelength in these experiments was 850 nm. The data collection time was 30 s per spectrum. Concentration profiles of NMF were determined semiquantitatively, using the relative signal contributions of NMF and keratin to the total *in vivo* Raman spectrum of stratum corneum (About 80% of the dry weight of the stratum corneum consists of keratin). This was done using multiple-least-squares fitting, in which the *in vivo* skin spectrum was fitted with the *in vitro* Raman spectra of NMF, keratin, ceramide, lactate and urea. A combination of these *in vitro* Raman spectra provides an adequate model for *in vivo* spectra of human SC.²³ The resulting fit coefficients represent the relative proportions in which these species contribute to the total SC Raman signal. The NMF/keratin ratio was the ratio between the fit coefficients of NMF and keratin. This ratio was normalized to 1 at the maximum value.

Raman spectra of structures in the skin (sweat ducts, sebaceous glands and blood capillaries) were measured in the fingerprint region. The excitation wavelength was 850 nm and the exposure time was 20 s per spectrum. Together with each recorded Raman spectrum, the corresponding CSLM image was captured and stored. For comparison with *in vivo* Raman spectra of dermal capillaries, *in vitro* spectra were recorded from fresh, human blood in glass capillaries. In all *in vivo* experiments the Raman laser power at the skin was 100 mW.

Data processing

The software used to control the CSLM enabled automatic recording and storage of confocal images as a stack of uncompressed bitmap files. For easy handling, a descriptor file was generated containing the filenames and depth-coordinates for each image in a stack. A complete stack represents a volume section of the tissue, with each pixel having an (x,y,z)-coordinate and a brightness level. Plotting the image stack in an *xy*-plane (that is, all pixels having the same *z*-coordinate) results in an image of a section parallel to the skin surface. Similarly, cross sectional images were obtained by plotting the image stack in an *xz*-plane or in a *yz*-plane.

Processing of images and of spectral data was done with software that was developed in-house using Matlab (MathWorks, Natick, MA). The Raman spectra were calibrated to relative wavenumbers and corrected for the wavelength dependent detection-efficiency of the Raman system.²⁴

Results

Figure 2a shows an *in vivo* cross sectional image (xz -plane) of the skin at the palm of the hand obtained with the CSLM, and a water concentration profile obtained simultaneously by Raman spectroscopy. The water concentration profile was determined from the Raman spectra that were measured on the dashed line. The solid line demarcates the boundary between the SC and the stratum granulosum (SG), at a depth of 145 μm below the skin surface. The confocal image in the xy -plane obtained at this position is shown in figure 2b. Clearly visible are the uppermost cells of the stratum granulosum at the SC/SG junction. Figure 2 shows a result that is representative of the results obtained in 10 experiments in which water concentration profiles were measured using Raman spectroscopy in combination with CSLM.

A similar experiment was carried out in order to determine the (semiquantitative) concentration profile of NMF in relation to skin architecture. Figure 3a shows an *in vivo* cross sectional image (xz -plane) of the skin at the palm of the hand obtained with the CSLM, and a concentration profile of natural moisturizing factor profile obtained simultaneously by Raman spectroscopy. The NMF concentration was determined as a ratio (in arbitrary

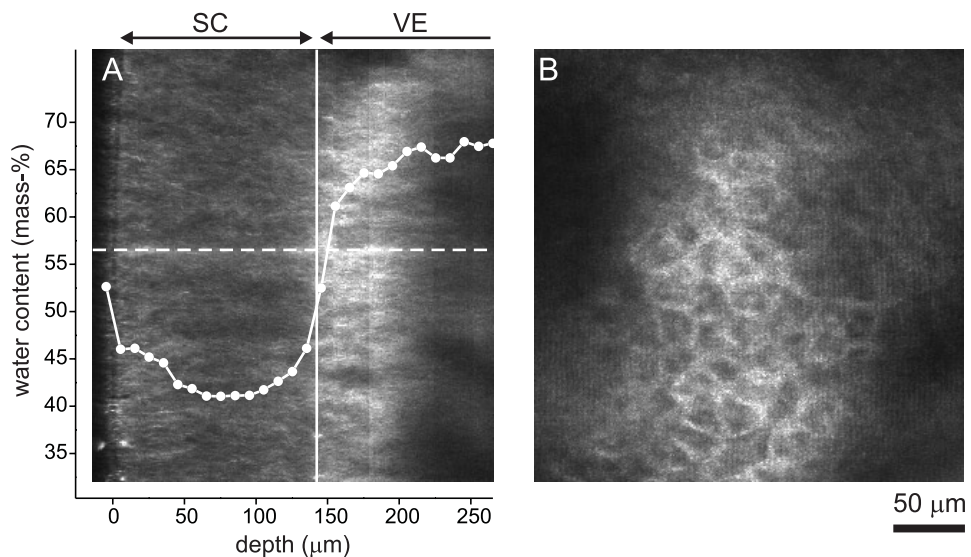


Figure 2. *In vivo* confocal images and a water concentration profile for the stratum corneum of the palm based on combined CSLM and Raman measurements. (A) Cross section of the skin (xz -plane, SC: stratum corneum, VE: viable epidermis). Plotted in the image is the water concentration profile as determined from Raman measurements on the dashed line. The x -axis represents the distance to the skin surface and applies to both the image and the graph. The y -axis represents the water concentration in mass percentage (grams of water per 100 g of wet tissue). The solid line locates the plane from which image B was obtained; (B) Confocal image parallel to the skin surface (xy -plane), recorded at 145 μm below the skin surface at the boundary between SC and VE.

units) between the intensities of the Raman signal contributions of NMF and keratin, where keratin is the main constituent of the SC. The dashed line indicates the line on which the Raman spectra were recorded. The solid line indicates the SC/SG boundary. Figure 3b shows a confocal image in the xy -plane that was obtained at this position. The result here is representative for the results of a total of eight experiments in which the NMF profiles were measured in combination with CSLM.

Figure 4 shows a confocal image of a sweat duct in the SC of the thenar at $30\ \mu\text{m}$ below the skin surface. Several Raman spectra were recorded in and around the sweat duct. Spectra from the center of the sweat duct, and from the area around the sweat duct are plotted next to the image. Clear spectral differences can be observed, of which the intensity difference seen in the Raman band at $856\ \text{cm}^{-1}$ (marked with an asterisk, see discussion) is the most prominent.

Figure 5 shows a confocal section of a sebaceous gland located on the lower forearm at a depth of $15\ \mu\text{m}$ below the skin surface. Several Raman spectra were recorded in and around the gland. A typical spectrum from the gland and a typical spectrum from the area around the gland are shown next to the image. A prominent spectral difference, the Raman band at $1296\ \text{cm}^{-1}$, is marked with an asterisk (see discussion).

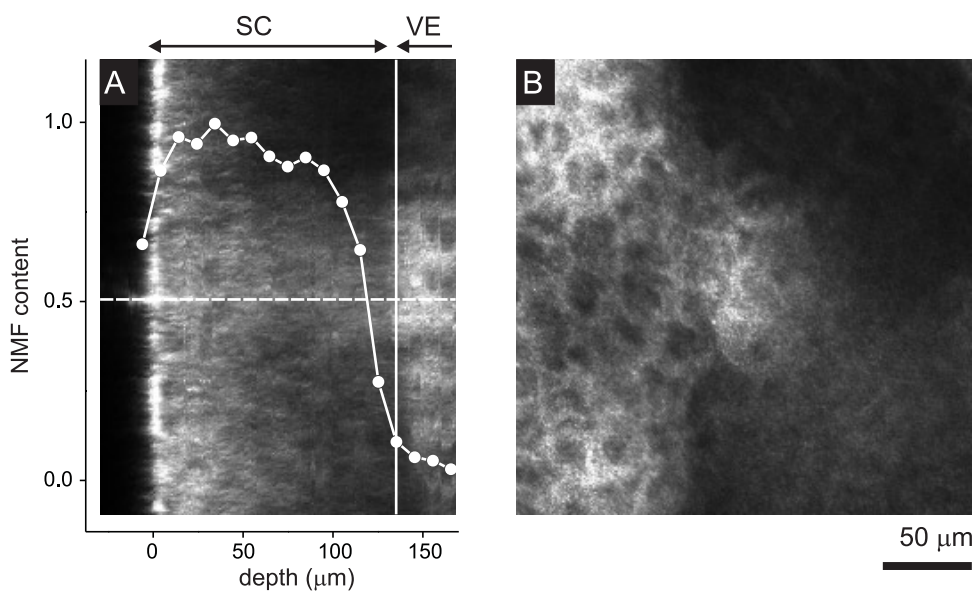


Figure 3. *In vivo* confocal images and a concentration profile of NMF for the stratum corneum of the palm. (A) Cross section of the skin (xz -plane, SC: stratum corneum, VE: viable epidermis). Plotted in the image is the relative amount of NMF as a function of depth, as determined from Raman measurements on the dashed line. The x -axis represents the distance to the skin surface and applies to both the image and the graph. The y -axis represents the relative amount of NMF, normalized to its maximum value. The solid line locates the plane from which image B was obtained. (B) Confocal image parallel to the skin surface (xy -plane) recorded $135\ \mu\text{m}$ below the skin surface at the boundary between SC and VE.

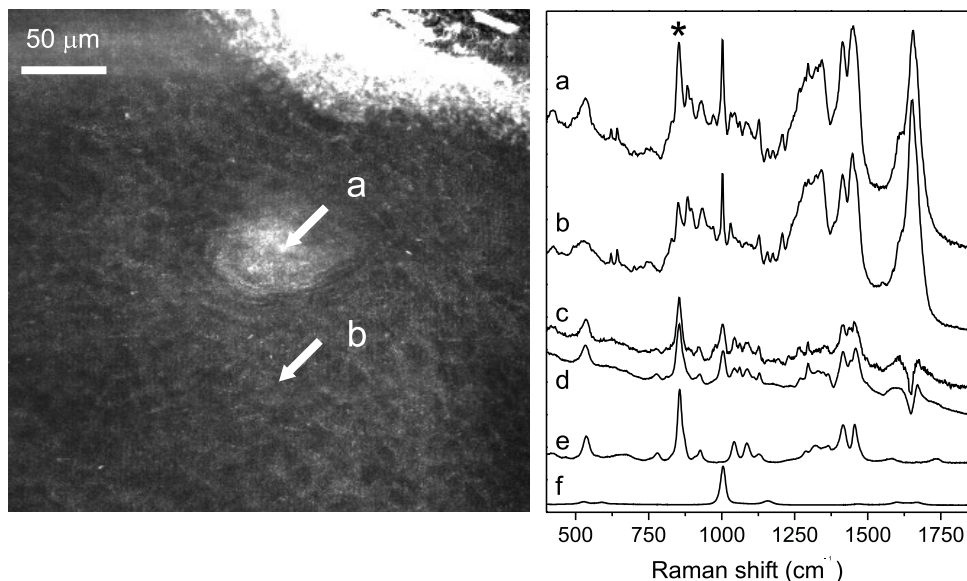


Figure 4. *In vivo* confocal image and Raman spectroscopy of a sweat duct on the palm of the hand, 30 μm below the skin surface. The bright area is a sweat duct. The arrows (*left*) mark the spots from which the Raman spectra were obtained. The asterisk marks the prominent Raman band of lactate at 856 cm^{-1} (see text). (*a, right*) Raman spectrum measured in the sweat duct; (*b, right*) Raman spectrum measured outside the sweat duct; (*c, right*) Difference spectrum (a minus b); (*d, right*) Fit result of spectrum a with spectrum b and spectra of NMF and sweat constituents (see text for details); (*e, right*) *In vitro* Raman spectrum of lactate; (*f, right*) *In vitro* Raman spectrum of urea.

In the lower part of the epidermis, dermal papillae can be observed. These structures show up in a CSLM image as bright circles around a darker central part.¹³ Blood flow within dermal capillaries can be observed in the center of dermal papillae. These capillaries ascend from the papillary plexus, which is a network of microcirculatory elements oriented parallel to the skin surface. The plexus is located in the upper part of the dermis. From this plexus, capillary loops are directed towards the epidermis and extend into the dermal papillae.¹ Figure 6 shows a confocal image of a dermal capillary. Although capillaries may be difficult to recognize in a single image, they clearly show up in the live video image, because of the circulating blood cells, which appear as bright dots moving along the same path.¹³ By positioning capillaries in the center of the cross-hair, Raman spectra were obtained of blood inside the capillary. Figure 6 shows an *in vivo* spectrum obtained from a capillary and for comparison, a spectrum of blood that was obtained *in vitro*.

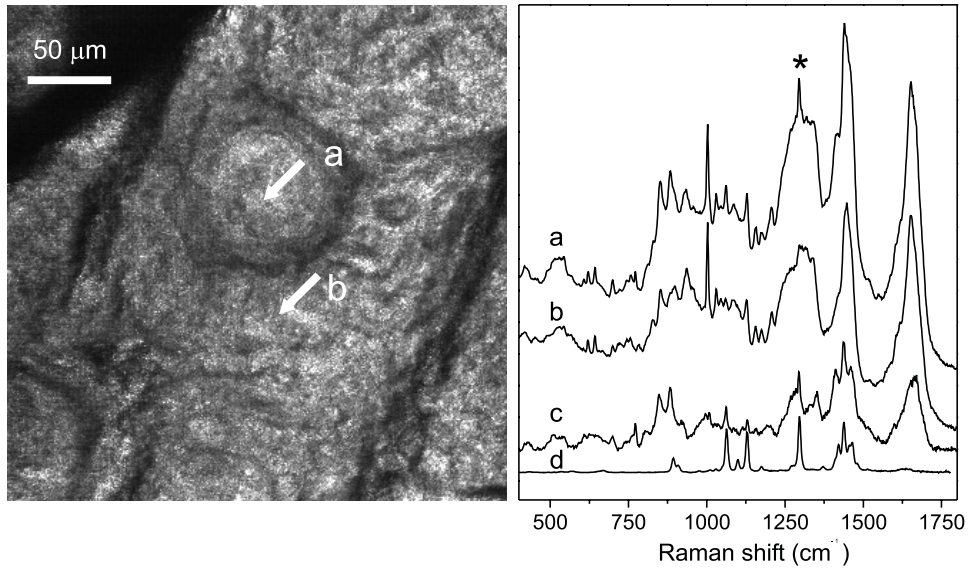


Figure 5. *In vivo* confocal image and Raman spectroscopy of a sebaceous gland on the lower forearm, 15 μm below the skin surface. The arrows (*left*) mark the spots from which the Raman spectra were obtained. The asterisk marks the prominent Raman band of lipid at 1296 cm^{-1} . (*a, right*) Raman spectrum measured in the sebaceous gland. (*b, right*) Raman spectrum measured outside the gland. (*c, right*) Difference spectrum (*a* minus *b*). (*d, right*) *In vitro* Raman spectrum of palmitic acid.

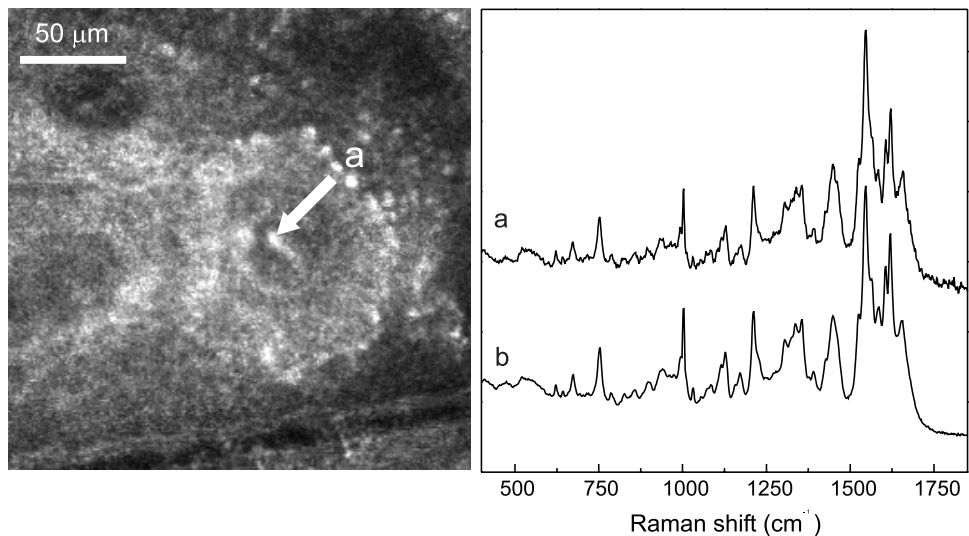


Figure 6. *In vivo* confocal image and Raman spectrum of a dermal capillary in the skin of the lower forearm. The depth is 60 μm below the skin surface. The arrow (*left*) indicates the location from which the Raman spectrum was obtained. (*a, right*) *In vivo* Raman spectrum of blood measured directly in a dermal capillary. Signal integration time: 30 s. (*b, right*) *In vitro* spectrum of blood.

Discussion

In the *in vivo* cross sectional CSLM images of the palm (figures 2A and 3A) the skin surface and the junction between the SC and the viable epidermis can be easily observed. Contrast in CSLM originates from differences in the amount of back-scattered light from structures in the skin. The amount of back-scattered light largely depends on variations in refractive index within the tissue.¹³ However, the SC is an optically homogeneous layer; the cells are flattened, and nuclei and other cell organelles are absent. As a result CSLM images of the SC are relatively dark and show little contrast. In comparison, the living cells of the viable epidermis contain cytoplasm, organelles and nuclei, from which light is scattered due to refractive index changes. Overall, images of the viable epidermis are therefore brighter than images of the SC. As a result, the cross sectional image shows a well-defined junction between the darker SC and the brighter viable epidermis (figures 2A and 3A).

The water concentration profile in the SC provides insight into the water holding capacity and barrier properties of the skin. This has implications for pharmacology, cosmetics and fundamental skin biology. Trans-epidermal water loss (TEWL) measurements and skin impedance measurements have been used in combination with mathematical modeling of water diffusion through a membrane to study the barrier properties of the SC.^{25; 26} These studies have provided indirect information about the location of the water barrier and the water concentration profile. However, they have not resulted in a clear understanding of the *in vivo* water concentration in the SC as a function of depth.

In contrast, confocal Raman spectroscopy combined with CSLM provides a direct method to study the water concentration profile in the SC. With the results presented here, we show for the first time a detailed *in vivo* water concentration profile for the SC in relation to the skin architecture. The water concentration within the SC of the palm is constant throughout most of the SC (figure 2). Only at the junction between the SC and viable epidermis does the water content increase with a steep gradient, reaching about 70% (mass %, or grams of water per 100 grams of wet tissue) in the viable epidermis. The slight increase of the water content at the skin surface has not been observed in earlier experiments using *in vivo* confocal Raman spectroscopy without CSLM^{23; 22} and must be dismissed as an artifact. It is presumably caused by the thin film of water between the window and the skin surface that was applied to improve optical refractive index matching between skin surface and cover glass (see *Materials and Methods*). The use of a different matching medium, such as oil, would avoid this problem. The presence of a steep gradient at the lower part of the SC implies that the water barrier is not homogeneously distributed over the entire SC of the palm, but located mostly at the junction between the SC and the SG. These observations do not confirm results obtained by TEWL measurements and mathematical modeling from which it was concluded that the SC of the arm is a homogeneous water barrier^{25; 26} Whether the *in vivo* water concentration profile for the SC of the arm has the same pattern of a slowly varying water concentration in most of the SC followed by a steep gradient at the lower SC boundary remains to be elucidated. Currently

the axial resolution of the combined Raman/CSLM system is not sufficient to answer this question, but an improvement with a factor of 3 to about 3 μm is feasible.

The relative changes in the concentration of NMF show a pattern quite different from the water concentration profile. Scott and co-workers have shown that a layer of stable filaggrin exists in the lowermost cell layers of the SC.^{27, 28} This precursor protein is broken down by hydrolytic enzymes, a process that produces the free amino acids and amino acid derivatives that, together with specific salts, form the NMF. Proteolytic activity of these enzymes is modulated by the water content in the tissue. Radio labeling and immunohistochemical studies in rats have shown that a high water content in the SC prevents the production of NMF by filaggrin proteolysis. In normal conditions, the relatively dry external environment dries out the outer layers of the SC resulting in a water gradient decreasing from the deeper SC toward the surface. The decreased water content triggers proteolysis of filaggrin in the deeper part of the SC.²⁷

Figure 3 visualizes this localized production of NMF in the lower part of the SC *in vivo*. The NMF-to-keratin ratio is zero in the viable epidermis. The steep gradient in the NMF profile indicates a very rapid increase of NMF at about 15 μm above the SC/SG junction. According to figure 2, the water concentration at the distance of about 15 μm from the SC/SG junction has dropped considerably with respect to the water concentration in the viable cells. These *in vivo* observations are in agreement with the findings by Scott and co-workers²⁷ that a decrease in water concentration is required before the proteolysis of filaggrin can start and the presence of NMF can be detected.

Absence or decreased production of NMF has been related to skin problems such as xerosis, ichthyosis and psoriasis.^{29, 28} Decrease in NMF has also been observed in aged skin.²⁸ *In vivo* confocal Raman spectroscopy combined with CSLM provides a method to study the distribution of NMF and water in the SC *in vivo*. It can therefore contribute to gaining insight into the cause and treatment of skin conditions such as those mentioned above.

Figures 4 to 6 illustrate the capability of combined confocal Raman spectroscopy and CSLM for study of the molecular composition of structures in the skin *in situ*. The real-time imaging capability of the CSLM was used to locate a structure of interest, such as a sweat duct (figure 4). Confocal Raman spectroscopy was then used to obtain spectroscopic information from this structure. Clearly the Raman band at 856 cm^{-1} is more intense in the spectrum of the sweat duct (a) than in the spectrum measured outside the duct (b). Multiple-regression fitting of spectrum (a) with spectrum (b) and the spectra of lactate, urea, and the predominant constituents of NMF was applied to interpret these spectral differences in terms of differences in molecular composition. Details of the fitting procedure have been described elsewhere.²³ The choice of these constituents for fitting purposes is based on the assumption that NMF, which is highly water soluble and present in high concentrations in the SC, can easily dissolve in sweat.³⁰ Lactate and urea are also present in sweat, as both are secreted by the sweat glands. The concentrations usually depend on the sweat rate. At low sweat rates, the concentration of lactate can be as high as 40 mM and that of urea 4 mM.³⁰ At the current spatial resolution of the instrument, signal from the tissue surrounding the sweat duct also unavoidably is collected. Therefore, spectrum b (figure 4) was also included in the fit to the spectrum obtained in the sweat duct. The dif-

ference spectrum and the fit with the aforementioned compounds (figure 4) showed that the concentration of lactate in the sweat duct is much higher than in the surrounding tissue. The significance of this result is that it demonstrates that information about the molecular composition of sweat can be obtained from a sweat duct *in situ*. For cosmetic research, in designing and improving antiperspirants, which involves modulation of sweat production, this may offer a new and valuable tool to study the effects of these formulations *in situ*.

A similar experiment was carried out for a sebaceous gland, located at the lower forearm. Human sebaceous glands secrete a lipid mixture of mainly triglycerides, wax esters, free fatty acids and squalene.³¹ The process of sebogenesis is complex and not entirely understood. It involves elongation and desaturation of free fatty acids in the sebaceous cells, and incorporation of free fatty acids into triglycerides and wax esters. At a later stage bacterial hydrolysis of triglycerides causes the release of free fatty acids.

The Raman spectrum (figure 5) from the sebaceous gland (a) shows a strong band at 1295 cm^{-1} , which is not present in the spectrum recorded outside the gland (b). The difference spectrum (c) shows many Raman bands, indicating a difference in molecular composition between the sebaceous gland and the skin around the gland. Although the Raman bands of spectrum (a) remain to be assigned, the comparison with the spectrum of palmitic acid (d) suggests the presence of this 16-carbon fatty acid in the sebaceous gland. The 16-carbon acids are predominant in sebaceous cells.³² This first result demonstrates the potential to study the lipid composition in a sebaceous gland *in vivo*. It also suggests the possibility to measure Raman spectra in various parts of the sebaceous gland, which would enable one to follow the complex process of sebogenesis *in vivo*.

Confocal Raman Spectroscopy combined with an imaging modality such as CSLM can be used to obtain direct chemical information about structures in the skin *in situ*. As such, the technique presented also provides a potential method to investigate *in vivo* the penetration of topically applied substances via shunt routes. This offers the possibility to apply substances to the skin and study their effects *in situ*, directly in the sebaceous glands, sweat glands, or hair follicles. This capability should be of particular interest in cosmetics research and pharmaceutical research on transdermal drug delivery.

In vivo recording of Raman spectra from dermal capillaries (figure 6) offers possibilities that reach well beyond skin research. Spectrum (a) was recorded *in vivo*, focusing on a capillary, whereas spectrum (b) is an *in vitro* spectrum of blood. The *in vivo* spectrum (a) is likely to contain signal contributions from the surrounding tissue, but clearly the majority of the spectrum originates from blood flowing through the dermal capillary. The collection time for spectrum (a) was only 30 s, demonstrating that high quality Raman spectra of blood can be rapidly measured in a completely noninvasive manner.

The Raman spectrum of blood largely depends on the oxygenation state of hemoglobin.^{33;}

³⁴ Due to the high spatial resolution of both CSLM and *in vivo* confocal Raman spectroscopy, it seems feasible to study the local hemoglobin-oxygen saturation at a microscopic scale. This is currently being investigated.

Several *in vitro* studies have shown the feasibility to use Raman spectroscopy to determine analyte concentrations in whole blood, in plasma or in serum.³⁵⁻³⁷ We therefore believe that the new technique presented here, enabling the *in vivo* recording of Raman spectra from dermal capillaries, has great potential for noninvasive monitoring of blood analytes, including glucose.

Conclusions

The combination of confocal Raman microspectroscopy and CSLM has been presented as a novel noninvasive method to obtain information about molecular composition in relation to skin architecture. CSLM is an imaging modality that can be used to image specific structures in the skin and to generate *in vivo* cross sectional images of the skin. By combining CSLM with confocal Raman microspectroscopy, we show that detailed information about molecular composition can be obtained from well-defined regions in the confocal image. This was demonstrated by obtaining *in vivo* concentration profiles of water and of NMF in the SC that were directly related to the layered skin architecture by simultaneous recording of cross sectional images of the skin. The possibility of studying the molecular composition of specific skin structures *in vivo* (sweat duct, sebaceous gland, dermal capillary) also was demonstrated. We believe that the technique presented provides the basis for a wide range of applications in fundamental skin research, as well as in pharmacology, dermatology and cosmetics. The fact that high quality spectra of blood can be obtained rapidly and completely noninvasively supports our great expectations for *in vivo* confocal Raman microspectroscopy in combination with CSLM as a method for non-invasive blood analysis.

References

1. Jakubovic, H. R., and A. B. Ackerman. 1992. Structure and function of skin: development, morphology, and physiology. *In* *Dermatology*. S. L. Moschella and H. J. Hurley, editors. W. B. Saunders company, Philadelphia. 3-87.
2. Odland, G. F. 1991. Structure of the skin. *In* *Physiology, Biochemistry and molecular Biology of the Skin*. L. A. Goldsmith, editor. Oxford University Press, New York. 3-62.
3. Steinert, P. M., and I. M. Freedberg. 1991. Molecular and cellular biology of keratins. *In* *Physiology, biochemistry and molecular biology of the skin*. L. A. Goldsmith, editor. Oxford University Press, New York. 113-147.
4. Huang, D., E. A. Swanson, C. P. Lin, J. S. Schuman, W. G. Stinson, W. Chang, M. R. Hee, T. Flotte, K. Gregory, C. A. Puliafito, and et al. 1991. Optical coherence tomography. *Science*. 254:1178-81.
5. Schmitt, J. M., M. J. Yadlowsky, and R. F. Bonner. 1995. Subsurface imaging of living skin with optical coherence microscopy. *Dermatology*. 191:93-8.

6. Wang, R. K., and J. B. Elder. 2002. High resolution optical tomographic imaging of soft biological tissues. *Laser Physics*. 12:611-616.
7. Bordenave, E., E. Abraham, G. Jonusauskas, N. Tsurumachi, J. Oberle, C. Rulliere, P. E. Minot, M. Lassegues, and J. E. S. Bazeille. 2002. Wide-field optical coherence tomography: imaging of biological tissues. *Appl Opt*. 41:2059-2064.
8. Knuttel, A., S. Bonev, A. Hoepfner, and C. Kugler. 2001. Sub-surface skin imaging and evaluation by Optical Coherence Tomography (OCT). *J Invest Dermatol*. 117:962.
9. Masters, B. R., P. T. So, and E. Gratton. 1998. Multiphoton excitation microscopy of in vivo human skin. Functional and morphological optical biopsy based on three-dimensional imaging, lifetime measurements and fluorescence spectroscopy. *Ann N Y Acad Sci*. 838:58-67.
10. Hendriks, R. F. M., and G. W. Lucassen. 2001. Two-photon fluorescence and confocal video microscopy of in-vivo human skin. In *Multiphoton microscopy in biomedical sciences*. A. Periasamy and P. T. So, editors. SPIE, San Jose, CA. 287-293.
11. So, P. T. C., C. Y. Dong, B. R. Masters, and K. M. Berland. 2000. Two-photon excitation fluorescence microscopy. *Annu Rev Biomed Engin*. 2:399-429.
12. Corcuff, P., and J. L. Leveque. 1993. In vivo vision of the human skin with the tandem scanning microscope [see comments]. *Dermatology*. 186:50-4.
13. Rajadhyaksha, M., M. Grossman, D. Esterowitz, R. H. Webb, and R. R. Anderson. 1995. In vivo confocal scanning laser microscopy of human skin: melanin provides strong contrast. *J Invest Dermatol*. 104:946-52.
14. Rajadhyaksha, M., S. Gonzalez, J. M. Zavislan, R. R. Anderson, and R. H. Webb. 1999. In vivo confocal scanning laser microscopy of human skin II: advances in instrumentation and comparison with histology. *J Invest Dermatol*. 113:293-303.
15. Gniadecka, M., O. Faurskov Nielsen, D. H. Christensen, and H. C. Wulf. 1998. Structure of water, proteins, and lipids in intact human skin, hair, and nail. *J Invest Dermatol*. 110:393-8.
16. Barry, B. W., H. G. M. Edwards, and A. C. Williams. 1992. Fourier Transform Raman and infrared vibrational study of human skin: assignment of spectral bands. *J Raman Spectrosc*. 23:641-645.
17. Schallreuter, K. U., J. Moore, J. M. Wood, W. D. Beazley, D. C. Gaze, D. J. Tobin, H. S. Marshall, A. Panske, E. Panzig, and N. A. Hibberts. 1999. In vivo and in vitro evidence for hydrogen peroxide (H₂O₂) accumulation in the epidermis of patients with vitiligo and its successful removal by a UVB-activated pseudocatalase. *J Invest Dermatol Symp Proc*. 4:91-6.
18. Wohlrab, J., A. Vollmann, S. Wartewig, W. C. Marsch, and R. Neubert. 2001. Noninvasive characterization of human stratum corneum of undiseased skin of patients with atopic dermatitis and psoriasis as studied by Fourier transform Raman spectroscopy. *Biopolymers*. 62:141-6.
19. Nijssen, A., T. C. Bakker Schut, F. Heule, P. J. Caspers, D. P. Hayes, M. Neumann, and G. J. Puppels. 2002. Discriminating basal cell carcinoma from its surrounding tissue by Raman spectroscopy. *J Invest Dermatol*. 119:64-69.
20. Caspers, P. J., G. W. Lucassen, R. Wolthuis, H. A. Bruining, and G. J. Puppels. 1998. *In vitro* and *in vivo* Raman spectroscopy of human skin. *Biospectroscopy*. 4:S31-39.
21. Caspers, P. J., A. C. Williams, E. A. Carter, H. G. M. Edwards, B. W. Barry, H. A. Bruining, and G. J. Puppels. 2002. Monitoring the penetration enhancer dimethylsulfoxide in human stratum corneum by in vivo confocal Raman spectroscopy. *Pharm Res*. 19:1577-1580.
22. Caspers, P. J., G. W. Lucassen, H. A. Bruining, and G. J. Puppels. 2000. Automated depth-scanning confocal Raman microspectrometer for rapid in vivo determination of water concentration profiles in human skin. *J Raman Spectrosc*. 31:813-818.

23. Caspers, P. J., G. W. Lucassen, E. A. Carter, H. A. Bruining, and G. J. Puppels. 2001. In vivo confocal Raman microspectroscopy of the skin: noninvasive determination of molecular concentration profiles. *J Invest Dermatol.* 116:434-442.
24. Wolthuis, R., T. Bakker Schut, P. Caspers, H. Buschman, T. Roemer, H. Bruining, and G. Puppels. 1999. Raman spectroscopic methods for in vitro and in vivo tissue characterization. *In Fluorescent and luminescent probes for biological activity.* W. Mason, editor. Academic Press, London. 433-455.
25. Kalia, Y. N., F. Pirot, and R. H. Guy. 1996. Homogeneous transport in a heterogeneous membrane: water diffusion across human stratum corneum in vivo. *Biophys J.* 71:2692-2700.
26. Schwindt, D. A., K. P. Wilhelm, and H. I. Maibach. 1998. Water diffusion characteristics of human stratum corneum at different anatomical sites in vivo. *J Invest Dermatol.* 111:385-9.
27. Scott, I. R., and C. R. Harding. 1986. Filaggrin breakdown to water binding compounds during development of the rat stratum corneum is controlled by the water activity of the environment. *Dev Biol.* 115:84-92.
28. Rawlings, A. V., I. R. Scott, C. R. Harding, and P. A. Bowser. 1994. Stratum corneum moisturization at the molecular level. *J Invest Dermatol.* 103:731-741.
29. Horii, I., Y. Nakayama, M. Obata, and H. Tagami. 1989. Stratum corneum hydration and amino acid content in xerotic skin. *Br J Dermatol.* 121:587-92.
30. Sato, K., W. H. Kang, and F. Sato. 1991. Eccrine sweat glands. *In Physiology, Biochemistry and molecular Biology of the Skin.* L. A. Goldsmith, editor. Oxford University Press, New York. 741-762.
31. Stewart, M. E., and D. T. Downing. 1991. Chemistry and function of mammalian sebaceous lipids. *Adv Lipid Res.* 24:263-301.
32. Pappas, A., M. Anthonavage, and J. S. Gordon. 2002. Metabolic fate and selective utilization of major fatty acids in human sebaceous gland. *J Invest Dermatol.* 118:164-71.
33. Venkatesh, B., S. Ramasamy, M. Mylrajan, R. Asokan, P. T. Manoharan, and J. M. Rifkind. 1999. Fourier transform Raman approach to structural correlation in hemoglobin derivatives. *Spectrochim Acta A Mol Biomol Spectrosc.* 55A:1691-7.
34. Wood, B. R., and D. McNaughton. 2002. Micro-Raman characterization of high- and low-spin heme moieties within single living erythrocytes. *Biopolymers.* 67:259-262.
35. Pilotto, S., M. T. Pacheco, L. Silveira, Jr., A. B. Villaverde, and R. A. Zangaro. 2001. Analysis of near-infrared Raman spectroscopy as a new technique for a transcutaneous non-invasive diagnosis of blood components. *Lasers Med Sci.* 16:2-9.
36. Berger, A. J., I. Itzkan, and M. S. Feld. 1997. Feasibility of measuring blood glucose concentration by near-infrared Raman spectroscopy. *Spectrochimica Acta A.* 53:287-292.
37. Berger, A. J., T. W. Koo, I. Itzkan, G. Horowitz, and M. S. Feld. 1999. Multicomponent blood analysis by near-infrared Raman spectroscopy. *Appl Opt.* 38:2916-2926.

Conclusions and prospects

Chapter

7

Conclusions

In vivo confocal Raman microspectroscopy is presented as a novel noninvasive method to study the molecular composition of the skin. The method is based on inelastic scattering of light upon interaction with molecular components in the skin. The inelastic component of the scattered light, the so-called Raman spectrum, is unique for a given molecule and its intensity is proportional to the number of molecules present in a studied material. Therefore, a Raman spectrum can be used to study both qualitatively and quantitatively the molecular composition of the skin. The use of *confocal* Raman microspectroscopy enables the recording of Raman spectra from a very small measurement volume. Thus, a sample can be investigated at high axial and lateral resolution. This offers unique possibilities for the *in vivo* study of the skin, being a layered structure with a strongly varying molecular composition on a microscopic scale.

The studies described in this thesis demonstrate that confocal Raman microspectroscopy enables the determination of *in vivo* molecular gradients of water, natural moisturizing factor (NMF) and topically applied dimethyl sulfoxide in the stratum corneum (SC). Some possibilities of combined Raman spectroscopy and *in vivo* confocal microscopy have been probed, which enabled the *in vivo* study of the interplay between skin architecture and its molecular composition, as well as *in situ* investigation of the molecular composition of morphological structures in the skin. The information obtained in these studies is unique, because as yet, no other technique combines molecular specificity, noninvasiveness and high spatial resolution to provide this kind of detailed *in vivo* information about the molecular composition of the skin and structures therein. It may therefore be concluded that *in vivo* confocal Raman microspectroscopy is a powerful noninvasive method for investigation of the skin. It is expected that the method presented in this thesis provides the basis for a wide range of applications in fundamental skin research, pharmacology, cosmetics and fundamental and clinical dermatology.

Prospects

Despite, or perhaps due to the enormous advance in our understanding of the biochemistry of the epidermis, many questions have been raised, which may benefit from the possibilities offered by *in vivo* confocal Raman spectroscopy. The various studies described in this thesis have resulted in a detailed understanding of Raman spectra of the human SC to the extent that most molecular compounds that significantly contribute to the Raman signal, have been identified. This knowledge can serve as a starting point for many *in vivo* Raman investigations targeting the skin.

Chapter 4 describes an *in vivo* experiment in which the water gradient in the SC is strongly altered upon hydration. This particular example shows a strong effect, but the method could also be used to study the more subtle influences of various agents that are thought to have a moisturizing effect on the SC. For instance, little unambiguous knowledge exists about the penetration of glycerol in the skin and its influence on skin hydra-

tion.¹ Raman spectroscopy provides a method to address these issues *in vivo*, or more generally, to study the effects or the penetration of a range of topically applied products. Moreover, since Raman spectroscopic measurements can be performed repeatedly on the same skin area, the effects of these products can be studied as a function of time.² The molecular specificity of the method provides the means to separate the Raman signal of the product from the skin Raman signal. This is a great advantage when the effects of a product are to be studied without interference from the product itself.

Skin pH has been a topic of interest³ for a long time and is often considered as a parameter of skin well being. Investigations have been directed at the relation between aberrant skin pH and diseases such as ichthyosis⁴ and pruritus.⁵ The irritation potential of skin cleansing products has been associated with the extent to which these products alter the natural skin pH.^{6; 7} The surface of the human skin is acidic. Although originally described as the “acid mantle”, it has become clear that the acidity extends well below the SC surface, ranging from about 5 on the surface to 7 in the viable cells. Numerous enzymatic processes in the SC, involving NMF synthesis, lipid metabolism, cornification and desquamation are influenced by pH. Hydrolytic enzymes, such as phosphatase, are stored in the lamellar bodies at neutral acidity. During the cornification process these enzymes are released and, upon activation by acidic pH, start to produce the NMF.⁸ Several pH-dependent enzymes are involved in the desquamation process where they play a role in the detachment of corneocytes in the upper SC.⁹⁻¹¹ The pH level also influences many enzymes that are active in epidermal lipid metabolism and which are crucial for epidermal homeostasis and barrier formation.¹² It is a reasonable assumption that a close relation exists between these processes and the pH changes over the thickness of the SC. Despite the efforts in this field the origin and the nature of the pH variation in the human SC is still under debate.^{4; 13; 14} Krien *et al.* have suggested that the pH gradient within the SC is largely dependent on the production rate of urocanic acid (UCA).¹³ UCA is a constituent of the NMF, and its Raman spectrum is strongly pH dependent within the acidity range that is encountered in the skin (see chapter 3). Hence, UCA is an intrinsic marker of the local acidity within the SC. This offers excellent opportunities for *in vivo* investigation of the pH gradient and pH related characteristics of the SC, based on the Raman spectroscopy.

UCA has received interest from a different perspective since it was discovered to absorb harmful ultraviolet (UV) radiation. Although initially regarded as potential sunscreen, UCA has been indicated as an important mediator of ultraviolet induced immunosuppression. UCA, present in the stratum corneum as *trans*-UCA, absorbs ultraviolet radiation and isomerizes to *cis*-UCA, which has been demonstrated to suppress immune responses in several experimental systems.^{15; 16} The process of UV-isomerization is dose dependent.¹⁷⁻¹⁹ The ratio between the two UCA isomers in the SC could therefore be an intrinsic marker of exposure to UV radiation. It has been demonstrated that UCA can be detected in the SC by *in vivo* Raman spectroscopy (see chapter 3). It was found that the two isomers of UCA, *trans*-UCA and *cis*-UCA, produce very distinct Raman spectra. Therefore, *in vivo* confocal Raman spectroscopy could provide a method to directly measure the ef-

fects of UV exposure and relate these to other biochemical changes in the SC. This also offers the potential to assess the actual protection of sunscreens against UV exposure *in vivo*.

Concentration profiles of NMF constituents (chapter 3) showed significant differences between individuals in the amount of NMF. Considering the complex of biochemical processes underlying the production of NMF and the interactions with skin hydration, *in vivo* determination of these properties could be the basis for a new method of skin typing. Studies are required in which a variety of parameters such as age, sex, environmental properties and perceivable symptoms of dry skin and other skin conditions are related to NMF content and hydration status of the skin. This could also include other biochemical properties of the skin such as pH and lipid composition and organization. This would provide a method for skin typing based on objective biochemical properties, which can serve as parameters to predict potential skin disorders and to monitor the effects of treatment.

Although dry skin may be considered a mild, predominantly cosmetic skin disorder, it is expected that *in vivo* Raman spectroscopy will prove beneficial in clinical dermatology as well, for instance in fundamental research of skin disorders such as diseases that involve a compromised skin barrier or an abnormal NMF production (e.g. psoriasis, ichthyosis). Also diagnosis and grading of skin diseases and the study and evaluation of effects of treatments may be complemented by this new noninvasive method. Monitoring the effects of treatment of skin diseases is a particularly tempting, since measurements can be performed repeatedly on the same skin area, and thus the process of treatments and healing can be followed in detail. Examples of clinical application of Raman spectroscopy have been presented by Schallreuter *et al.*, who utilized FT-Raman spectroscopy to study elevated epidermal levels of hydrogen peroxide and phenylalanine in vitiligo and to monitor the effects of topical substitution with an UVB-activated pseudocatalase on the removal of hydrogen peroxide from the epidermis.^{20; 21} Nijssen *et al.* have demonstrated *in vitro* that basal cell carcinoma can be discriminated from the surrounding noncancerous tissue, based on a detailed analysis of the biochemical differences using Raman spectroscopy. This exploratory study was directed to the development of an *in vivo* technique for tumor border demarcation of basal cell carcinoma, which in the future may be used as an intra-operative assisting and guiding technique for onco-surgical procedures.²²

As these many examples show, *in vivo* confocal Raman microspectroscopy promises to throw light on a wide range of problems in fundamental skin research, pharmacology, cosmetics and fundamental and clinical dermatology.

References

1. Rieger, M. 1998. Water, water, everywhere. *Cosmetics & Toiletries magazine*. 113:75-87.
2. Caspers, P. J., A. C. Williams, E. A. Carter, H. G. M. Edwards, B. W. Barry, H. A. Bruining, and G. J. Puppels. 2002. Monitoring the penetration enhancer dimethylsulfoxide in human stratum corneum by in vivo confocal Raman spectroscopy. *Pharm Res*. 19:1577-1580.
3. Schade, H., and A. Marchionini. 1928. Der Säuremantel de Haut. *Klin Wochenschr*. 7:12-14.
4. Öhman, H., and A. Vahlquist. 1998. The pH gradient over the stratum corneum differs in X-linked recessive and autosomal dominant ichthyosis: A clue to the molecular origin of the "acid skin mantle"? *J Invest Dermatol*. 111:674-677.
5. Yosipovitch, G., E. Tur, G. Morduchowicz, and G. Boner. 1993. Skin surface pH, moisture, and pruritus in haemodialysis patients [see comments]. *Nephrol Dial Transplant*. 8:1129-32.
6. Baranda, L., R. Gonzalez-Amaro, B. Torres-Alvarez, C. Alvarez, and V. Ramirez. 2002. Correlation between pH and irritant effect of cleansers marketed for dry skin. *Int J Dermatol*. 41:494-9.
7. Schmid, M. H., and H. C. Korting. 1995. The concept of the acid mantle of the skin: its relevance for the choice of skin cleansers. *Dermatology*. 191:276-80.
8. Meyer, J., H. Grundmann, and S. Knabenhäus. 1990. Properties of acid phosphatase in human stratum corneum. *Dermatologica*. 180:24-29.
9. Menon, G. K., R. Ghadially, M. L. Williams, and P. M. Elias. 1992. Lamellar bodies as delivery systems of hydrolytic enzymes: implications for normal and abnormal desquamation. *Br J Dermatol*. 126:337-45.
10. Ekholm, I. E., M. Brattsand, and T. Egelrud. 2000. Stratum corneum tryptic enzyme in normal epidermis: a missing link in the desquamation process? *J Invest Dermatol*. 114:56-63.
11. Freinkel, R. K., and T. N. Traczyk. 1983. Acid hydrolases of the epidermis: subcellular localization and relationship to cornification. *J Invest Dermatol*. 80:441-6.
12. Forslind, B. 1995. The skin: upholder of physiological homeostasis. A physiological and (bio) physical study program. *Thromb Res*. 80:1-22.
13. Krien, P. M., and M. Kermici. 2000. Evidence for the existence of a self-regulated enzymatic process within the human stratum corneum -an unexpected role for urocanic acid. *J Invest Dermatol*. 115:414-20.
14. Harding, C. R., A. Watkinson, and A. V. Rawlings. 2000. Dry skin, moisturization and corneodesmolysis. *Int J Cosmet Science*. 22:21-52.
15. Wille, J. J., A. F. Kydonieus, and G. F. Murphy. 1999. cis-urocanic acid induces mast cell degranulation and release of preformed TNF-alpha: A possible mechanism linking UVB and cis-urocanic acid to immunosuppression of contact hypersensitivity. *Skin Pharmacol Appl Skin Physiol*. 12:18-27.
16. Termorshuizen, F., J. Garssen, M. Norval, L. Koulu, J. Laihia, L. Leino, C. T. Jansen, F. De Gruijl, N. K. Gibbs, C. De Simone, and H. Van Loveren. 2002. A review of studies on the effects of ultraviolet irradiation on the resistance to infections: evidence from rodent infection models and verification by experimental and observational human studies. *Int Immunopharmacol*. 2:263-75.
17. Hanson, K. M., B. Li, and J. D. Simon. 1997. A spectroscopic study of the epidermal ultraviolet chromophore trans-urocanic acid. *J Am Chem Soc*. 119:2715-2721.
18. Hanson, K. M., and J. D. Simon. 1997. The photochemical isomerization kinetics of urocanic acid and their effects upon the in vitro and in vivo photomerization action spectra. *Photochem Photobiol*. 66:817-820.

19. Hug, D. H., and J. K. Hunter. 1994. Adventitious interconversion of cis- and trans-urocanic acid by laboratory light. *Photochem Photobiol.* 59:303-8.
20. Schallreuter, K. U., M. Zschiesche, J. Moore, A. Panske, N. A. Hibberts, F. H. Herrmann, H. R. Metelmann, and J. Sawatzki. 1998. In vivo evidence for compromised phenylalanine metabolism in vitiligo. *Biochem Biophys Res Commun.* 243:395-9.
21. Schallreuter, K. U. 1999. Successful treatment of oxidative stress in vitiligo. *Skin Pharmacol Appl Skin Physiol.* 12:132-8.
22. Nijssen, A., T. C. Bakker Schut, F. Heule, P. J. Caspers, D. P. Hayes, M. Neumann, and G. J. Puppels. 2002. Discriminating basal cell carcinoma from its surrounding tissue by Raman spectroscopy. *J Invest Dermatol.* 119:64-69.

Summary

Samenvatting

Dankwoord

Curriculum vitae

Publications

Chapter

8

Summary

The number of noninvasive research methods to study the molecular composition of the skin is limited. Existing methods lack either the spatial resolution or the molecular specificity to enable investigation of the presence and distribution of molecular compounds in the stratum corneum (SC). The objective of the work described in this thesis was to develop a method based on confocal Raman spectroscopy as a noninvasive technique for qualitative and quantitative analysis of the molecular composition of the human skin and the SC in particular.

Raman spectroscopy is based on scattering of light upon interaction with molecular components. The inelastic component of the scattered light, the so-called Raman spectrum, is unique for a given molecule and its intensity is proportional to the concentration of the molecule. Therefore, Raman spectroscopy can be used to study both qualitatively and quantitatively the molecular composition of the skin.

In vivo confocal Raman microspectroscopy enables the recording of Raman spectra with from a specific region within the living skin. The method provides the high spatial resolution required to study different layers of the skin and to detect in-depth variations in the molecular composition of the SC.

Chapter 1 presents an introduction into the morphology and the molecular composition of the human skin, which serves as the basis for the discussions throughout this thesis. Several commonly applied invasive methods for (biochemical) skin characterization are discussed. A specific disadvantage of these methods is that they require extraction of skin material, thereby affecting the molecular composition of the skin. Noninvasive methods can avoid this problem. The most dominant methods for noninvasive (biochemical) characterization of the skin are discussed and an introduction to Raman spectroscopy is given from both a technical and a historical perspective.

Chapter 2 describes the exploratory work that served as the basis for the development of *in vivo* confocal Raman spectroscopy of human skin. In this study *in vitro* Raman measurements were performed on human skin sections and on pure skin constituents. A Raman instrument was realized that enabled *in vivo* collection Raman spectra of the skin with high spatial resolution.

A crucial step was the development of methods to interpret Raman spectra of the skin, which are composed of signal contributions from a large number of molecular compounds. Moreover, different skin layers have different molecular compositions. *In vitro*

Raman spectra of skin sections and skin constituents provided insight in the different Raman signatures of the different skin layers. Clear differences between spectra from the SC and the viable epidermis could be observed, which were interpreted as possible variations in the ceramide content. Spectra of the dermis showed much resemblance to that of collagen, being the major constituent of the dermis.

Using the confocal Raman microspectrometer that had been developed, *in vivo* spectra were recorded from several locations of the arms and hands of volunteers. It was demonstrated that the instrument provided the necessary depth resolution required to study different layers of the skin. Raman spectra were obtained from the dermis (ca. 85 μm below the skin surface) and from the SC, by changing the depth in the skin at which the laser light was focused. The initial *in vivo* measurements also uncovered local variations in the SC composition. Differences observed between SC spectra of the dorsal surface of the finger and the lower forearm could be assigned to large variations in the concentration of natural moisturizing factor (NMF).

Chapter 3 presents *in vivo* confocal Raman microspectroscopy as a novel noninvasive method to measure molecular concentration profiles in the human SC. The method was demonstrated by determination of water concentration profiles for the SC of the lower forearm and for palmar SC (thenar).

The resulting *in vivo* concentration profiles are in qualitative and quantitative agreement with published data obtained by *in vitro* methods. Water concentration profiles for the arm showed a continuous rise from 30% (wt.) at the SC surface to about 65% at a depth of ca. 15 μm . In the much thicker palmar SC the water profile was almost constant throughout the SC, showing a very steep rise at a depth of 80 to 120 μm below the skin surface.

The composition and distribution of NMF in the SC was investigated *in vivo* and a detailed description is given of the signal analysis methodology that was developed to extract the information about NMF composition and distribution from the Raman spectra. The *in vivo* results obtained by Raman spectroscopy were in agreement to in published data on NMF composition obtained by *in vitro* methods. Semi-quantitative concentration profiles were determined for the major constituents of NMF, providing *in vivo* evidence that NMF is produced in a narrow region in the lower part of the SC.

Chapter 4 describes an automated version of the Raman instrument, in which the microscope objective is mounted in a piezo-electric positioner. This modification allowed computer controlled, high precision focusing of the objective. This enabled rapid, automated determination of water concentration profiles for the SC. A detailed description is given of the signal analysis method that was used to determine water concentrations from Raman skin spectra.

Rapid measurement of water concentration profiles is required to limit occlusion effects. During the measurements the skin was covered by a window, which obstructed evaporation of water from the skin surface. This might affect the hydration level of the skin. Successive measurements of water concentration profiles on the same skin area, however,

gave highly reproducible results, showing that occlusion of the skin did not alter the skin hydration within the short time frame that was needed to record the profiles.

Intentionally induced changes in skin hydration could be clearly detected. This was demonstrated by hydrating the skin for 45 minutes, which resulted in a clearly altered water concentration profile, showing an enormous increase in the water content of the SC.

In **chapter 5** the application of Raman spectroscopy for monitoring of topically applied substances was investigated. A small dose of the penetration enhancer dimethyl sulfoxide (DMSO) was applied to the skin and concentration profiles were measured in order to monitor the distribution of DMSO as a function of depth and time. The recordings started directly after the application of DMSO and were continued at irregular time intervals. As expected, most of the dose permeated through the SC within 20 min. Surprisingly, a small fraction remained within the tissue for several days. This study particularly underlines one of the great advantages of a completely noninvasive method, in that it shows that same skin area can be monitored *in vivo* for an extended period.

Chapter 6 describes the combination of *in vivo* confocal Raman spectroscopy with the imaging technique, *in vivo* confocal scanning laser microscopy (CSLM). This unique combination enabled the *in vivo* study of the interplay between skin architecture and its molecular composition.

Simultaneous recording of confocal images and Raman spectra resulted in cross sectional images and molecular concentration profiles for the same section of the epidermis. This provided a visualization of the locations of the concentration profiles of water and NMF within the epidermis. These results confirmed *in vivo* that NMF is produced in the lower part of the SC.

Another possibility that was demonstrated was targeting of specific skin structures for Raman spectroscopic investigation, guided by real-time confocal microscopic images. High quality Raman spectra were obtained of sweat ducts and sebaceous units in the skin, which provided information about their molecular compositions in the natural state. Furthermore, targeting dermal capillaries yielded high quality Raman spectra of blood, which may open the door to the development of a method for noninvasive blood analysis.

Samenvatting

Het aantal niet-invasieve technieken om de moleculaire samenstelling van de huid te onderzoeken is beperkt. Bestaande methoden ontbreekt het of aan ruimtelijk oplossend vermogen of aan de moleculaire specificiteit die vereist zijn om de aanwezigheid en de verdeling van moleculaire bestanddelen het stratum corneum (SC) te onderzoeken. Het doel van het werk dat in dit proefschrift wordt beschreven, is het ontwikkelen van een niet-invasieve methode voor kwalitatieve en kwantitatieve analyse van de moleculaire samenstelling van de menselijke huid en van het SC in het bijzonder, op basis van confocale Raman spectroscopie.

Raman spectroscopie maakt gebruik van verstrooiing van licht door interactie met moleculen. De inelastische component van het verstrooide licht, het zogenaamde Raman spectrum, is uniek voor een gegeven molecuul en de intensiteit is evenredig met de concentratie van het molecuul. Raman spectroscopie kan daarom worden gebruikt om, zowel kwalitatief als kwantitatief, de moleculaire samenstelling van de huid te bestuderen.

In vivo confocale Raman microspectroscopie is een techniek om Raman spectra van de levende huid te meten met een hoge ruimtelijke resolutie. Hiermee wordt het mogelijk de verschillende lagen van de huid te bestuderen en diepte afhankelijke variaties in de moleculaire samenstelling van het SC te meten.

Hoofdstuk 1 geeft een introductie van de structuur en de moleculaire samenstelling van de menselijke huid. Deze dient als basis voor de verdere discussies in dit proefschrift. Een aantal veel gebruikte invasieve methoden voor het bestuderen van de huid wordt besproken. Een nadeel van deze methoden is de noodzaak om materiaal aan de huid te onttrekken, waarmee de moleculaire samenstelling van de huid wordt beïnvloed. Met niet-invasieve methoden kan dit probleem worden vermeden. De belangrijkste niet-invasieve methoden voor (biochemische) karakterisering van de huid worden besproken. Tenslotte wordt een inleiding in de Raman spectroscopie gegeven vanuit een technisch en historisch perspectief.

Hoofdstuk 2 beschrijft het verkennende werk dat als basis heeft gediend voor de ontwikkeling van *in vivo* confocale Raman spectroscopie van de menselijke huid. Voor deze studie zijn *in vitro* Raman spectra gemeten van humane huidcoupes en van moleculaire bestanddelen van de huid. Daarnaast is een confocale Raman opstelling gebouwd, waarmee het mogelijk is om *in vivo* en met hoge ruimtelijke resolutie metingen aan de huid te verrichten.

Een belangrijke onderdeel van deze studie is de ontwikkeling van methoden om Raman spectra van de huid te interpreteren. Raman spectra van de huid vormen een complex geheel van signaalbijdragen van een groot aantal moleculaire bestanddelen. Daarnaast verschilt de moleculaire samenstelling van de verschillende huidlagen. De *in vitro* metingen aan huidcoupes en aan huidbestanddelen hebben inzicht verschaft in de specifieke kenmerken van Raman spectra van verschillende huidlagen. Zo zijn duidelijke verschillen gevonden tussen de spectra van het SC en van de vitale epidermis, die wijzen op een verschil in de concentratie van ceramide. Het spectrum van de dermis blijkt hoofdzakelijk te zijn opgebouwd uit signaalbijdragen van collageen, het belangrijkste bestanddeel van de dermis.

Met de in deze studie ontwikkelde confocale Raman microspectrometer zijn *in vivo* spectra gemeten op verschillende plaatsen op armen en handen van vrijwilligers. Hiermee is aangetoond dat met confocale Raman microspectroscopie verschillende huidlagen *in vivo* kunnen worden bestudeerd. Door op verschillende dieptes in de huid te focuseren, konden onafhankelijk van elkaar Raman spectra van de dermis (ca. 85 μm onder het huidoppervlak) en van het SC worden gemeten. Voorts werden lokale variaties gevonden in de moleculaire samenstelling van het SC. Zo kon op basis van niet-invasieve Raman metingen worden aangetoond dat er grote verschillen bestaan tussen de concentratie “natural moisturizing factor” (NMF) in het SC op de dorsale zijde van de vingers en het SC aan de binnenkant van de onderarm.

In **hoofdstuk 3** wordt *in vivo* confocale Raman microspectroscopie gepresenteerd als een nieuwe niet-invasieve methode om moleculaire concentratieprofielen in de menselijke huid te bepalen. De methode wordt gedemonstreerd door concentratieprofielen van water en van NMF in het SC te bepalen. Hiervoor zijn metingen verricht aan de binnenkant van de onderarm en op de muis van de hand. De methodologie van de signaalanalyse die ontwikkeld is om de moleculaire concentratieprofielen uit de Raman spectra te verkrijgen, wordt in detail besproken.

De *in vivo* concentratieprofielen van water komen kwalitatief en kwantitatief overeen met gepubliceerde resultaten van *in vitro* bepalingen. Voor de arm laten de *in vivo* profielen een continue stijging zien van de waterconcentratie van 30% (gewichtspcent) aan het huidoppervlak naar ongeveer 65% op een diepte van 15 μm . In het veel dikkere SC van de handpalm is de waterconcentratie nagenoeg constant (ca. 35%) en vertoont pas vanaf een diepte van 80 à 120 μm onder het huidoppervlak een sterke stijging naar ongeveer 65%.

Op basis van *in vivo* Raman metingen is tevens de samenstelling van NMF bepaald. Deze komt overeen met gepubliceerde gegevens over de NMF samenstelling op basis van *in vitro* bepalingen. Voor de belangrijkste componenten van NMF zijn semi-kwantitatieve concentratieprofielen bepaald, waarmee *in vivo* bewijs wordt geleverd dat NMF onder in het SC wordt geproduceerd.

Hoofdstuk 4 beschrijft een geautomatiseerde versie van het Raman instrument. Het microscoop objectief is in een piëzo-elektrische houder gemonteerd. Dat maakt het mogelijk om snel en nauwkeurig op verschillende dieptes in de huid te focuseren. Bovendien kan

de diepte waarop gefocuseerd wordt vanuit een computer worden aangestuurd. De opstelling is gebruikt om snel en geautomatiseerd concentratieprofielen van water in het SC te bepalen. De methode waarmee concentratieprofielen van water uit de Raman metingen kunnen worden bepaald, wordt in dit hoofdstuk in detail beschreven.

Het snel kunnen meten van een concentratieprofiel van water is van belang om de invloed van occlusie te beperken. Doordat tijdens de metingen het huidoppervlak tegen een glaasje ligt, wordt de vrije verdamping van water aan het huidoppervlak belemmerd. Hierdoor zou de hydratatie van de huid kunnen worden beïnvloed. Achtereenvolgende metingen op hetzelfde stukje van de huid laten zien dat de metingen goed reproduceerbaar zijn. Hieruit blijkt dat de metingen snel genoeg kunnen worden uitgevoerd om verandering van de hydratatie van de huid door occlusie te voorkomen.

Een experiment is uitgevoerd waarbij de hydratatietoestand van de huid opzettelijk werd veranderd door de huid 45 minuten lang te bedekken met een natte lap. Een vergelijking van de hydratatieprofielen die voor en na de behandeling gemeten werden, liet een enorme toename van water in het SC zien. Dit experiment maakt duidelijk dat de methode geschikt is voor het in detail bestuderen van geïnduceerde veranderingen van de hydratatie van de huid.

In **hoofdstuk 5** wordt de mogelijkheid onderzocht om Raman spectroscopie te gebruiken voor het monitoren van op de huid aangebrachte middelen. Hiertoe werd een kleine dosis van de penetratiebevorderaar dimethyl sulfoxide (DMSO) op de huid aangebracht. Vervolgens werden er concentratieprofielen bepaald, met het doel om de distributie van DMSO in de huid te volgen als functie van diepte en tijd. De metingen werden direct na het aanbrengen van de stof gestart en voortgezet met tussenposen. Zoals verwacht drong het grootste gedeelte van de aangebrachte dosis DMSO binnen 20 minuten door het SC. Verrassend genoeg bleef een kleine fractie gedurende meerdere dagen in het weefsel aanwezig. Deze studie benut een van de grote voordelen van een niet-invasieve methode, namelijk door hetzelfde gebied van de huid over een langere periode te bestuderen.

Hoofdstuk 6 beschrijft de combinatie van *in vivo* confocale Raman spectroscopie met een afbeeldende techniek, te weten *in vivo* confocale scanning laser microscoopie (CSLM). Deze unieke combinatie maakt het mogelijk om de wisselwerking tussen de bouw van de huid en zijn moleculaire samenstelling *in vivo* te bestuderen.

De beide modaliteiten, Raman spectroscopie en CSLM, konden simultaan op dezelfde locatie in de huid worden toegepast. Dit is gebruikt om *in vivo* een afbeelding van de dwarsdoorsnede van de huid te maken en tegelijkertijd moleculaire concentratieprofielen te bepalen. Hiermee konden de locaties van de concentratieprofielen van water en NMF in de epidermis zichtbaar worden gemaakt. De resultaten bevestigen *in vivo* dat NMF onder in het SC wordt geproduceerd.

Met de combinatie is het ook mogelijk om Raman metingen te verrichten aan specifieke structuren in de huid, geleid door de real-time confocale beelden. Op deze manier konden kwalitatief goede spectra worden gemeten van zweetkanaaltjes en talgkliertjes in de huid. Hieruit werd informatie verkregen over hun moleculaire samenstelling in natuurlijke staat. Op dezelfde wijze werden spectra gemeten in dermale capillairen, hetgeen kwalitatief mooie spectra opleverde van bloed. Dit biedt vooruitzichten op een methode voor niet-invasieve analyse van de samenstelling van bloed.

Dankwoord

Het dankwoord is meestal het meest gelezen stukje tekst in een proefschrift. En waarom ook niet? Dit boekje is tot stand gekomen met de steun en bijdragen van veel mensen. Op deze plek wil ik iedereen daarvoor van harte bedanken. Dat mag best gelezen worden. Het valt niet mee om alles in een paar dankwoorden uit te drukken. Toch wil ik een poging wagen en een aantal mensen bij naam noemen.

Om te beginnen mijn promotor, Professor Bruining. Wil je je als fysicus lang genoeg binnen een geneeskundige faculteit handhaven om een boekje bij elkaar te kunnen schrijven, dan heb je een stevig draagvlak nodig. U hebt dat draagvlak gecreëerd en, op een voor mij vaak onzichtbare wijze maar beslist niet onopgemerkt, al die tijd weten te onderhouden.

Gerwin Puppels, de Baas, met in de ene hand een zweep en in de andere een toverstafje. Jouw inzet grenst aan het onwaarschijnlijke. Je hebt het lab van de grond af opgebouwd en vervolgens een groot aantal lijnen van onderzoek uitgezet. Ik ben blij dat je me een van die lijnen toevertrouwd hebt. Ver voor die tijd heb je je positieve invloed al op mijn wetenschappelijke bezigheden laten gelden. Als afstudeerder in Twente heb ik samen met jou, op een vrijdag na werktijd (toen al!), mijn eerste Raman spectrum met een zelf in elkaar gesleutelde opstelling gemeten. Er zouden er nog vele volgen. Ik heb heel veel van je geleerd en heel veel aan je te danken!

Gerald Lucassen, de man van Philips. Jij bent uiterst dankbaar publiek als het gaat om nieuwe onderzoeksresultaten. Je weet er telkens weer voor te zorgen dat elk wetenschappelijk succesje van mijn kant een vervolg krijgt. Daarnaast is er je eigen belangstelling en gedrevenheid als onderzoeker pur sang. Dat pakje dextro, onder het motto ‘alles voor de wetenschap’, verdient respect. Enne, dat jammen komt echt nog wel een keer.

Mensen van LICROS, met jullie had ik slechtere collega's kunnen treffen. Raman spectroscopie vindt vooral in het donker plaats en het is goed als je je nu en dan omringd weet met verlichte geesten. Senada Koljenovic, de sociale spil van de groep en meesters in het relativeren, jouw constante aanvoer van snoep, koek en Turkse koffie heeft ons meer dan eens over een glucosedip getrokken; Annieke Nijssen, ambassadrice van de Raman spectroscopie op ‘de Derma’ en even bedreven als Senada in het konfijten van van onze ingewanden; Bas de Jong, onze opmerkingen over je cavia's altijd sportief opnemend; Gilbert Tjiang, de skatende dokter, onze zweedse Gunilla Hagevi, Karan Kanhai, bedankt voor jullie gezelligheid. Bill and Renate Riggs, thanks for all the pleasant

conversations and for proving that all Americans may be equal, but that they're not all alike. Dan zijn er nog de mannen van het eerste uur Tom Bakker Schut, Kees Maquelin en Rolf Wolthuis. Tom, onze grote steun en toeverlaat. Jarenlang hebben wij een gangkast in het EDC gedeeld en elkaar geregeld met veel plezier van het werk gehouden als we weer eens van gedachten wisselden over de meest vreemde onderwerpen. Als je nog eens het plan opvat om je memoires uit te brengen behoor ik tot de eerste lezers. Rolf, in de gangen van het EDC bekend om je bulderende lach. Ik vermoed dat Wolthuis oud Grunnings is voor eigenwijs. Lastig is alleen dat je het zo vaak bij het rechte eind blijkt te hebben. Let wel: vaak, niet altijd! Je creatieve manier van werken is voor je collega's niet de makkelijkste. Toch heb je daarmee een bijdrage aan dit proefschrift geleverd die wellicht groter is dan je zelf beseft. Bedankt. Kees, jij dwingt respect af met de grondige en georganiseerde manier waarop je dingen aanpakt. Het verdient minder respect - maar leuk is het wel - dat wij aan een half woord genoeg hebben om elkaars grappen te vatten, waarbij jij en passant alle mogelijke associaties en perspectieven meeneemt. 'Specifiek gevoel voor humor' noem je dat geloof ik...En ach, sommige grappen vallen nou eenmaal een beetje rauw op het lijf, zo 's ochtends vóór het eerste kopje koffie. Rolf en Kees, fantastisch dat jullie mijn paranimfen willen zijn.

Alle vrienden en familie, jullie belangstelling en support zijn zeer gewaardeerd. Natasja en Chris, bedankt voor het proeflezen en de vele, vele tips. De 'yupclub', jullie zijn nooit voorzichtig met relativerende opmerkingen, maar als het er op aan komt is de interesse warm en oprecht. Tanneke en Raymond, jammer dat jullie het laten afweten, maar ja, een huwelijksreis is ook belangrijk ;-). Vrienden muzikanten, jullie hebben bij het tot stand komen van dit boekje niet met de neus vooraan gestaan. Het is natuurlijk ook een beetje als een experimentele plaat van Miles Davis: knap, maar 't swingt niet echt lekker. De muziek was in al die jaren een welkome afwisseling en de soms ietwat vermoeide maandagochtenden meer dan waard.

Belinda, mijn maatje. Jij hebt direct de gevolgen moeten ervaren van een promovende vriend. Uitgestelde vakanties en vooral de laatste tijd ongezellige avonden als ik meer wel dan niet achter de compu zat. Met de wijsheid van een ervaren process manager heb je me rustig m'n gang laten gaan en op de juiste momenten een zetje in de goede richting gegeven. En als het dan echt nodig is ben je er ook helemaal! Dankjewel.

Mam, Maarten en Margo, jullie hebben me letterlijk vanaf het allereerste begin onvoorwaardelijk gesteund en daarmee bedoel ik de afgelopen 34 jaar. Wat dit voor mij betekent, is niet in een paar woorden uit te drukken. Jullie zullen genoeg moeten nemen met één, dank!

A handwritten signature in black ink. The word "Peter" is written in a cursive, lowercase font. Above the 'P' is a large, sweeping horizontal stroke that extends across the width of the signature.

Curriculum vitae

Peter Jacobus Caspers werd geboren in Amsterdam op 10 mei 1969. In 1987 behaalde hij het diploma van het Voorbereidend Wetenschappelijk Onderwijs aan het Christelijk Lyceum Arnhem. In datzelfde jaar verhuisde hij naar het land tussen Regge en Dinkel om Technische Natuurkunde te studeren aan de Universiteit Twente. Hier deed hij zijn eerste ervaring met Raman spectroscopie op bij de vakgroep Technische Optica en Biofysische Techniek, waar hij zijn afstudeeronderzoek verrichtte. In mei 1994 werd hij opgeroepen voor de militaire dienstplicht als sergeant verbindingdienst te Ede. Kort daarna, in augustus 1994, werd de studie afgerond met het behalen van het ingenieursdiploma. Na het vervullen van de militaire dienst verrichtte de auteur gedurende acht maanden onderzoek bij zijn oude vakgroep in Twente. Begin 1997 verhuisde hij Twente voor Rotterdam, waar de medische faculteit van de Erasmus Universiteit het Laboratorium voor Intensive Care Research en Optische Spectroscopie herbergt. In deze onderzoeksgroep begon hij aan een ‘kortdurend onderzoek naar de mogelijkheden van Raman spectroscopie voor het karakteriseren van de huid’. Dit onderzoek bood voldoende aanknopingspunten voor een vervolg, hetgeen heeft geleid tot dit proefschrift. De auteur zet het onderzoek thans voort.

Publications

- Salmaso, B. L., G. J. Puppels, P. J. Caspers, R. Floris, R. Wever, and J. Greve. 1994. Resonance Raman microspectroscopic characterization of eosinophil peroxidase in human eosinophilic granulocytes. *Biophys J.* 67:436-446.
- Puppels, G. J., T. van Aken, R. Wolthuis, P. J. Caspers, T. C. Bakker Schut, H. A. Bruining, T. J. Römer, H. P. J. Buschman, M. L. Wach, and J. S. Robinson. 1998. "In vivo tissue characterization by Raman spectroscopy" in *Infrared spectroscopy: New tool in medicine*. H. H. Mantsch and M. Jackson, editors. Proc. SPIE Vol 3257, pp. 78-85.
- Lucassen, G. W., P. J. Caspers, and G. J. Puppels. 1998. "In vivo infrared- and Raman spectroscopy of human stratum corneum" in *Infrared spectroscopy: New tool in medicine*. H. H. Mantsch and M. Jackson, editors. Proc. SPIE Vol. 3257, pp. 52-61.
- Caspers, P. J., G. W. Lucassen, R. Wolthuis, H. A. Bruining, and G. J. Puppels. 1998. In vitro and in vivo Raman spectroscopy of human skin. *Biospectroscopy*. 4:S31-39.
- Caspers, P. J., G. W. Lucassen, R. Wolthuis, H. A. Bruining, and G. J. Puppels. 1999. "In-vivo Raman spectroscopy of human skin: determination of the composition of natural moisturizing factor" in *Biomedical applications of Raman spectroscopy*. M. D. Morris, editor. Proc. SPIE Vol. 3608, pp. 99-102.
- Wolthuis, R., T. C. Bakker Schut, P. J. Caspers, H. P. J. Buschman, T. J. Römer, H. A. Bruining, and G. J. Puppels. 1999. "Raman spectroscopic methods for in vitro and in vivo tissue characterization" in *Fluorescent and luminescent probes for biological activity*. W. T. Mason, editor. Academic Press, London. 433-455.
- Lucassen, G. W., P. J. Caspers, and G. J. Puppels. 2000. "Water content and water profiles in skin measured by FTIR and Raman spectroscopy" in *Controlling tissue optical properties: Applications in clinical study*. V. V. Tuchin, editor. Proc. SPIE Vol. 4162, pp. 39-45.
- Caspers, P. J., G. W. Lucassen, H. A. Bruining, and G. J. Puppels. 2000. Automated depth-scanning confocal Raman microspectrometer for rapid in vivo determination of water concentration profiles in human skin. *J Raman Spectrosc.* 31:813-818.

- Puppels, G. J., T. C. Bakker Schut, P. J. Caspers, R. Wolthuis, M. van Aken, H. P. J. Buschman, A. van der Laarse, M. G. Shim, B. C. Wilson, and H. A. Bruining. 2001. "In vivo Raman spectroscopy" in *Handbook of Raman Spectroscopy*. I. R. Lewis and H. G. M. Edwards, editors. Marcel Dekker, New York, pp. 549-574.
- Caspers, P. J., G. W. Lucassen, E. A. Carter, H. A. Bruining, and G. J. Puppels. 2001. In vivo confocal Raman microspectroscopy of the skin: noninvasive determination of molecular concentration profiles. *J Invest Dermatol*. 116:434-442.
- Caspers, P. J., A. C. Williams, E. A. Carter, H. G. M. Edwards, B. W. Barry, H. A. Bruining, and G. J. Puppels. 2002. Monitoring the penetration enhancer dimethyl sulfoxide in human stratum corneum by in vivo confocal Raman spectroscopy. *Pharm Res*. 19:1577-1580.
- Lucassen, G. W., P. J. Caspers, and G. J. Puppels. 2002. "Infrared and Raman spectroscopy of human skin in vivo" in *Handbook of Optical Biomedical Diagnostics*. V. V. Tuchin. SPIE Press, Bellingham. Vol. PM107, chapter 14.
- Nijssen, A., T. C. Bakker Schut, F. Heule, P. J. Caspers, D. P. Hayes, M. Neumann, and G. J. Puppels. 2002. Discriminating basal cell carcinoma from its surrounding tissue by Raman spectroscopy. *J Invest Dermatol*. 119:64-69.
- Bakker Schut, T. C., R. Wolthuis, P. J. Caspers, and G. J. Puppels. 2002. Real-time tissue characterization on the basis of in vivo Raman spectra. *J Raman Spectrosc*. 33:580-585.
- Caspers, P. J., G. W. Lucassen, and G. J. Puppels. 2003. Combined in vivo confocal Raman spectroscopy and confocal microscopy of human skin. *Biophys. J*. 85:572-580.
- Lucassen, G. W., M. van der Voort, G. J. Puppels, P. J. Caspers, and J. S. Cohen. "Beamcombiners for imaging and Raman spectroscopy for analysis of local composition" Patent nr: PHNL 010053 18.01.2001 US60/262582, PHNL010534US 20.07.2001 US09/912127.

